



universität  
wien

# DISSERTATION

Titel der Dissertation

„Regulatory tools and the characterization of insulinergic cells in the annelid *Platynereis dumerilii*“

Verfasser

Dipl.-Biol. Benjamin Backfisch

angestrebter akademischer Grad

Doktor der Naturwissenschaften (Dr.rer.nat.)

Wien, 2013

Studienkennzahl lt.  
Studienblatt:

A 091 490

Dissertationsgebiet lt.  
Studienblatt:

Molekulare Biologie

Betreuerin / Betreuer:

Dr. rer. nat. Florian Raible



## Acknowledgment

I am very thankful to Dr. Florian Raible for his excellent supervision, for his financial support during my work and stimulating discussions and for critically reading this manuscript.

I want to thank Dr. Kristin Tessmar for her advice and constructive criticism and for sharing materials that I used in this study.

I am very thankful to Dr. Maria Ina Arnone and Prof. Ulrich Technau for accepting to review my thesis.

I want to thank Dr. Alexander Stark and Prof. Ulrich Technau for their advice and their help as the members of my thesis advisory committee.

I want to say thanks to all past and present members of the Raible group and the Tessmar group for a great working atmosphere, for sharing their knowledge with me, for their help and for fruitful discussions. In particular, I want to thank the „founding members“ of the Raible and Tessmar labs, Claudia Lohs and Juliane Zantke who have given me a great start in my PhD project when I arrived in Vienna.

I want to thank the MFPL animal care and the marine facility animal care for the maintenance of the *Platynereis dumerilii* culture.

I want to say thanks to Charlotte Nikbakht and Filip Nikic for outstanding librarian services.

I want to say thanks to the organizing committee of the VBC PhD Symposium 2011 „Think alternative - New insights from unconventional model organisms“ for the great time that we had in organizing such an event.





# Table of Contents

<b>1. Introduction .....</b>	<b>12</b>
<b>1.1. Phylogeny of <i>Platynereis dumerilii</i> .....</b>	<b>12</b>
<b>1.2. <i>Platynereis dumerilii</i> as a model system for evolutionary and developmental biology .....</b>	<b>14</b>
<b>1.3. The molecular toolkit in <i>Platynereis dumerilii</i> .....</b>	<b>14</b>
<b>1.4. The lifecycle of <i>Platynereis dumerilii</i>.....</b>	<b>15</b>
<b>1.5. Morphology and anatomy of <i>Platynereis dumerilii</i> larval and postlarval stages.....</b>	<b>16</b>
<b>1.6. Posterior regeneration of <i>Platynereis dumerilii</i> .....</b>	<b>19</b>
<b>1.7. Transposon-based transgenic approaches as powerful tools for research.....</b>	<b>19</b>
<b>1.7.2. Transient transgenesis and stable transgenic reporter lines .....</b>	<b>21</b>
<b>1.8. Insulin and insulin-like peptides .....</b>	<b>22</b>
<b>1.8.1 The insulin family in vertebrates .....</b>	<b>22</b>
1.8.1.1. Insulin is produced by the pancreatic $\beta$ -cell .....	22
1.8.1.2. The role of insulin in vertebrates .....	24
1.8.1.3 Transcriptional regulation of the insulin gene .....	24
1.8.1.4. Posttranslational modifications of the insulin molecule .....	25
1.8.1.6. Additional members of the vertebrate insulin family .....	26
<b>1.8.2. Insulin-like peptides in ecdysozoans.....</b>	<b>26</b>
1.8.2.2. The role of insulin-like peptides in insects .....	27
1.8.2.3. Transcriptional regulation of insulin-like peptides in insects .....	28
<b>1.8.3. Insulin-like peptides in lophotrochozoans .....</b>	<b>28</b>
1.8.3.1. Expression and secretion of insulin-like peptides in molluscs .....	28
1.8.3.2. Neurosecretory centers of annelids.....	29
1.8.3.3. Insulin-like peptides in annelids .....	29
<b>1.9. Non-cephalic photoreceptor cells .....</b>	<b>30</b>
<b>1.10. Aims of the thesis.....</b>	<b>30</b>
<b>2. Results .....</b>	<b>33</b>
<b>2.1. Molecular specification of insulinergic cells in <i>Platynereis dumerilii</i> .....</b>	<b>33</b>
<b>2.1.1. Identification and characterization of insulinergic cell-types in <i>Platynereis</i> .....</b>	<b>33</b>
2.1.1.1. Identification and phylogenetic analyses of five insulin-like peptides in <i>Platynereis dumerilii</i> .....	33
2.1.1.2. Genomic loci of <i>Platynereis dumerilii</i> insulin-like peptides .....	37
2.1.1.3. Detection of insulin-like peptide transcripts in larval and nectochaete brains .....	39
2.1.1.4. Brain-specific expression of insulin-like peptides in atokous worms .....	43
2.1.1.5. Insulin-like peptide expressing cells are located within clusters of axons that are detected by anti-acetylated tubulin antibody .....	45
<b>2.1.2. Characterization of neurosecretory centers of atokous worms .....</b>	<b>45</b>
2.1.2.1. <i>Platynereis dumerilii pc2</i> is prominently expressed in the posterior brain lobes in atokous worms .....	46
2.1.2.2. Expression pattern of the neuronal marker <i>syt</i> in <i>Platynereis dumerilii</i> atokous worms.....	46
2.1.2.3. <i>Platynereis dumerilii nk2.1</i> is expressed in a medial cluster of cells and the pars intercerebralis .....	48
<b>2.1.3. Characterization of <i>Platynereis dumerilii</i> orthologues of genes that relate to the function of the vertebrate pancreas.....</b>	<b>48</b>

2.1.3.1. <i>Platynereis glut2</i> is expressed in the region of the infracerebral organ.....	49
2.1.3.2. <i>Platynereis dumerilii npy</i> is expressed in distinct cells in the medio-dorsal part of the brain and ventral nervous system .....	49
<b>2.2. Regulation of insulin-like peptides in <i>Platynereis dumerilii</i>.....</b>	<b>51</b>
<b>2.2.1. Characterization of potential upstream factors of <i>Platynereis</i> insulin-like peptides .....</b>	<b>51</b>
2.2.1.1. <i>Platynereis dumerilii IMaf</i> is expressed in insulinergic cell-types during early development.....	51
2.2.1.1.1. Identification of a large Maf gene in <i>Platynereis dumerilii</i> .....	51
2.2.1.1.2. <i>Platynereis dumerilii IMaf</i> is expressed in the larval and postlarval brain .....	53
2.2.1.1.3. <i>IMaf</i> is expressed in insulinergic cells of the trochophore larva .....	53
2.2.1.1.4. <i>IMaf</i> and insulin-like peptide 2 are not co-expressed in atokous worms.....	55
2.2.1.1.5. Transient expression of a reporter construct recapitulates endogenous <i>IMaf</i> expression in the central larval brain .....	55
2.2.1.1.6. Knockdown of <i>IMaf</i> expression reveals inconclusive data .....	58
2.2.1.2. <i>Platynereis dumerilii pax6</i> expression is associated to <i>ilp2</i> in atokous worms .....	59
2.2.1.3. <i>Platynereis dumerilii</i> insulin-like peptides are not co-expressed with <i>xlox</i> .....	62
2.2.1.4. <i>Platynereis dumerilii islet</i> gene is prominently expressed in the posterior lobes and the nuchal organ .....	62
<b>2.2.2. Elevated expression levels of insulin-like peptide mRNA after food intake in <i>Platynereis dumerilii</i> .....</b>	<b>63</b>
<b>2.2.3. Circadian expression of insulin-like peptides in <i>Platynereis dumerilii</i> .....</b>	<b>65</b>
2.2.3.1. <i>Platynereis dumerilii</i> ilps are expressed in a 24h rhythm.....	65
2.2.3.2. <i>Platynereis dumerilii</i> ilps keep their expression rhythm in the dark .....	65
2.2.3.3. Insulin-like peptides are expressed in a constant number of cells during the day .....	68
<b>2.3. Establishing transgenesis in <i>Platynereis dumerilii</i>.....</b>	<b>68</b>
<b>2.3.1. Transposase activity in <i>Platynereis dumerilii</i>.....</b>	<b>68</b>
2.3.1.1. Minos Transposase mediates genomic integration of reporter constructs in <i>Platynereis dumerilii</i> .....	69
2.3.1.2. Transient Expression of reporter constructs using tol2 Transposase.....	71
2.3.1.3. Heritable genomic integrations and expression of reporter constructs using Mos1 transposase.....	74
<b>2.3.2. Generation of stable transgenic reporter lines in <i>Platynereis dumerilii</i> .....</b>	<b>77</b>
2.3.2.1. A transgenic reporter line for <i>alpha-tubulin</i> demarcates ciliated cells of the prototroch .....	77
2.3.2.2. phiC31 integrase is active in <i>Platynereis dumerilii</i> .....	79
2.3.2.3. A transgenic reporter line for <i>r-opsin</i> revealed previously uncharacterized photoreceptor cells in <i>Platynereis dumerilii</i> .....	80
<b>2.3.3. Molecular specification of non-cephalic photoreceptors .....</b>	<b>83</b>
2.3.3.1. <i>Dachshund</i> correlates with <i>r-opsin</i> expression in cells of the ventral trunk.....	83
2.3.3.2. Correlating <i>pax6</i> and <i>r-opsin</i> expression .....	85
2.3.3.2.1. <i>Pax6</i> and <i>r-opsin</i> are co-expressed in the frontal lateral eyelets of juvenile worms .....	85
2.3.3.2.2. No correlation of <i>pax6</i> and <i>r-opsin</i> in atokous worms.....	85
2.3.3.3. <i>G(q)</i> is present in photoreceptor cells.....	88
2.3.3.4. <i>brn3</i> is detected in <i>r-opsin</i> neighboring cells.....	89
2.3.3.5. <i>pax2/5/8</i> is expressed in regenerated tails.....	89
<b>3. Discussion .....</b>	<b>92</b>
<b>3.1. Expanding the molecular toolkit to study cell types in <i>Platynereis</i> larvae and at postlarval stages.....</b>	<b>92</b>
<b>3.1.1. The tol2 transposon is a powerful tool for transient transgenic approaches in <i>Platynereis dumerilii</i> .....</b>	<b>92</b>
<b>3.1.2. Establishing of the first stable transgenic strains in <i>Platynereis</i> using the Mos1 transposable element.....</b>	<b>94</b>
3.1.2.1. Possible reasons for the discrepancy of endogenous and EGFP expression in the <i>alpha-tubulin</i> transgenic reporter strain .....	95
<b>3.1.3. phi C31 integrase system as a potential improvement in transgenic technology .....</b>	<b>96</b>

3.1.4. Optimized in-situ Hybridization protocols allow studying and comparisons of gene expression patterns at postlarval stages in <i>Platynereis dumerilii</i> .....	97
3.2. Molecular analyses reveal new insights into the neurosecretory centers of the adult <i>Platynereis</i> brain .....	97
3.3. New insights into the regulation of insulin-like peptides in <i>Platynereis dumerilii</i> .....	98
3.3.1. Phylogenetic analyses of the <i>Platynereis</i> insulin-like peptides .....	98
3.3.2. Expression analyses in larval and postlarval stages indicate that <i>Platynereis</i> insulin-like peptides are differentially regulated and have diverse functions .....	99
3.3.3. Assessing the regulatory code of insulinergic cells in <i>Platynereis dumerilii</i> .....	100
3.3.3.1. Expression analyses suggest a function of <i>Platynereis lMaf</i> in insulinergic cell types during larval development .....	100
3.3.3.2. Evidence for a conserved function of <i>Platynereis pax6</i> as a regulator of <i>ilp2</i> expression in atokous worms .....	101
3.3.3.3. Indication for a function of <i>Platynereis islet</i> in sensory cells .....	101
3.3.3.4. <i>Platynereis xlox</i> is not a regulator of insulin-like peptides in <i>Platynereis</i> .....	102
3.3.4. Evidence for circadian clock-controlled expression of <i>Platynereis</i> insulin-like peptides .....	102
3.3.5. Food-dependent expression suggests conserved functions of <i>Platynereis</i> insulin-like peptides in glucose metabolism .....	103
3.4. Expression patterns analyses of <i>glut2</i> and insulin-like peptides in atokous worms indicate a possible mechanism of glucose sensing and insulin-secretion in <i>Platynereis dumerilii</i> .....	104
3.5. Neuronal expression of <i>Platynereis</i> insulin-like peptides provide evidence for a neural origin of insulinergic cells .....	105
3.6. Molecular analyses of non-cephalic photoreceptors in <i>Platynereis</i> reveal similarities to the amphioxus Hesse organ .....	106
3.7. Co-expression of <i>pax6</i> and <i>r-opsin</i> in frontal lateral eyelets reveal <i>pax6</i> -positive photoreceptors in <i>Platynereis</i> .....	107
4. Materials and Methods .....	109
4.1. <i>Platynereis dumerilii</i> culture .....	109
4.2. <i>Platynereis</i> Whole-Mount in-situ Hybridization .....	109
4.2.1. Protocol .....	109
4.2.2. Preparation of DIG-labeled antisense-riboprobes .....	110
4.2.3. Preparation of Polyvinylalcohol stock solution .....	111
4.2.4. Two-color in-situ protocol .....	111
4.3. Microinjection .....	112
4.4. Salt-extraction protocol for genomic DNA .....	112
4.5. Southern blot and radioactive Hybridization .....	113
4.5.1. Detection of genomic insertions .....	113
4.5.1.1. Blotting of genomic DNA to nylon membrane .....	113
4.5.1.2. Radiolabeling of egfp probe .....	114
4.5.1.3. Southern Hybridization .....	114
4.5.2. Identification of specific RACE-PCR fragments and Colony lift .....	114
4.5.2.1. Blotting of RACE-PCR fragments to nylon membrane .....	114
4.5.2.2. Radiolabeling of probes .....	115
4.5.2.3. Southern Hybridization .....	115
4.5.2.4. Cloning of specific RACE-PCR products and Colony lifts .....	115
4.6. Rapid Amplification of c-DNA Ends (RACE-PCR) .....	116

4.6.1. Protocol RACE-PCR .....	116
4.7. Microscopy.....	117
4.7.1. Preparation of specimens for live imaging.....	117
4.7.2. Confocal laser microscopy.....	117
4.7.3. DIC microscopy.....	117
4.7.4. Lumar stereomicroscopic images .....	117
4.8. PhiC31 activity and plasmid recombination assay.....	118
4.8.1. Construction of attB-rps9::egfp.....	118
4.8.2. Construction of attP-tuba::egfp.....	118
4.8.3. Synthetic phiC31 integrase mRNA.....	118
4.8.4. Microinjection and analysis .....	118
4.9. Generation of reporter constructs .....	119
4.9.1. tuba::egfp reporter .....	119
4.9.2. rps9::egfp reporter.....	119
4.9.3. lMaf::egfp reporter .....	120
4.9.4. r-opsin::egfp reporter .....	121
4.10. Morpholino antisense oligo design.....	121
4.10.1. lMaf Morpholino antisense oligo .....	121
4.10.2. egfp Morpholino antisense oligo .....	122
4.10.3. Morpholino antisense oligo injections .....	122
4.11. Starvation assay.....	122
4.12. Quantitative RT-PCR .....	122
4.12.1. Primer design.....	122
4.12.2. Extraction of total RNA from tissues .....	123
4.12.3. cDNA synthesis.....	123
4.12.4. quantitative RT-PCR.....	124
4.12.5. Analysis .....	124
4.13. Standard cloning procedures .....	124
4.13.1. TA-cloning .....	124
4.13.2. blunt-end cloning.....	125
4.14. Plasmid preparation.....	125
4.14.1. Miniprep .....	125
4.14.2. Endotoxin-free Maxiprep .....	125
4.15. Thermal asymmetric interlaced PCR (TAIL-PCR).....	126
4.15.1. Protocol .....	126
4.15.2. Detection of genomic integrations of reporter constructs .....	127
4.15.2.1. Mos integrations .....	127
4.15.2.2. Tol2 integrations.....	128
4.15.3. Enhancer isolation.....	128
4.16. Construction of Phylogenetic trees .....	128
4.17. PCR Primer design.....	129
4.18. Identification of genomic loci of Platynereis insulin-like peptide1 and insulin-like peptide2 .....	129
4.19. Transposase activity test.....	130
4.19.1. Tol2 excision test .....	130
4.19.2. Mos1 excision test.....	130
4.20. Transposases .....	131
4.20.1. Minos Transposase.....	131

4.20.2. Mos1 Transposase .....	131
4.20.3. Tol2 Transposase.....	132
4.21. Vectors for Transgenesis .....	132
4.21.1. pMiSce.....	132
4.21.2. pMosSce .....	132
4.21.3. pTol2Sce.....	133
4.22. <i>Platynereis dumerilii</i> primary cell culture .....	133
4.23. Standard sequencing of plasmid DNA .....	133
4.24. Genotyping PCR for transgenic animals .....	133
4.25. <i>Platynereis dumerilii</i> rps9 gene-structure.....	134
4.26. List of genes that were cloned in this study using specific primers .....	134
4.27. Equipment.....	134
5. References .....	138
6. Appendix .....	152
Summary .....	155
Zusammenfassung.....	157
Erklärung.....	161
Curriculum vitae .....	164

## Index of Figures

Figure 1: Phylogenetic tree.....	13
Figure 2: <i>Platynereis dumerilii</i> .....	17
Figure 3: <i>Platynereis dumerilii</i> brain sections .....	18
Figure 4: Mechanism of Transposition.....	21
Figure 5: Development and function of insulinergic cells.....	23
Figure 6: Alignment of insulin-related peptides .....	35
Figure 7: Phylogeny of insulin-related peptides .....	36
Figure 8: Genomic loci of insulin-like peptides .....	39
Figure 9: Larval expression of insulin-like peptides .....	41
Figure 10: Expression of insulin-like peptides in nectochaete larvae .....	43
Figure 11: Expression of insulin-like peptides in atokous worms.....	44
Figure 12: Neurosecretory centers in atokous worms.....	48
Figure 13: Expression analyses of genes related to pancreatic functions.....	50
Figure 14: Phylogenetic analyses of <i>Platynereis</i> Maf genes .....	52
Figure 15: Expression of <i>IMaf</i> in larval and postlarval stages .....	54
Figure 16: Co-expression analyses of <i>IMaf</i> and insulin-like peptides in trochophore larvae .....	56
Figure 17: Double-staining analyses of <i>IMaf</i> and <i>ilp2</i> in atokous worms .....	57
Figure 18: <i>IMaf</i> reporter expression in larval stages .....	58
Figure 19: Expression analyses of <i>pax6</i> and insulin-like peptides in trochophore larvae .....	60
Figure 20: Double-staining analyses of <i>pax6</i> and <i>ilp2</i> in atokous worms .....	61
Figure 21: <i>islet</i> gene expression.....	63
Figure 22: Food-dependent expression of insulin-like peptides .....	64
Figure 23: Circadian expression of insulin-like peptides.....	66
Figure 24: Relative expression of insulin-like peptides under constant darkness .....	67
Figure 25: Genomic integrations of Minos-derived reporter constructs.....	70
Figure 26: Tol2 transposase activity and F <sub>0</sub> transgenesis of a Tol2-based ubiquitous fluorescent reporter construct delivered by microinjection.....	73
Figure 27: Mos1 transposase activity and genomic insertions of Mos1-based reporter constructs .....	77
Figure 28: Stable expression and inheritance of a ciliated cell-specific reporter construct using Mos1-based transgenesis.....	78
Figure 29: Expression of <i>alpha-tubulin</i> during development .....	79
Figure 30: phi C31 integrase is capable to recombine two plasmids in vivo.....	80
Figure 31: Stable transgenic expression of an <i>r-opsin</i> fluorescent reporter in cephalic photoreceptors .....	82
Figure 32: Expression analyses of dachshund in atokous worms reveal correlations with <i>r-opsin</i> in ventral non-cephalic photoreceptors.....	84
Figure 33: Co-expression of <i>r-opsin</i> and <i>pax6</i> in frontal lateral islets .....	86
Figure 34: Expression analyses of <i>pax6</i> in atokous worms reveal <i>pax6</i> -independent non-cephalic photoreceptors .....	87
Figure 35: <i>Platynereis g(q)</i> demarcates photoreceptor cells .....	88
Figure 36: Expression of <i>brn3</i> and <i>pax2/5/8</i> in cells adjacent to non-cephalic photoreceptors....	90
Figure 37: Assembly of Southern blot .....	113
Figure 38: Principle of TAIL-PCR .....	126



# 1. Introduction

## 1.1. Phylogeny of *Platynereis dumerilii*

The marine bristle worm *Platynereis dumerilii* is an annelid species and belongs to the superphylum of the lophotrochozoan animals. Figure 1 illustrates the phylogenetic position of *Platynereis dumerilii* within the animal kingdom. Along with the ecdysozoans, the lophotrochozoans constitute the protostomian branch of animals. The ecdysozoans comprise the phyla nematodes and arthropods, the latter encompasses large subphyla like crustaceans, chelicerata and insects. Protostomes and deuterostomes together, form the two main branches of bilaterian animals that diverged about 600 Million years ago. The deuterostomian branch of animals comprises the phyla ambulacraria and chordates. The Chordates include the subphyla cephalochordates, tunicates and vertebrates. Bilaterian animals are eumetazoan animals with left-right symmetry whereas the body of radially symmetrical eumetazoan animals like cnidarians has a radial symmetry.

Molecular biological research focuses on few species that have been established as model organisms and are accessible for a broad range of molecular techniques. The dipterian *Drosophila melanogaster*, the nematode *Caenorhabditis elegans*, the zebrafish *Danio rerio* and the mouse *Mus musculus* represent examples of well-established model organisms from different bilaterian branches. However, the lophotrochozoans as a major branch of bilaterian animals, are under-represented in terms of well-established model organisms for molecular biological research. In particular, lophotrochozoan species can provide new insights into the deep evolution of bilaterian animals. Lophotrochozoans are phylogenetically distant to insects, nematodes and vertebrates and are therefore interesting for long-range evolutionary comparisons with the conventional bilaterian model organisms. In this context, *Platynereis dumerilii* has emerged as a molecular reference species within the super-phylum of the lophotrochozoans.



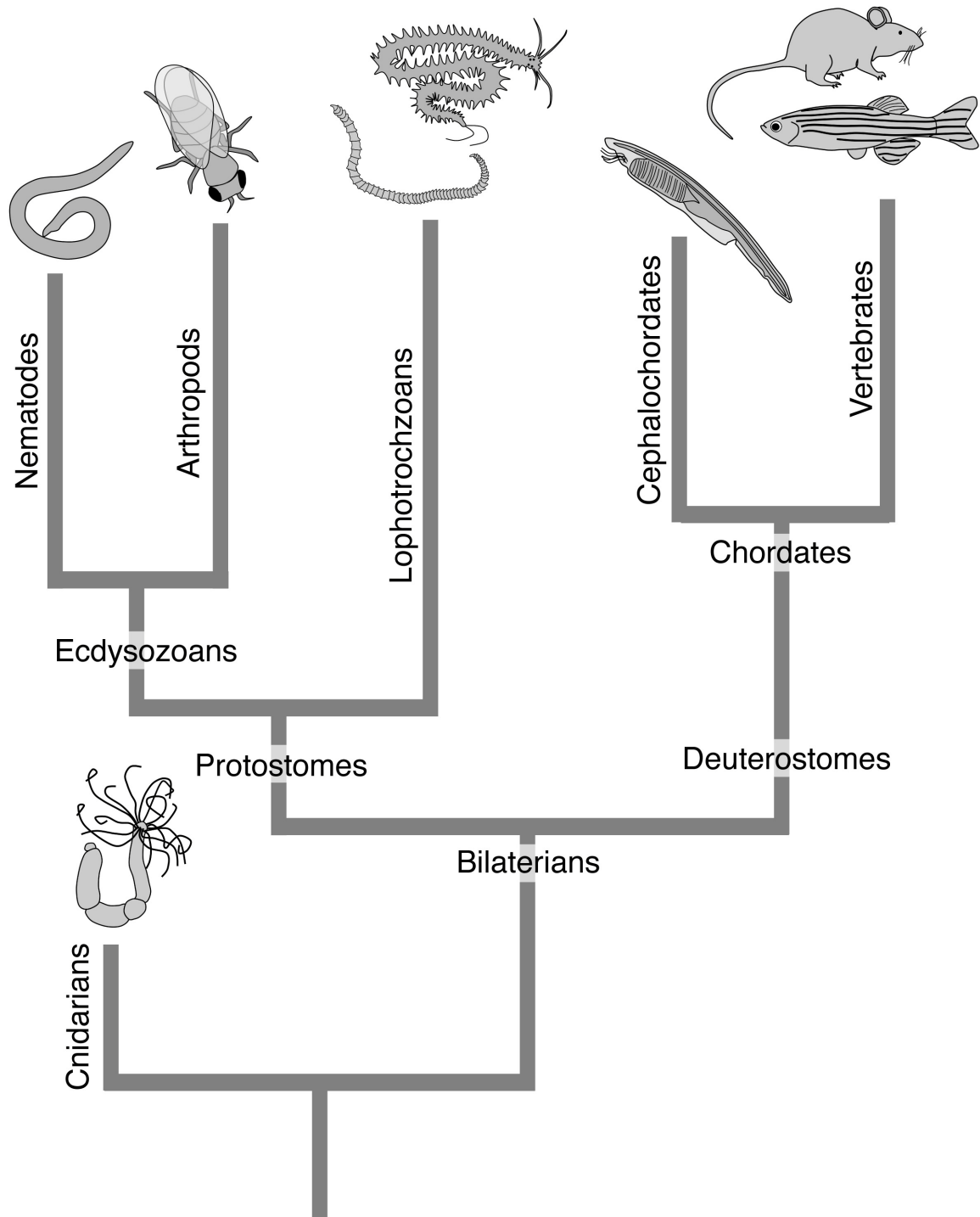


**Figure 1: Phylogenetic tree**

Schematic view of animal phylogeny. Species shown: Cnidarians: *Nematostella vectensis*; Nematodes: *Caenorhabditis elegans*; Arthropods: *Drosophila melanogaster*; Lophotrochozoans: *Capitella teleata*, *Platynereis dumerilii*; Cephalochordates: *Branchiostoma floridae*; Vertebrates: *Mus musculus*, *Danio rerio*

## 1.2. *Platynereis dumerilii* as a model system for evolutionary and developmental biology

*Platynereis dumerilii* has long served as a model species to study maturation, regeneration and development in annelids and has been bred in laboratory culture since 1953 without interruption. In the past years, the establishment of methods to investigate gene-expression and the availability of transcriptome and genome sequence data have paved the way for studies on *Platynereis* development and neurobiology using molecular biological approaches. Thus, *Platynereis* has become an attractive model species for evolutionary developmental biology (evo-devo), a relatively new field in biology that seeks to uncover how developmental processes have evolved in animals by investigating and comparing developmental processes in different species (Raff 2000).

Compared to ecdysozoan model species like *Drosophila melanogaster* and *Caenorhabditis elegans*, *Platynereis dumerilii* was shown to be a relatively slowly evolving species. Hence, it is assumed that *Platynereis dumerilii* reflects a more ancestral-type state in terms of cell-types, gene-repertoire and genome structure than the conventional ecdysozoan model organisms (Raible et. al., 2005). In several recent studies, *Platynereis dumerilii* has successfully been used to investigate the origin and evolution of vertebrate cell-types and elaborate organs such as the brain and eyes by their molecular fingerprints, the unique combination of genes expressed in a specific cell-type (Tomer et. al., 2010, Christodoulou et. al., 2010, Tessmar-Raible et. al., 2007, Denes et. al., 2007, Arendt et. al., 2004, Arendt & Wittbrodt, 2001).

## 1.3. The molecular toolkit in *Platynereis dumerilii*

As mentioned above (section 1.2), methods to investigate in-situ gene-expression patterns in larval stages and transcriptome and genome sequence resources have been established in *Platynereis dumerilii*. As an aquatic organism, *Platynereis dumerilii* is accessible for extrinsic treatment with chemical agents that, i.e. interfere with signaling pathways which are applied in solution. Moreover, an efficient microinjection protocol was developed for *Platynereis dumerilii* zygotes. Based on this, molecular methods to modify target gene-expression like gene-knockdown and mutagenesis are currently being established in several labs. However,

compared to conventional model organisms, the molecular toolkit for *Platynereis dumerilii* is limited. At the beginning of this study, robust protocols for labeling cells in later stages of development were still missing. This is why as a part of this study, I developed a robust protocol for transient and stable transgenesis in *Platynereis dumerilii*. Moreover, as part of my work to validate this method, I also established a two-color in-situ Hybridization protocol for comparing gene expression patterns at postlarval stages.

## 1.4. The lifecycle of *Platynereis dumerilii*

The maturation of *Platynereis dumerilii* is driven by the lunar periodicity and mature animals reproduce only once in their lifetime. The early embryonic and larval development is highly synchronized in a clutch of fertilized eggs and their developmental speed is temperature-dependent. Figure 2A gives an overview of the lifecycle of *Platynereis dumerilii*. Mature males and females are pelagic and reproduce after a remarkable spawning ritual - the „mating dance“ - in the open water. The female releases its eggs, which are subsequently fertilized by the male's sperm. Fertilized eggs develop a viscous egg jelly and stay afloat. The fertilized eggs undergo a series of spiral cleavages and develop into freely swimming, non-feeding trochophore larvae within one day that exhibit a positive phototactic swimming behavior. After 3 days, the trochophore larvae have developed via metatrochophore stages into nectochaete larvae that have a mixed pelago-benthic lifestyle. At 5 days of development, the late nectochaete larvae start to feed. In the following days the errant juveniles become benthic and subsequently grow as atokous worms that live in self-built tubes on the ground. After 2-18 months, worms undergo sexual metamorphosis and transform into epitokous worms that become mature males and females. In laboratory breeding culture, the lifecycle of *Platynereis dumerilii* is completed within 2-3 months and mature worms for breeding are obtained throughout the year. For an extensive overview of larval and postlarval development and the lifecycle of *Platynereis dumerilii*, I would like to refer to Fischer and Dorresteijn (2004) and Fischer et. al. (2010).

## 1.5. Morphology and anatomy of *Platynereis dumerilii* larval and postlarval stages

As mentioned in the previous section (1.4), the development of *Platynereis dumerilii* occurs indirectly via a ciliated trochophore larva that exhibits a planktonic lifestyle. Figure 2B illustrates schematically the trochophore larva and indicates its morphological features, body axes and definitions of the views shown in this study. A feature of *Platynereis dumerilii* larvae is that they are transparent and therefore easily accessible for *in-vivo* imaging and staining procedures.

The body of atokous worms appears homonomously-segmented (Figure 2C). Each of the segments has a pair of parapodia that are used for locomotion. A schematic view of a parapodia is shown in Figure 2C'. The head of an atokous worm possesses two pairs of adult eyes and specialized appendages, which are described in Figure 2D.

In Figure 3 sections through the adult brain of an atokous worm are shown and different structures are indicated (Müller 1976).

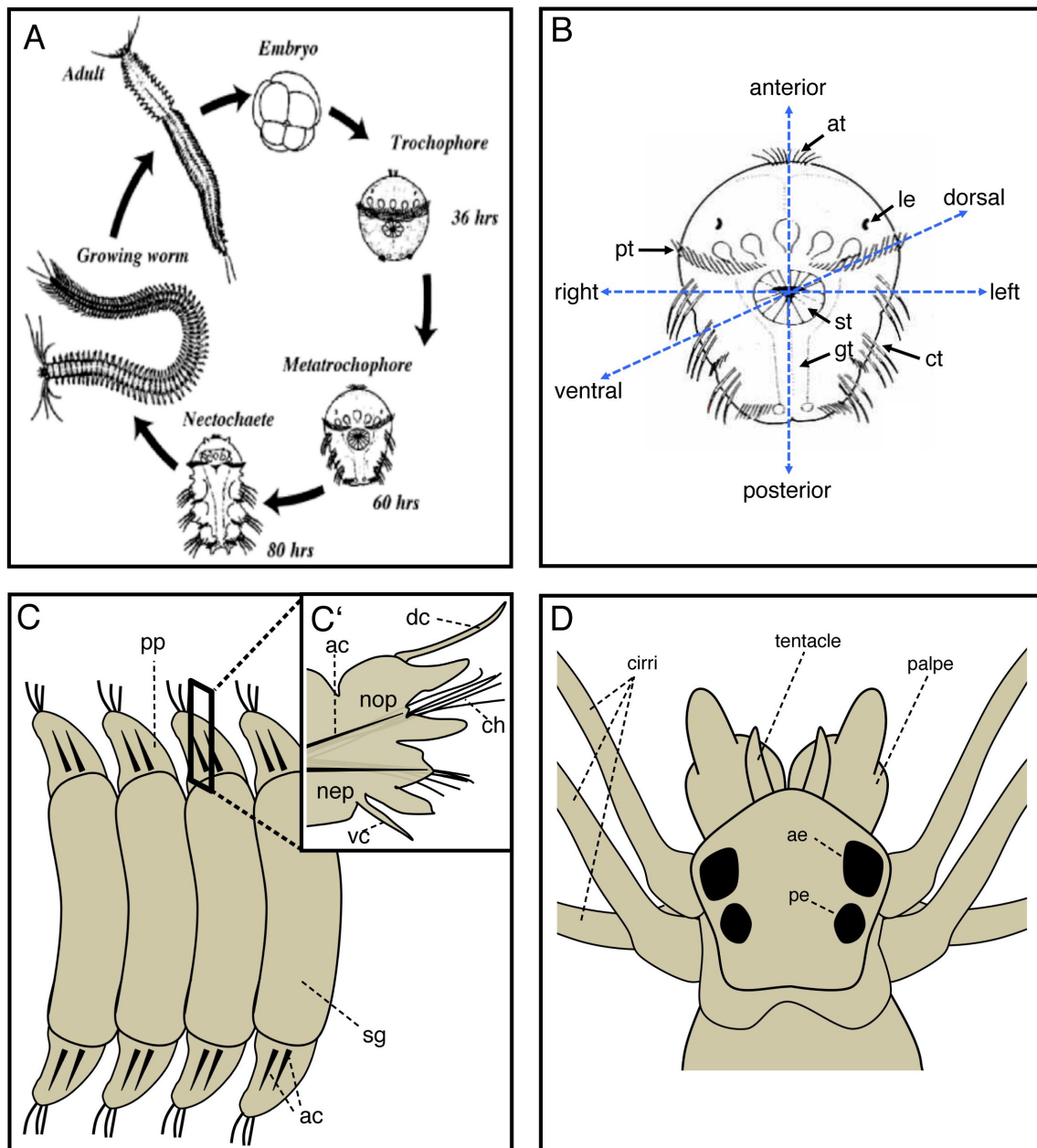


**Figure 2: *Platynereis dumerilii***

(A) The lifecycle of *Platynereis dumerilii* (Drawing from Hauenschild, 1969). (B) *Platynereis dumerilii* trochophore larva. Blue axes indicate the different views used in this study. at: apical tuft, ct: chaetae, gt: gut, le: larval eye, pt: prototroch, st: stomodeum (Drawing modified from Dorrestein et al., 1993). (C) Schematic view of 4 trunk segments (ventral view). ac: aciculae; pp: parapodia; sg: body segment. (C') Schematic drawing of a parapodia. Section indicated in C. ch: chaetae; dc: dorsal cirrus; vc: ventral cirrus; nep: neuropod; nop: notopod. (D) Schematic view of the *Platynereis* head with appendages from dorsal view. ae: anterior adult eye; pe: posterior adult eye.

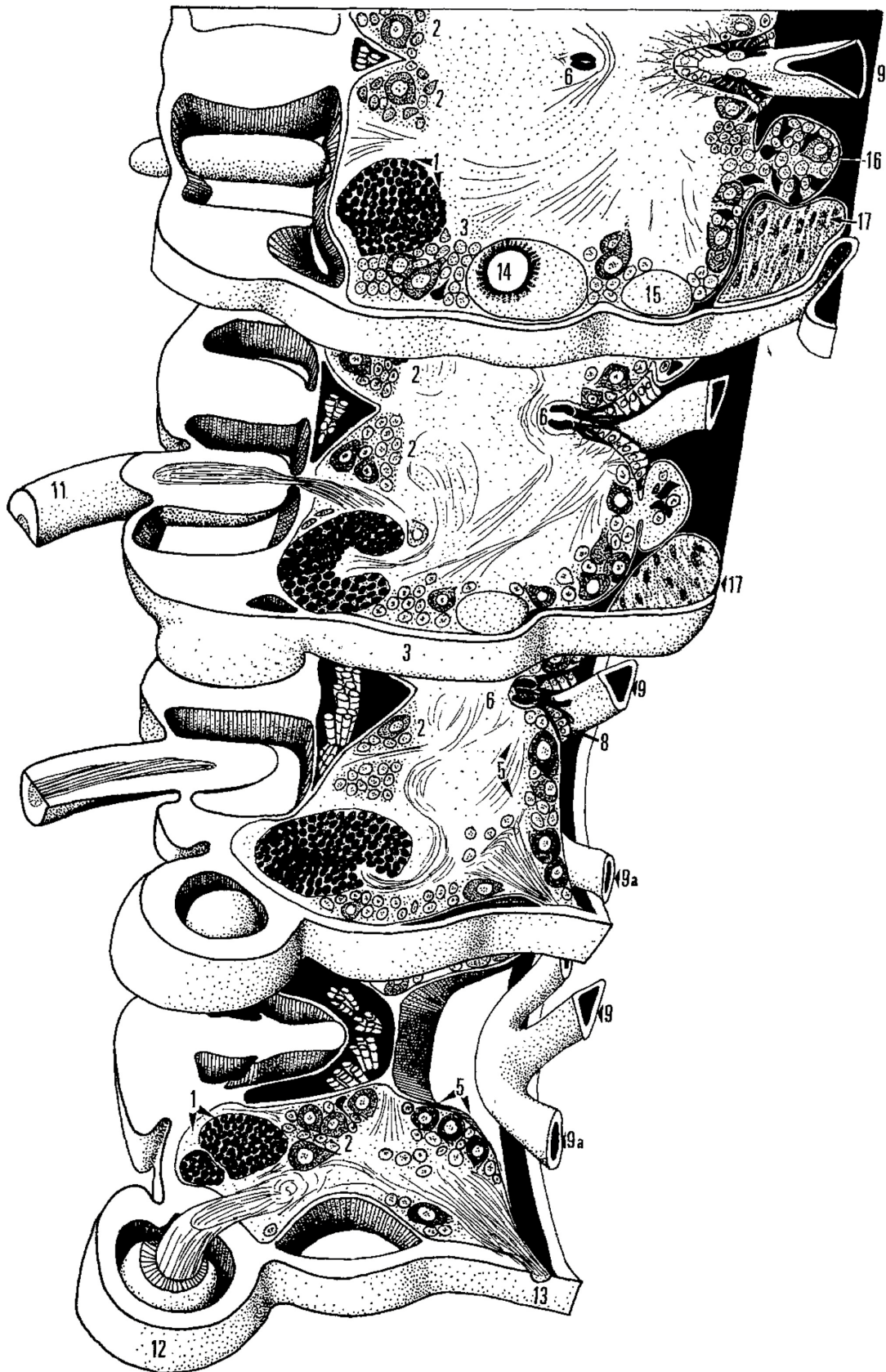


**Figure 3: *Platynereis dumerilii* brain sections**

Frontal sections through the protostomium of *Platynereis dumerilii*. Upper right corner: dorsal most section, lower left corner: ventral most section. Numbers indicate the different brain structures

(drawing from Müller 1973). 1: corpora pedunculata, 2 pars intercerebralis, pars lateralis, 6 anterior strand of connective tissue, 7 posterior strand of connective tissue, 8 infracerebral organ, 9 dorsal blood vessel, 11 antennae, 12 palpe, 14 anterior adult eye, 15 posterior adult eye, 16 posterior brain lobes, 17 nuchal organ (from Müller 1973).

## 1.6. Posterior regeneration of *Platynereis dumerilii*

A remarkable feature of *Platynereis dumerilii* is that atokous worms have the capacity to regenerate the posterior body part when it has been cut off. It was shown that this process is triggered by a specific brain region, which is supposed to produce a juvenile hormone responsible for regeneration and maturation (Hofmann 1976). The ability of posterior regeneration has been exploited to investigate formation and growth of segments in *Platynereis dumerilii* (Saudemont et. al., 2008). In 8-day-old posterior regenerated worms, a series of newly formed segments exists, representing different stages in segment development that can be analyzed morphologically, anatomically or on the molecular level. Moreover, genotyping assays can be performed with tail tips without severe harming of the animals.

## 1.7. Transposon-based transgenic approaches as powerful tools for research

As mentioned above (section 1.3), an intermediate goal of my study was to develop methodology in *Platynereis dumerilii* to label specific cells in the living animals using transgenic approaches. To achieve this, I explored the use of transposable elements mediating genomic integrations of fluorescent reporter constructs in *Platynereis dumerilii*. Transgenic techniques have become a powerful tool for various research purposes, like the study of spatio-temporal gene-expression pattern, targeted isolation and ablation of cell-types, mutagenesis, or enhancer activity tests (Plasterk et. al., 1992, Cooley et. al., 1988, Cooley et. al., 1988, Palmiter et. al., 1987, Breitmann et. al., 1987, Bessa et. al., 2009, Asakawa et. al., 2009). In particular, the use of transposable elements (transposons), which are mobile genetic elements, has become a major approach to generate transgenic organisms. Robust transposon-based protocols for transgenesis have been established in a variety of different species ranging from plants to insects and vertebrates.

### 1.7.1. Mechanism of transposon-mediated genomic integrations of reporter constructs

Barbara McClintock has discovered the phenomenon of transposition in maize in the middle of the last century (McClintock 1950). Since then, scientists have described different types of transposable elements and have extensively studied their mechanisms of transposition in various species. Two classes of transposable elements are being distinguished. Retrotransposons of the class I copy themselves by a reverse transcription mechanism via RNA stages (copy-and-paste) and DNA transposons of the class II encode for a transposase enzyme, which mediates excision and integration of the transposon (cut-and-paste). To date, transposable elements of the class II (DNA Transposons) have been engineered as tools to generate transgenic organisms. The DNA Transposons sleeping beauty, Mos1 and Minos that belong to the Tc1/mariner transposon-family or the Tol2 Transposon are prominent examples of transposable elements that have been adopted for transgenic applications in a variety of species.

Similar to unmodified class II transposons, engineered DNA transposons integrate into the host genome via a „cut-and-paste“ mechanism, too. Engineered transposons consist of the transgene, which is supposed to be integrated into the host genome instead of the transposase enzyme encoding sequence. The transgene is flanked on both sides by inverted terminal repeats that are recognition sites for the transposase and this construct is enclosed in a donor vector (Figure 4A). The transgene plasmid is co-delivered into the host cell along with the transposase as synthetic mRNA, protein or encoded on a second helper plasmid. In the host cell, the active transposase enzyme binds to both inverted terminal repeat sequences and excises the transgene from the donor vector (Figure 4B). At the genomic integration site, the transposase cleaves the DNA double-strand and inserts the transgene into the host genome (Figure 4C). Most transposons for transgenic approaches integrate randomly into the host genome but have preferred sites for integration, like TA-dinucleotides for members of the Tc1/mariner family.



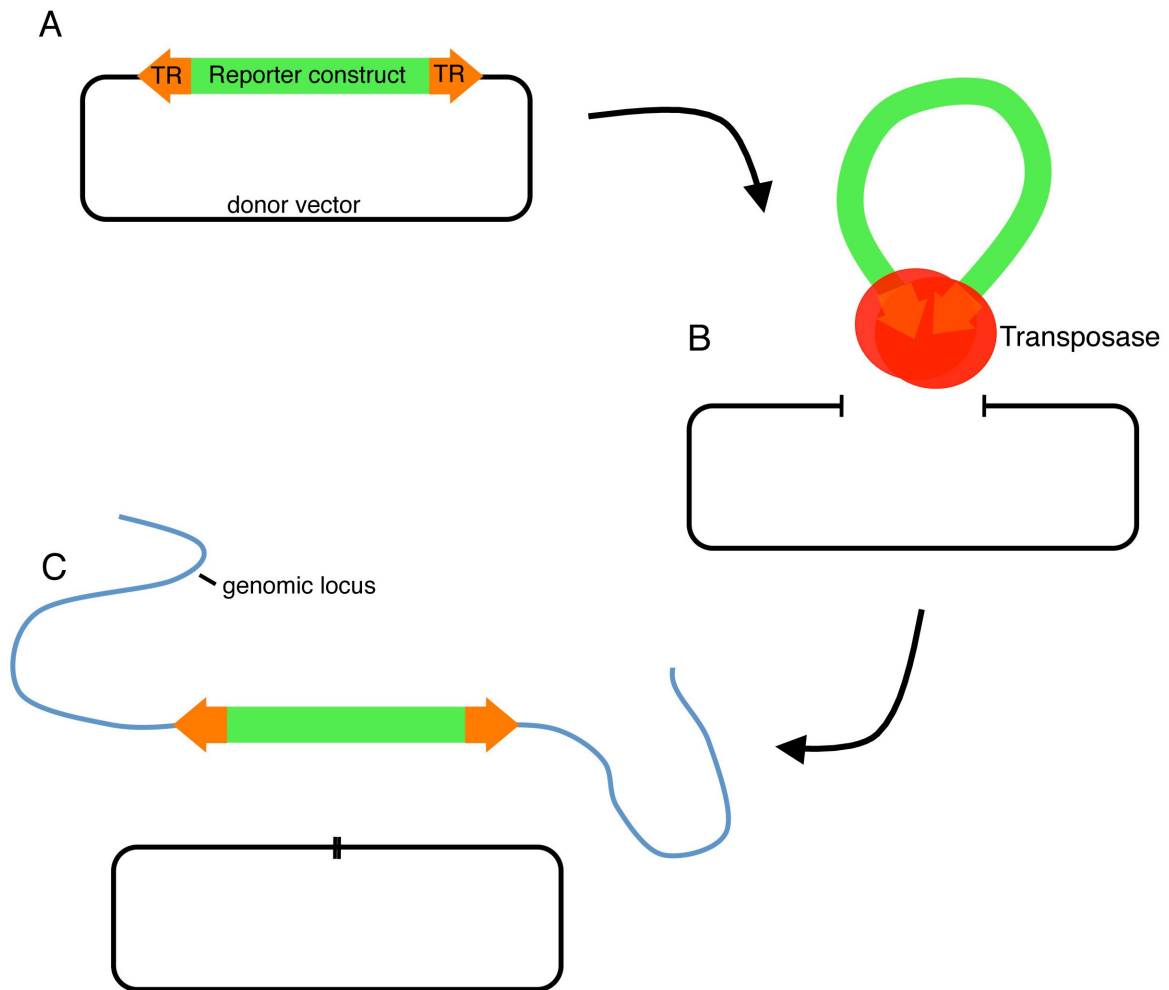


**Figure 4: Mechanism of Transposition**

(A) Fluorescent reporter construct consisting of enhancer sequences of the target fused with the reporter gene, flanked on both sides with terminal repeat (TR) sequences. The transposase enzyme that recognizes TR and cleaves at the end of the TR (B) mediates excision of the reporter construct from its donor vector. The transposase cleaves the DNA double-strand at the target locus and mediates insertion of the reporter construct into the host genome (C).

### 1.7.2. Transient transgenesis and stable transgenic reporter lines

The generation of stable transgenic reporter lines that carry single or more genomic integrations of a reporter construct is ideal for model organisms that can be bred in laboratory culture. Reporter constructs are inherited from one generation to the next and transgenic animals can be analyzed at any time during development. Usually, the offspring ( $F_1$ ) of genetically modified individuals is analyzed to minimize the risk of mosaic and ectopic expression.

Notably, for organisms that cannot breed under laboratory conditions or animals that have long generation times, transient transgenic approaches can be an alternative. In contrast to stable transgenic lines that are analyzed in F<sub>1</sub> and subsequent generations, transient transgenic animals are analyzed directly (F<sub>0</sub>). Hence, a prerequisite for transient transgenic approaches are a high-throughput delivery methods to overcome potentially mosaic and ectopic expression pattern of reporter constructs.

## 1.8. Insulin and insulin-like peptides

A main focus of my work was to investigate the regulation of insulin-like peptides in *Platynereis dumerilii*. Insulin-like peptides belong to a superfamily of peptide hormones that play key roles in the regulation of metabolism, reproduction and aging and are present throughout animal kingdom. Members of the insulin superfamily have been characterized in insects and nematodes, molluscs, tunicates and cephalochordates and even found in unicellular eukaryotes and plants (Nagasawa et. al., 1984, Duret et. al., 1998, Ebberink and Joosse 1985, Galloway et. al., 1988, Chan et. al., 1990, LeRoith 1980, LeRoith 1981). The insulin superfamily is characterized by structural and functional conservation among different species.

### 1.8.1 The insulin family in vertebrates

#### 1.8.1.1. Insulin is produced by the pancreatic $\beta$ -cell

Banting and Best discovered insulin in 1922 in vertebrates and ever since it has become one of the best studied hormones. Insulin is produced and secreted by the pancreas, a multifunctional organ with both endocrine and exocrine function (Figure 5A). Digestive enzymes and pro-enzymes like amylase or trypsinogen are produced and secreted by the pancreatic acini, which form the exocrine part of the pancreas. The endocrine part is formed by the islets of Langerhans that are scattered endocrine cell clusters within the pancreatic tissue. Islets of Langerhans consist of five endocrine cell-types: glucagon-producing  $\alpha$ -cells,

insulin-producing  $\beta$ -cells, somatostatin-expressing  $\delta$ -cells,  $\epsilon$ -cells that express grehlin and pp-cells which produce pancreatic polypeptide.

The vertebrate pancreas develops from endodermal progenitor cells and differentiates into the different exocrine and endocrine cell-types during embryogenesis (Figure 5B). A gene-regulatory program governs the differentiation process and different cell fates are specified by the combination of transcription factors that they express. A key player during pancreas development is *pdx1/ipf1*, a homeobox transcription factor that is expressed in the pancreatic progenitor cells and later becomes restricted to endocrine  $\beta$ - and  $\delta$ -cells (Jonsson et. al., 1994, Miller et. al., 1994). Another important gene for pancreas development is the bHLH transcription factor *ptf1a*. *Ptf1a* together with *pdx1/ipf1* specifies the early pancreatic progenitors. Later in development, *ptf1a* becomes a key gene in the development and maintenance of the exocrine pancreas (Zecchin et. al., 2004).

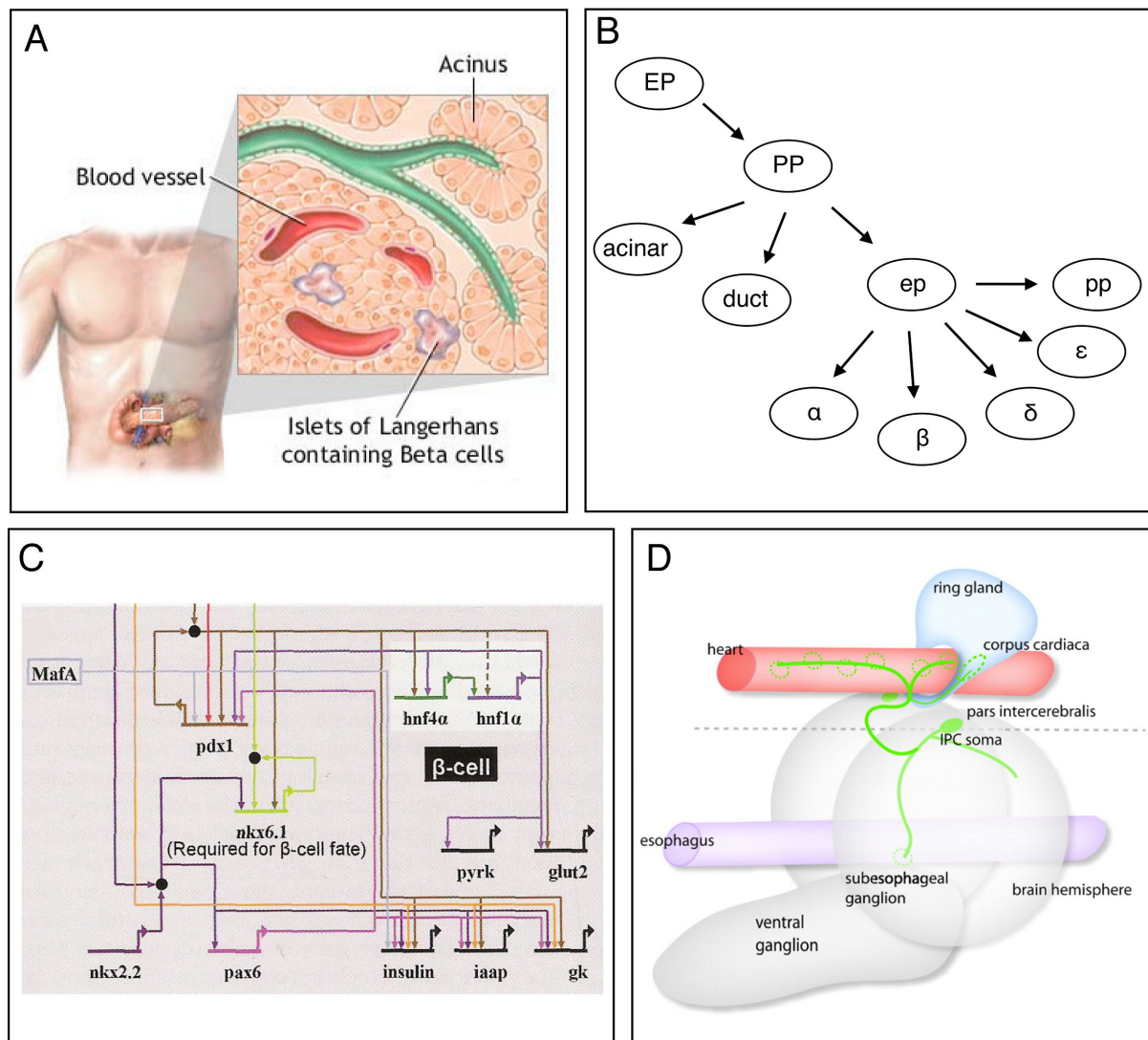


**Figure 5: Development and function of insulinergic cells**

(A) The vertebrate pancreas has exocrine and endocrine functions. Digestive enzymes are produced and secreted by acini, hormones are produced in different cell-types by the islet of Langerhans. (image from: <http://www.healthcentral.com/diabetes/more-images-7214-146.html>) (B) Development of the vertebrate pancreas. The different pancreatic cell-types develop from an endodermal progenitor (EP) via pancreatic progenitor (PP) into endocrine precursor-cells (ep) and acinar- and duct-cells that constitute the exocrine part of the pancreas. ep-cells differentiate into the different endocrine cell-types constituting the islet of Langerhans. Transcriptional networks control pancreas development and cell-type differentiation and each cell-type expresses a specific combination of transcription factors.  $\alpha$ : alpha cell,  $\beta$ : beta cell,  $\delta$ : delta cell,  $\epsilon$ : epsilon cell, pp: pancreatic polypeptide-expressing cell (drawing after: Bonal & Herrera 2008). (C) Gene-regulatory network of the pancreatic beta-cell (taken from EH Davidson, “The regulatory genome”, 2006). (D) Illustration of *Drosophila melanogaster* insulinergic cells. Insulin-like peptides are expressed by insulin-producing cells (IPC) of the pars intercerebralis that project to the dorsal blood vessel and the corpus cardiaca of the ring gland (drawing taken from Rulifson et. al., 2002).

### 1.8.1.2. The role of insulin in vertebrates

Insulin has a major role in carbohydrate and fat metabolism by regulating blood glucose levels. It is secreted in response to high blood glucose levels after food intake and stimulates glucose uptake in liver- and muscle-cells and fat tissue by insulin-receptor signaling. The vertebrate insulin receptor is a transmembrane receptor that belongs to the class of tyrosine kinases (TK). Ligand binding to the receptor leads to conformational changes and autophosphorylation of several tyrosin residues in the TK domain, which induces an intracellular signal cascade.

Expression and secretion of insulin is highly regulated on different levels and impaired insulin production causes the severe metabolic disease diabetes mellitus. Hence, the function of the pancreatic  $\beta$ -cell as well as the transcriptional regulation of insulin expression is being extensively studied.

### 1.8.1.3 Transcriptional regulation of the insulin gene

The transcriptional regulation of the insulin gene is well-characterized and important vertebrate insulin regulators and their binding specificities to the insulin promoter have been determined (Figure 5C). Pdx1/ipf1 has not only a role in endocrine pancreas development but is also a potent activator of insulin expression in mature  $\beta$ -cells (Ohlsson et. al., 1993). *Pax6* is expressed in all endocrine cell-types of the vertebrate pancreas and is known to activate insulin transcription (Sander et. al., 1997). MafA is specifically expressed in  $\beta$ -cells and binds

the RIPE3b element of the insulin enhancer (Olbro et. al., 2002). B2/NeuroD is an activator of insulin that binds the E-box sequence of the insulin promoter (Mutoh et. al., 1997, Naya et. al., 1997). Nkx2.2 is expressed in pancreatic  $\alpha$ -,  $\beta$ - and pp-cells and has been shown to activate insulin transcription in  $\beta$ -cells (Sussel et. al., 1998, Cissell et. al., 2003).

#### 1.8.1.4. Posttranslational modifications of the insulin molecule

Before secreted, the insulin precursor is enzymatically processed in the pancreatic  $\beta$ -cell. The insulin precursor consists of a signal peptide, A, B and C chains, whereas the secreted insulin molecule has A and B chains that are linked by several disulfide bridges. The nascent insulin polypeptide is directed through the plasma membrane of the rough endoplasmatic reticulum by its signal peptide. The process of peptide maturation is catalyzed by endoproteolytic cleavage performed by two protease enzymes, prohormone convertase 1/3 and prohormone convertase 2 in the endoplasmatic reticulum (Neerman-Arbez et. al., 1993, Neerman-Arbez et. al., 1994, Smekens et. al., 1991). The two prohormone convertase enzymes cleave the proinsulin and transform it into its mature form consisting of A and B chains. The mature insulin peptide is stored in vesicles in the  $\beta$ -cell and released by metabolic signaling.

#### 1.8.1.5. Insulin metabolism and the circadian clock are interconnected

Insulin biosynthesis and insulin secretion are highly regulated on different levels. Moreover, insulin production and the circadian clock are interconnected and can influence each other. Energy metabolism and circadian rhythms are interconnected to coordinate physiological processes and behavior with the day-night cycle. In mammals, the suprachiasmatic nucleus (SCN) of the hypothalamus is considered as the master pacemaker that integrates circadian and physiological processes. Different mammalian tissues possess peripheral oscillators and are synchronized by the SCN (Dunlap 1999, Ripperger 2001). In pancreatic  $\beta$ -cells, genes that are involved in insulin production and secretion are circadian regulated and insulin secretion follows a 24h-rhythm (Allaman-Pillet et. al., 2004, Boden et. al., 1996, La Fleur 1999). Recently, a self-sustained circadian clock that coordinates insulin secretion with the sleep-wake cycle was discovered in pancreatic  $\beta$ -cells (Marcheva et. al., 2010). In reverse, insulin expression in response to food intake can alter expression of components of the circadian

clock (Tahara et. al., 2011). These findings are evidence that circadian rhythms and insulin production are highly coordinated and influence each other in mammals. It is hypothesized that the coupling of glucose-metabolism and circadian rhythms is an ancient paradigm (Rutter et. al., 1999).

#### 1.8.1.6. Additional members of the vertebrate insulin family

The vertebrate insulin family comprises not only insulin, but as well igf1, igf2, insulin-like peptides and relaxins. Insulin-like growth factor I (igf1) acts as a growth hormone and is expressed in different tissues, i.e. liver and lung. Igf1 is involved in growth and aging and has anabolic effects (Richardson et. al., 2004, Van Heemst et. al., 2005). Insulin-like factor II (igf2) is transcribed from different promoters in various tissues (Holthuizen et. al., 1993). It is a potent mitogen and is involved in fetal development. In contrast to igf1, igf2 is considered to be more active in early development during fetal growth. Moreover, igf2 has a function in learning and memory (Chen et. al., 2011). The vertebrate relaxins are found in female ovary and male sperm semen and play a role in reproduction (Kelly & Posse 1956, Hall 1957, Essig et. al., 1982). Furthermore, relaxins have a function in wound healing (Beiler et. al., 1960).

#### 1.8.2. Insulin-like peptides in ecdysozoans

As mentioned above, members of the insulin superfamily have a conserved function across species and insulin-like peptides in arthropods and nematodes have similar functions than their vertebrate relatives. A highly variable number of insulin-like peptides exist in different ecdysozoan species. For instance, 42 insulin-like peptide-encoding genes are found in the nematode *C. elegans*, 32 are present in the silk moth *bombyx mori* and 8 insulin-like peptides have been identified in *Drosophila melanogaster*.

### 1.8.2.1. Neurosecretory centers of insulin-like peptide expression in insects

In insects, mainly neurosecretory cells of the pars intercerebralis express insulin-like peptides. The pars intercerebralis (PI) is a neurosecretory center and located in the dorso-medial brain. Insulin-like peptides are expressed by clusters of median-neurosecretory cells (MNC) of the PI and delivered via axonal transport to the corpora cardiacum (CC), a neurohemal release sites. The CC is a neurohemal organ in insects and part of the ring gland, which surrounds the aorta. As crucial regulators of glucose homeostasis, cells of the CC sense levels of blood glucose in *Drosophila melanogaster* (Kim et. al., 2004). The insulin-like peptide producing MNC have analogous function to the vertebrate  $\beta$ -cells together with the CC, they form a glucose sensing and insulin-producing unit similar to the pancreatic islets in vertebrates (Figure 5D).

### 1.8.2.2. The role of insulin-like peptides in insects

Like the vertebrate insulin, *Drosophila melanogaster* insulin-like peptides 2, -3 and -5 are expressed in a food-dependent manner in the MNC and ablation of MNC causes a diabetic phenotype in the flies with adults of smaller size and elevated trehalose levels (Ikeya et. al., 2002, Rulifson et. al., 2002). Beside MNC, insulin-like peptide expression is also found in other tissues in *Drosophila melanogaster*. Similar to vertebrate relaxins, insulin-like peptide 7 is expressed in neurons that innervate the female reproductive tract (Yang et. al., 2008, Miguel-Aliaga et. al., 2008). Insulin-like peptide 4 is present in the embryonic midgut and mesoderm (Brogiolo et. al., 2001) and insulin-like peptide 6 is expressed in the larval fat body and resembling the vertebrate igf (Okamoto et. al., 2009). *Drosophila melanogaster* possesses a single insulin-like peptide receptor that is widely expressed in different tissues with high levels in the nervous system and ovaries (Garofalo et. al., 1988). The insulin-receptor signaling pathway is highly conserved between vertebrates and *Drosophila melanogaster* (Yamaguchi et. al., 1997).

### 1.8.2.3. Transcriptional regulation of insulin-like peptides in insects

Expression of the different *Drosophila melanogaster* insulin-like peptides is differentially regulated. The *Drosophila melanogaster* insulin-like peptides have their individual expression pattern in different tissues and different developmental stages (Brogiolo et. al., 2001). The transcriptional regulation of *Drosophila melanogaster* insulin-like peptides remains largely unknown. However, it has been shown that the transcription factor *pax6/eyeless* is involved in MNC differentiation and regulates insulin-like peptide 3 expression. In contrast, expression of insulin-like peptides 2 and -5 is unaffected in *Drosophila melanogaster pax6/eyeless* mutants, which implies that these genes have different regulators of expression (Clements et. al., 2008).

### 1.8.3. Insulin-like peptides in lophotrochozoans

#### 1.8.3.1. Expression and secretion of insulin-like peptides in molluscs

Insulin-like peptides have been described in the nervous system and gut of different mollusc species (Ebberink and Joosse 1985, Smit 1988, Boquist et. al., 1971, Davidson 1971, Fritsch 1976).

In the pond snail *Lymnaea stagnalis*, five insulin-like peptides (I, II, III, V, VII) and two pseudogenes (IV, VI) are present. The center of insulin-like peptide expression in *Lymnaea stagnalis* are the light green cells (LGC), which are neuroendocrine cells located in the cerebral ganglia. Moreover, insulin-like peptide VII is expressed in the buccal ganglia which are neurons involved in feeding behavior (Smit et. al., 1996).

In *Lymnaea stagnalis*, insulin-like peptides that are produced by the LGCs are delivered via axonal transport to neurohemal axon terminals and released into the haemolymph (van Heumen et. al., 1990, van Heumen et. al., 1991).

*Lymnaea stagnalis* insulin-like peptides have crucial roles in regulating carbohydrate metabolism, growth and reproduction, similar to the function of the vertebrate insulin, igfs and relaxins (Smit 1988, Meester et. al., 1992, van Minnen et. al., 1989, Geraerts et. al., 1992, Geraerts et. al., 1976). Moreover, insulin-like peptides might play a role in the formation of long-term memory of *Lymnaea stagnalis* (Ito et. al., 2012, Azami et. al., 2006).



An insulin-like peptide receptor gene has been identified in *Lymnaea* but its function remains to be elucidated (Roovers et. al., 1995).

It is unclear how insulin-like peptide expression is regulated in *Lymnaea stagnalis* or other mollusc species, although studies on insulin-like peptide regulation in lophotrochozoans could provide new insights into the evolution of the gene-regulatory network present in  $\beta$ -cells and the origin of the vertebrate pancreas.

### 1.8.3.2. Neurosecretory centers of annelids

In annelids, groups of neurosecretory cells are located in different regions of the adult brain. Moreover, annelid species possess an infracerebral gland which is an epithelium covering the medio-ventral surface of the brain adjacent to the dorsal blood vessel. A function of the infracerebral gland as neurohemal release site of neuropeptides has been proposed (Dhainaut-Courtois 1986, Golding 1967, Golding 1977, Bashkin 1976). In *Platynereis dumerilii*, the neurosecretory brain centers are groups of cells in the anterior-dorsal and posterior-ventral brain and the pars intercerebralis/pars lateralis. Additionally, the posterior lobes may also have neurosecretory potential (Müller 1973). The infracerebral gland of *Platynereis dumerilii* is a leaf-shaped epithelium on the medio-ventral side of the brain capsule adjacent to the dorsal blood vessel and its efferent branches. An endocrine function for the *Platynereis* infracerebral gland was suggested by Hofmann (Hofmann 1976).

At the beginning of my studies, gene-expression patterns in the neurosecretory centers and the infracerebral gland in *Platynereis dumerilii* adult brains have not been investigated since in-situ staining protocols were not available. Therefore, a goal of my project was to develop in-situ staining methods to study gene-expression in the adult brain.

### 1.8.3.3. Insulin-like peptides in annelids

Insulin-like peptides are present in annelid species (LeRoith 1981, Hrzenjak et. al., 1993), but little is known about their number, expression and function in annelids. At the beginning of this study, insulin-like peptides have not been described in *Platynereis dumerilii* and a major goal of my project was to investigate insulin-like peptides, their expression and their regulation in this species.

## 1.9. Non-cephalic photoreceptor cells

Research on photoreceptors has mostly focused on cephalic photoreceptor cells and eyes. However, eyes and other photoreceptive cells are not only present in the head but also in the periphery of cephalized animals. For instance, the chordate amphioxus possesses photoreceptors arranged along the ventral neural tube that are referred to as Hesse organs (Hesse, 1898). Some polychaete species have been shown to possess segmental ocelli, too, like the opheliid worms of the genus *Polyophthalmus* (Dujardin, 1839, Purschke, 1995), or the Sabellid polychaete *Branchiomma* (Dragesco-Kernéis, 1980). In the polychaete *Platynereis dumerilii*, peripheral photoreceptors have not yet been reported.

Extensive research has been done on the molecular characterization of cephalic photoreceptors, in contrast to non-cephalic photoreceptors that have been poorly characterized on a molecular level. The main light sensors of photoreceptor cells in bilaterian animals are Opsin-type G-protein-coupled receptors. Among these, rhabdomeric opsins (r-opsins) are an ancient group of opsins, particularly widespread in invertebrates and typically expressed in larval photoreceptor cells and/or cephalic eyes.

A key regulator for the development of cephalic eyes is the homeodomain transcription factor *pax6*, which is commonly associated with cephalic photoreceptors across different species. However, there are examples for *pax6*-independent photoreceptors. The Hesse organs of amphioxus for instance, do not express *pax6* (Glargdon et. al., 1998). Instead, amphioxus Hesse organs express *dachshund*, a gene that is known to be a regulator of eye and leg development in *Drosophila*. (Candini et. al., 2003). In *Platynereis dumerilii*, adult eyes develop independently of *pax6* while larval eyes do express *pax6* (Arendt et. al., 2002). It is unclear if *pax6*-independent development of photoreceptors like amphioxus Hesse organs or *Platynereis dumerilii* adult eyes underlie an ancient regulatory mechanism that was already present in the last common ancestor of both species or if it has been independently evolved.

## 1.10. Aims of the thesis

The aim of this thesis was fourfold:

The main focus of my PhD thesis was (1) the comparative analysis of insulinergic cells to study the regulation of insulin-like peptides in *Platynereis dumerilii* larvae and in adult worms. For this, I worked on the establishment of tools to study gene expression in the adult

animal. As part of my project, I explored the use of transposable elements to (2) establish protocols for transient transgenesis and stable transgenic reporter lines in *Platynereis dumerilii* to study gene-expression in adult worms in vivo. To analyze and compare gene-expression patterns in adult worms in-situ, a goal of this study was to (3) develop and optimize in-situ Hybridization protocols and two-color staining protocols for postlarval stages. Moreover, in-situ Hybridization protocols developed in this study were applied to (4) analyze the molecular specification of newly discovered non-cephalic photoreceptors in *Platynereis dumerilii* to investigate their evolution and function.



## 2. Results

### 2.1. Molecular specification of insulineric cells in *Platynereis dumerilii*

#### 2.1.1. Identification and characterization of insulineric cell-types in *Platynereis*

At the beginning of my project, neither insulin-like peptides, nor cells that produce insulin-like peptides were investigated in *Platynereis*. Thus, as part of my study, I determined the number of insulin-like peptides and explored their expression patterns to identify insulineric cells in *Platynereis* larval and postlarval stages.

##### 2.1.1.1. Identification and phylogenetic analyses of five insulin-like peptides in *Platynereis dumerilii*

Firstly, I wanted to explore, how many different members of the insulin superfamily are present in the *Platynereis* transcriptome. Therefore, I compiled a set of vertebrate and invertebrate insulin-family related peptides and performed searches by similarity in different *Platynereis* transcriptome libraries. Four different candidate sequences were extracted from the transcriptome resources and confirmed as members of the insulin-family by reciprocal BLAST and by conserved protein domain search. F. Raible and A. Polo identified an additional *Platynereis* insulin-like peptide candidate. The complete coding sequences of *insulin-like peptide 3 (ilp3)*, *insulin-like peptide 4 (ilp4)* and *insulin-like peptide 5 (ilp5)* were extracted from the databases. In contrast, transcript sequences of *insulin-like peptide 1 (ilp1)* and *insulin-like peptide 2 (ilp2)* were lacking the 5'- and 3'-ends of their coding sequences and I performed RACE-PCR to obtain the full-length coding sequences of *Platynereis ilp1* and *ilp2*. Overall, there is little sequence conservation between different insulin-family members across different species. The most characteristic feature of insulin-family members is a motif consisting of six cystein residues that is conserved across species and among the different insulin family members. Amino acid sequence alignments with human and murine

*insulin*, *relaxin*, *igf1* and *igf2* and *Lymnaea stagnalis* insulin-like peptides revealed that these six highly conserved cysteine residues are present in the *Platynereis* insulin-like peptide candidates (Figure 6). Unlike vertebrate insulin and mollusc insulin-like peptides, *Platynereis* insulin-like peptides have extended C-termini and resemble in this aspect the vertebrate *igf1* and *igf2*. Hence, I performed phylogenetic analyses to examine whether *Platynereis* insulin-like peptides are more similar to *igf's*, *relaxin* or *insulin*. Phylogenetic analysis revealed that the different *Platynereis* insulin-like peptides group together with *Lymnaea stagnalis* insulin-like peptides and insect insulin-like peptides whereas the vertebrate insulin-family members form a distinct group (Figure 7A). Phylogenetic comparison of *Platynereis* insulin-like peptides with human insulin family members show that no distinction can be made if *Platynereis* insulin-like peptides are closer related to the human *igf's*, *relaxin* or *insulin* (Figure 7B). Among *Platynereis* insulin-like peptides, *ilp3* and *ilp4* shared the highest sequence similarities (see also section 2.1.1.2.) and group together with *ilp1*. *Platynereis ilp5* is closer related to the group of *ilp1/3/4* than to *ilp2*. *Ilp2* is the most distant one within the group of *Platynereis* insulin-like peptides. To investigate if insulin-like peptides from another lophotrochozoan species split into peptides that are more similar to the different vertebrate insulin-family members, I performed phylogenetic analyses to compare human *igf's*, *insulin* and *relaxin* to the five *Lymnaea stagnalis* insulin-like peptides. Similar to *Platynereis*, *Lymnaea stagnalis* insulin-like peptides are not allocated to the different human insulin family members (Figure 7C). These findings are in line with the current view that in invertebrates, insulin-like peptides are not discriminated into *insulin*, *igf* or *relaxin*.

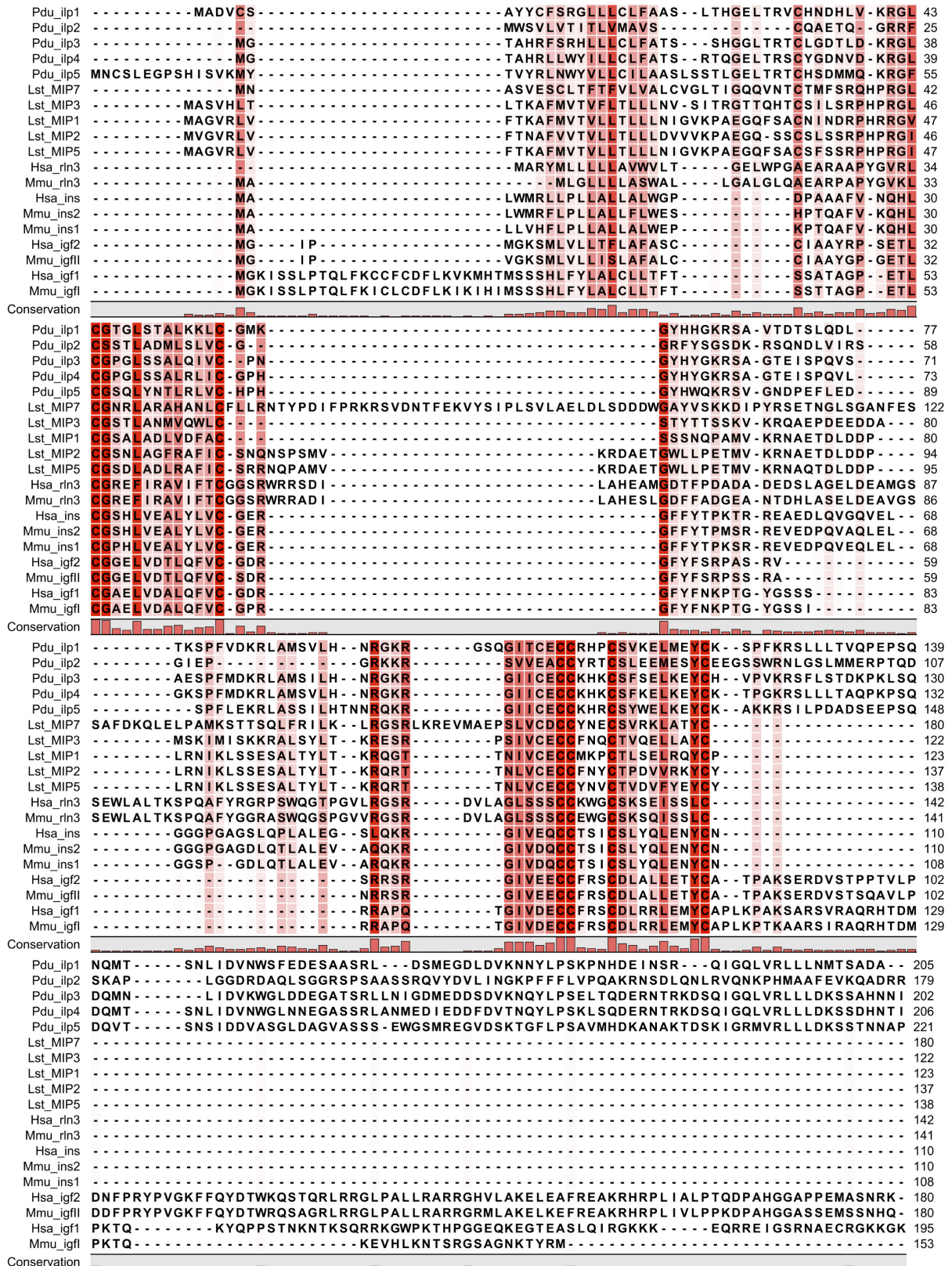


**Figure 6: Alignment of insulin-related peptides**

Amino acid sequence alignment of insulin-related peptides from *Platynereis dumerilii* (*Pdu*): *ilp1*, *ilp2*, *ilp3*, *ilp4*, *ilp5*; *Lymnaea stagnalis* (*Lst*): *MIP1*, *MIP2*, *MIP3*, *MIP5*, *MIP7*; *Mus musculus* (*Mmu*): *ins1*, *ins2*, *igf1*, *igf2*, *rln3* (=relaxin3); *Homo sapiens* (*Hsa*): *ins*, *igf1*, *igf2*, *rln3*. Sequences conservation is indicated as red bars below the alignment. Red color gradient indicates conservation of amino acids.

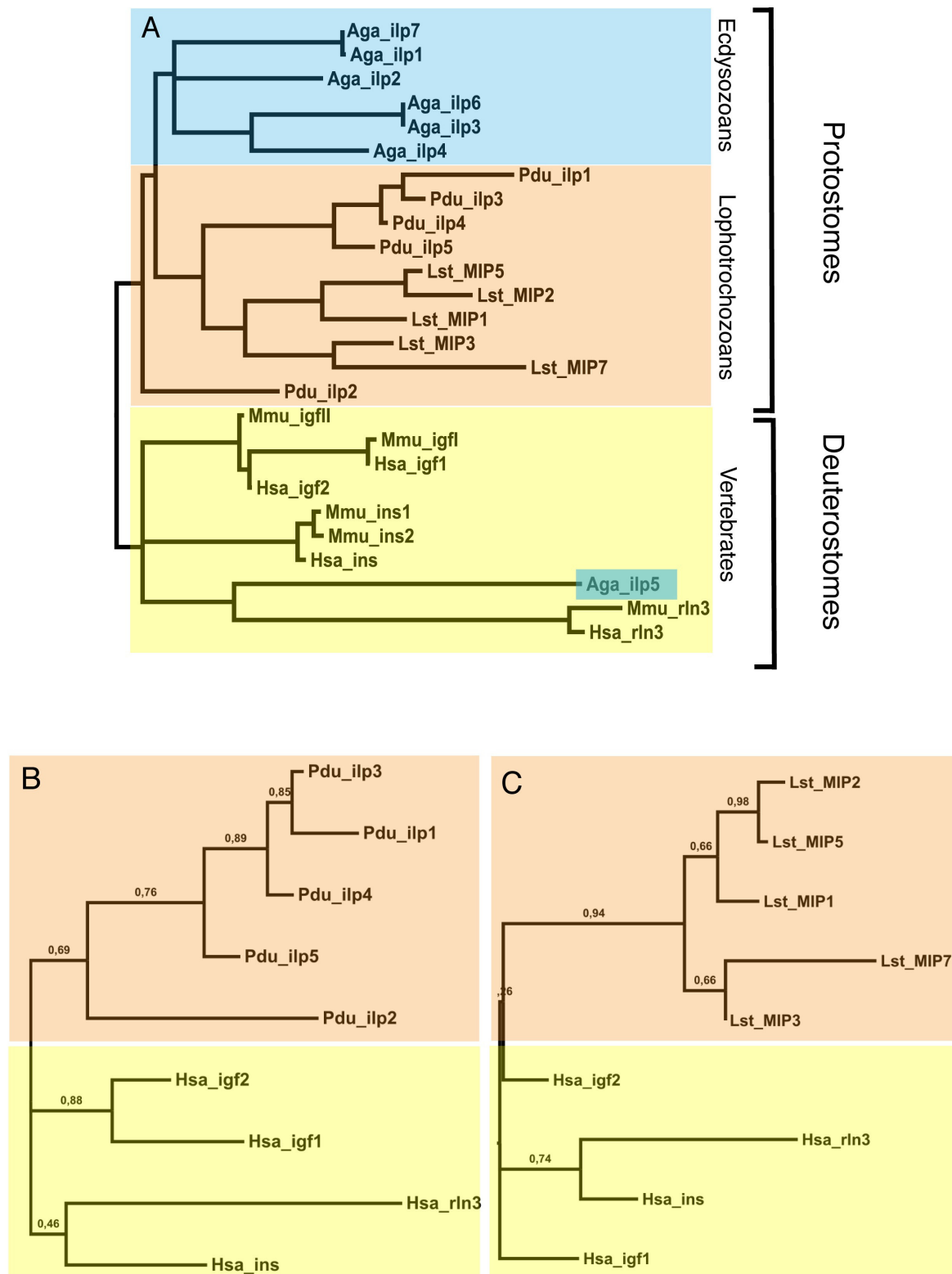


**Figure 7: Phylogeny of insulin-related peptides**

(A) Maximum-likelihood phylogenetic tree constructed with amino acid sequences of insulin-related peptides from *Mus musculus* (Mmu), *Homo sapiens* (Hsa), *Lymnaea stagnalis* (Lst), *Platynereis dumerilii* (Pdu) and *Anopheles gambiaensis* (Aga). Insulin-related peptides from protostomes form distinct groups within species. Pdu ilps and Lst MIPs and constitute the lophotrochozoan insulin-related peptides (orange) and Aga ilps contribute the ecdysozoan branch of insulin-related peptides



(blue). *Mmu* and *Hsa* insulin-family members form the deuterostome branch of insulin-related peptides (yellow). An exception is *Aga ilp5*, which has strong sequence similarities with vertebrate relaxin. (B) Phylogenetic comparison of *Pdu* and *Hsa* insulin-related peptides. (C) Phylogenetic comparison of *Lst* and *Hsa* insulin-related peptides.

### 2.1.1.2. Genomic loci of *Platynereis dumerilii* insulin-like peptides

As described in the previous section, I identified five different *Platynereis* insulin-like peptide transcripts. Next, I wanted to determine their gene-structures and their genomic loci. To get the genomic sequences of the different insulin-like peptides, I screened a *Platynereis* BAC-library and identified BAC-clones containing the genomic loci of *ilp1* and *ilp2*. For each of the two genes, one BAC-clone was extracted and sequenced. Annotations of the BAC-clones revealed that in addition to *ilp1* and *ilp2*, the genomic loci of *ilp3* and *ilp4* are also present on one of the sequenced BAC-clones. *Ilp1*, *ilp3* and *ilp4* are located in a genomic cluster of about 21kbp total length on one BAC-clone (Figure 8A). *Ilp1* has four exons of 33bp, 198bp, 432bp and 73bp that are separated by three introns of 562bp, 656bp and 11bp in length. *Ilp1* is separated by around 10kb of non-coding genomic DNA from the next gene, *ilp4*. The sequences of *ilp3* and *ilp4* are highly similar with only a few exchanges in this amino acid sequences. *Ilp3* has three exons of 215bp, 184bp and 422bp in length and two introns of 1850bp and 500bp. The coding sequence of *ilp4* is distributed on two exons of 193bp and 422bp and separated by a 281bp intron. *Ilp3* and *ilp4* are located in a head-to-head orientation and separated by about 15kbp of non-coding genomic DNA. The amino acid sequences of their transcripts are highly similar. Moreover, *ilp3* and *ilp4* have conserved exon-intron boundaries at amino acid positions 62 and 64, respectively.

*Platynereis ilp2* is located on the second BAC that was sequenced (Figure 8B). The genomic locus stretches across 30kb of genomic DNA. *Ilp2* has four exons of 24bp, 154bp, 128bp and 332bp in size that are separated by intron of 5.5kbp, 14.4kbp and 9.5kbp in length.

The *Platynereis ilp5* transcript sequence could not be mapped on a BAC. However, the transcript sequence of *ilp5* matches with a 2kbp fragment from a genomic sequence resource (Figure 8C). Mapping of the two sequences revealed that the *ilp5* coding sequence is distributed on two exons of 201pb and 425bp in length and separated by a 300bp intron. UTR-regions could not be determined for *ilp5*.

As mentioned above, analyses of exon-intron boundaries of *ilp3* and *ilp4* revealed conserved positions of introns in their amino acid sequences. To investigate if a conserved exon-intron structure is a general feature of *Platynereis* insulin-like peptides, I determined the positions of

introns in the amino acid sequences of *ilp1*, *ilp2* and *ilp5* and compared them among all *Platynereis* insulin-like peptides. I found that *ilp1*, *ilp3*, *ilp4* and *ilp5* all have a conserved exon-intron boundary after the characteristic motif GYH\*\*KRS\* (Figure 8D). Similarly, *ilp2* has an exon-intron boundary after the motif \*KRS. To investigate if this exon-intron boundary is conserved not only in worms but also in insulin-family members of mammals, I compared exon-intron boundaries of insulin-related peptides of mouse, human and *Platynereis*. The exon-intron boundaries among mammalian *insulin*, *igf1*, *igf2* and *relaxin3* are highly conserved, but exon-intron boundaries between the subfamily members are not highly conserved. Based on the comparison of exon-intron boundaries, *Platynereis* insulin-like peptides are not distinguishable into peptides that are closer related to mammalian *insulin*, *igf* or *relaxin*. These findings support the data from phylogenetic analyses of *Platynereis* insulin-like peptides (section 2.1.1.1.) and are in line with the current view that in invertebrates, insulin-like peptides are not discriminated into *insulin*, *igf* or *relaxin*.

Four of the *Platynereis* insulin-like peptides were mapped on two BAC-clones and their genomic loci were determined. *Ilp1*, *ilp3* and *ilp4* are located in a genomic cluster and two genes of this cluster - *ilp3* and *ilp4* - are highly similar in terms of amino acid sequences. Moreover, *Platynereis* insulin-like peptides have a highly conserved exon-intron boundary.

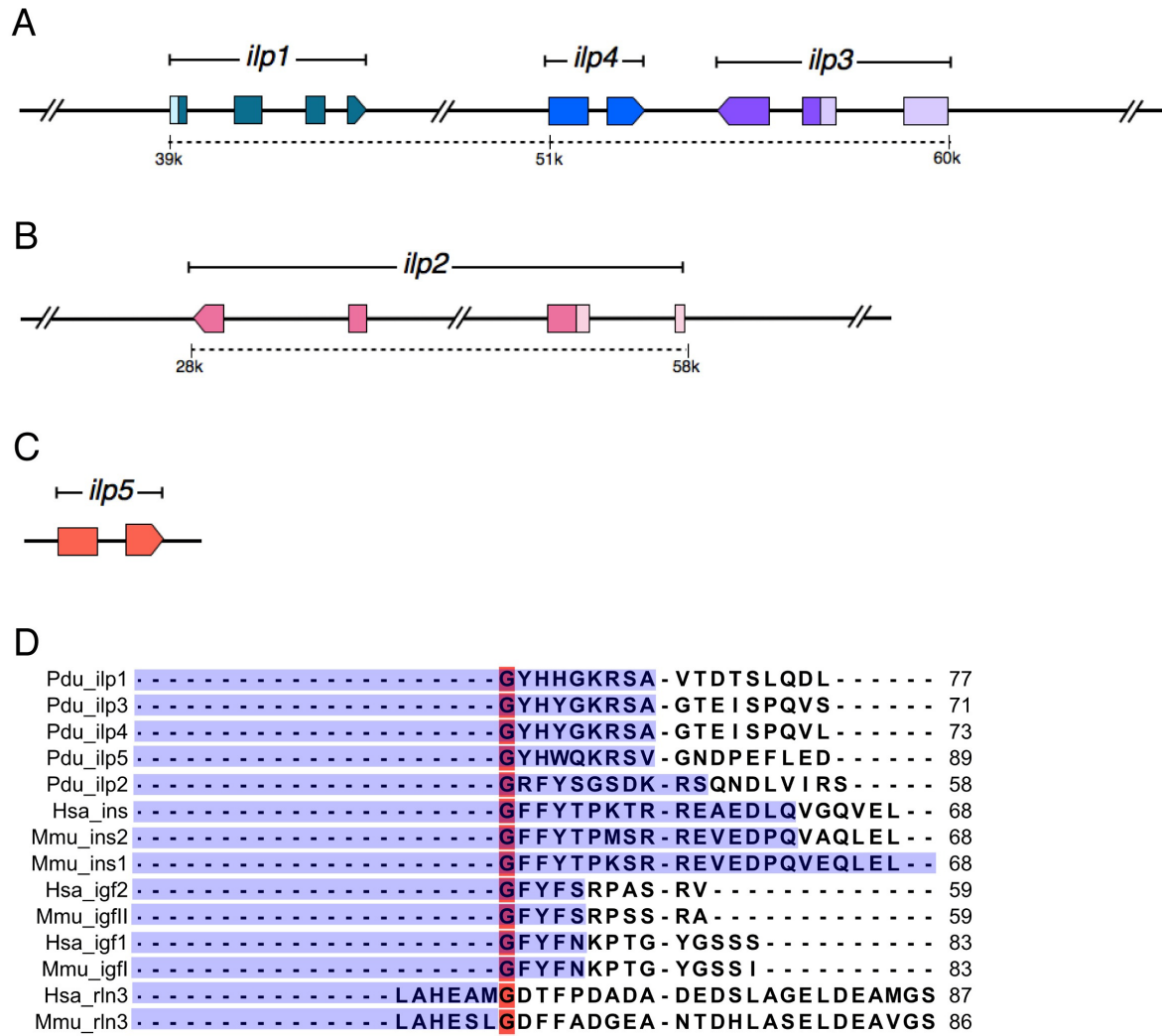


**Figure 8: Genomic loci of insulin-like peptides**

(A) Genomic cluster of *Platynereis* *ilp1* (turquoise), *ilp3* (blue) and *ilp4* (purple) within a 20kbp BAC locus. (B) *Platynereis* *ilp2* (pink) covers a locus of 30kbp in length on a sequenced BAC. (C) Partial locus of *Platynereis* *ilp5* (orange) was extracted from genomic resources database. (D) Amino acid sequence alignments of *Platynereis* and vertebrate insulin-related peptides reveal conserved exon-structure among *Platynereis* insulin-like peptides and among vertebrate *insulin*, *igf1*, *igf2* and *relaxin3*. Foregoing exon in blue, end of blue bar indicates exon boundary.

### 2.1.1.3. Detection of insulin-like peptide transcripts in larval and nectochaete brains

Next, I wanted to characterize the expression patterns of the different insulin-like peptides during larval development by in-situ Hybridization. In trochophore larvae, *ilp2*, *ilp3* and *ilp5* are expressed but no expression of *ilp1* and *ilp4* is detectable. *Ilp2* is expressed in 1-2 cells located in the center of the larval brain directly below the apical tuft in the region of the apical

organ (Figure 9A-C). Expression of *ilp3* is detectable in three cells of the medial larval brain that are located 5-6 cell diameters dorsal to the apical tuft (Figure 9D-F). The larval expression pattern of *ilp5* is more complex: *ilp5* is detected 2-4 cells that are located in the center of the larval brain, directly below the apical tuft. Moreover, *ilp5* is expressed in a bilateral pair of cells that are located 3-6 cell diameters ventrolateral of the apical tuft and weak *ilp5* expression is detectable in two cells that are located 3-5 cell diameters dorso-lateral the apical tuft. *Ilp5* expression is also found in two cells that are located dorso-medial, about 6 cell-diameters dorsal to the apical tuft (Figure 9G-K). *Ilp4* expression is detectable in 5-days-old late nectochaete stages in a pair of bilateral cells located in the dorsolateral brain Figure 10A,B). A similar expression pattern is observed for *ilp2* at the same developmental stage but the cells expressing *ilp2* are not the same as the *ilp4* expressing cells (Figure 10C,D). In 5-days-old individuals, *ilp3* is expressed in two cells in the dorso-medial part of the brain (Figure 10E,F). Anterior-ventral of the first pair of *ilp3* expressing cells; a bilateral pair of cells located lateral to the center of the brain is detected by in-situ Hybridization. *Platynereis ilp5* is expressed in late nectochaete brain in three clusters that consist of 2-4 cells each Figure 10G,H). One cluster is located in the anterior part of the central brain. Two bilateral clusters of cells are detected posterior-lateral of the apical cluster of *ilp5* expressing cells. Altogether, the three clusters of cells resemble the basic points of an equal-sided triangle.

In contrast to the other *Platynereis* ilps, *ilp1* expression is not detectable in larval and nectochaete stages by in-situ Hybridization.

*Platynereis* insulin-like peptides are expressed in different subsets of cells in the larval and nectochaete brain. *Ilp2*, *ilp3* and *ilp5* transcripts are present in 48hpf trochophore larvae and *ilp4* is detected in 5-days-old nectochaetes. No insulin-like peptide expression is found outside the brain.

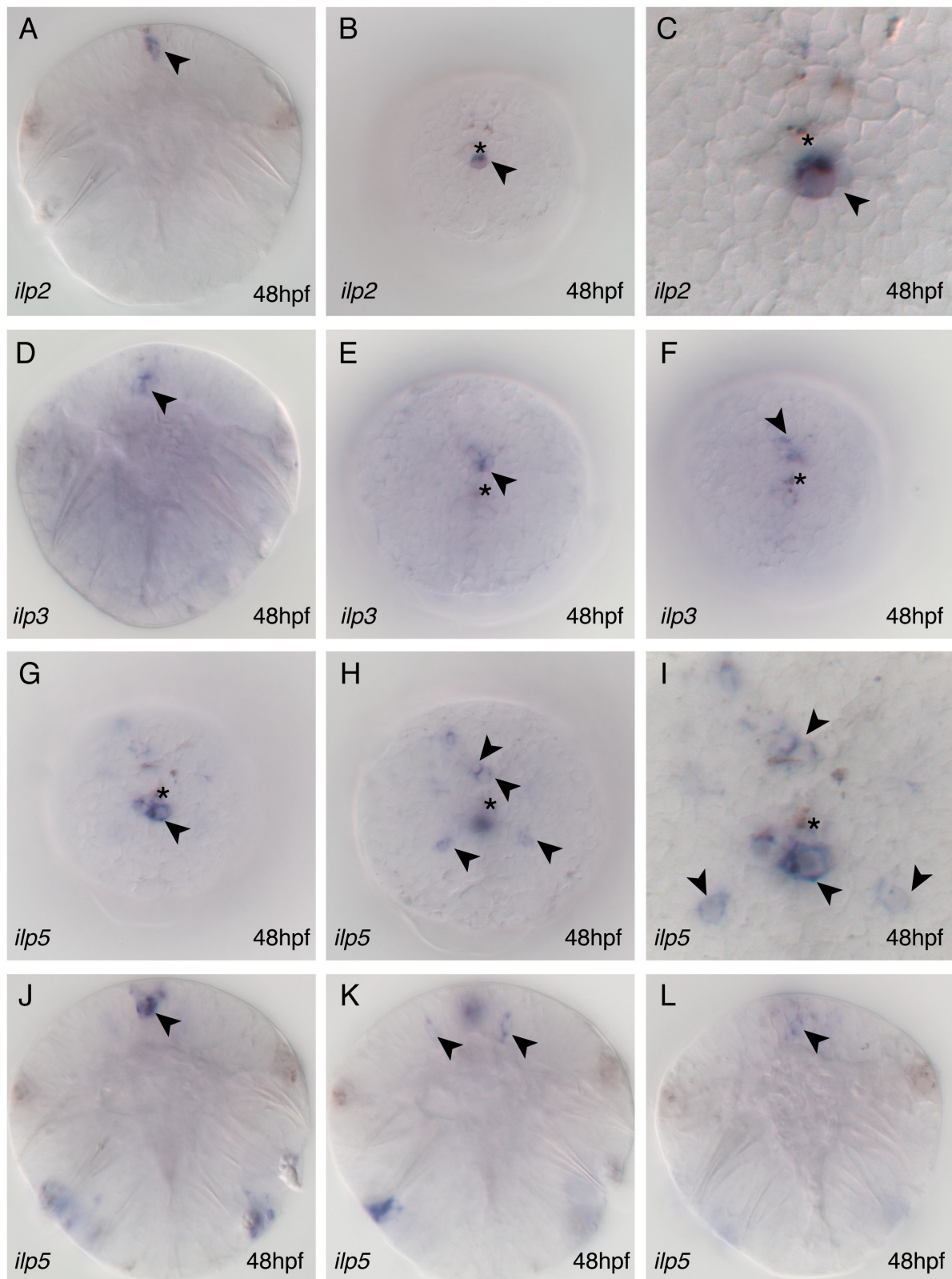


### Figure 9: Larval expression of insulin-like peptides

In-situ Hybridization of *Platynereis* insulin-like peptides in 48hpf trochophore larvae. (A-C) *Ilp2* expression in a single cell of the central larval brain. (D-F) *Ilp3* is expressed in a cluster of cells of the medial-dorsal brain. *Ilp5* is expressed in the central brain (G, J), a bilateral pair of cells ventro-lateral to the apical tuft (H, I, K) and a cluster of cells of the medio-dorsal brain (H, I, L).

Black arrowheads indicate expression; black asterisk: apical tuft; A, D, G, J, K, L: dorsal views (anterior to the top); B, C, E, F, I, H: apical views (dorsal to the top).



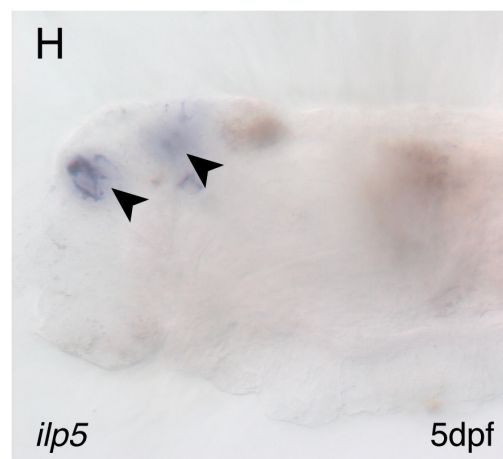
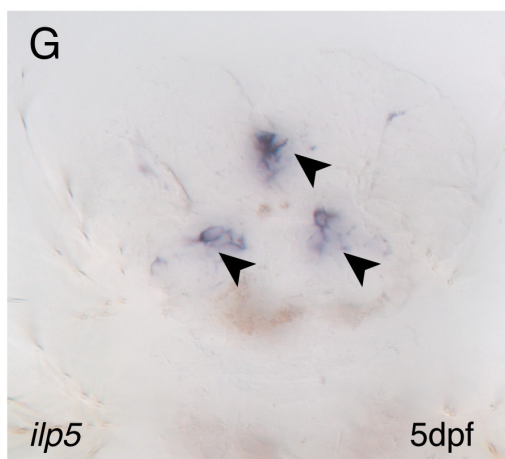
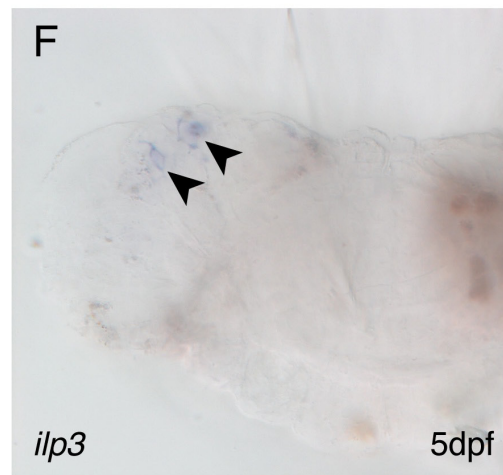
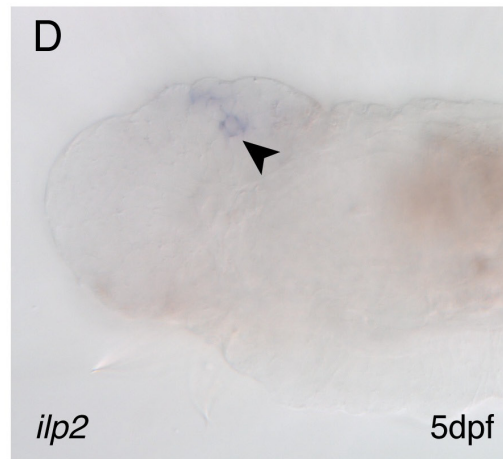
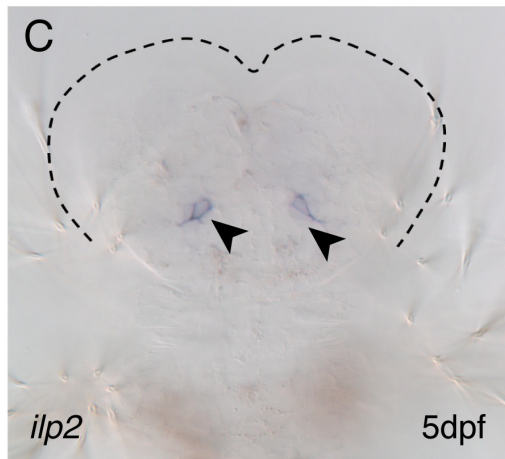
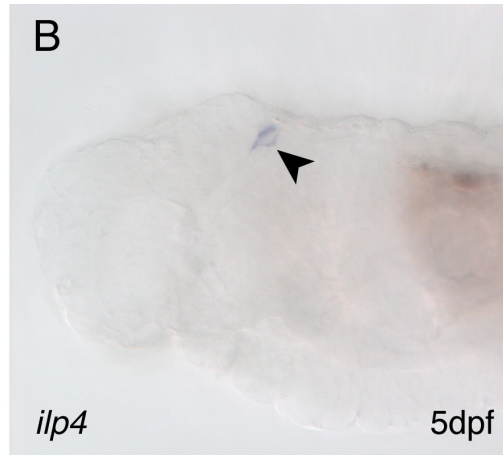
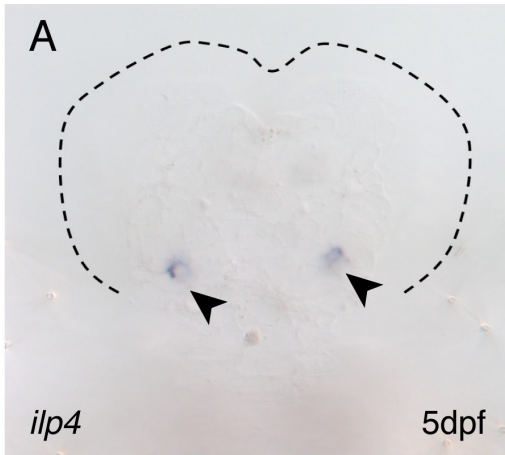


**Figure 10: Expression of insulin-like peptides in nectochaete larvae**

In-situ Hybridization of *Platynereis* insulin-like peptides in 5-days-old nectochaete larvae. (A, B) *Ilp4* is expressed in a bilateral pair of cells of the dorsal brain. (C, D) *Ilp2* is found in two cells of the dorso-lateral part of the brain. (E, F) Detection of *ilp3* mRNA in a bilateral pair of cells and a cluster of median cells of the dorsal brain. (G,H) *Ilp5* is expressed in a bilateral cluster of cells and a median cluster of cells in the dorsal brain.

Black arrowheads indicate expression; dotted black line: outline of the head; A, C, E, G: dorsal views (anterior to the top); B, D, F, H: lateral views (anterior to the left).

#### 2.1.1.4. Brain-specific expression of insulin-like peptides in atokous worms

In addition to insulin-like peptide expression in larval and nectochaete stages, I studied insulin-like peptide expression in atokous worms to investigate if there is insulin-like peptide expression outside the brain and if there is a center of insulin-like peptide expression in adult worms. For this purpose, I modified a whole-mount in-situ Hybridization protocol for *Platynereis* larvae to that effect that it was applicable to detect gene expression in atokous worms. By analyzing the expression of the five *Platynereis* insulin-like peptides, I found that the center of insulin-like peptide expression is located in the posterior lobes of the adult brain. The posterior lobes are paired structures of the dorsal part of the adult brain that are located between the nuchal organs and behind the posterior pair of adult eyes. No expression of insulin-like peptides was observed outside the brain. Figure 11 shows an overview of insulin-like peptide expression in atokous worms. The five *Platynereis* insulin-like peptides are expressed in distinct subsets of cells of the posterior brain lobes with the exception of *ilp2*, which is expressed most prominently in two cells adjacent to the posterior lobes (Figure 11B). Moreover, *ilp2* is expressed in a cell located in the center of each of the posterior lobes and in 1-2 cells located in close proximity to each of the anterior adult eyes. *Ilp1*, *ilp3* and *ilp4* have individual expression patterns in the posterior and medial part of the posterior lobes (Figure 11A,C,D). Furthermore, *ilp4* is expressed in cells that are located in the center of the posterior lobes (Figure 11D). *Ilp5* expressing cells are detected along the posterior margin of the posterior lobes of the adult brain (Figure 11E). The five *Platynereis* insulin-like peptides have individual expression patterns in different subsets of cells of the adult brain.

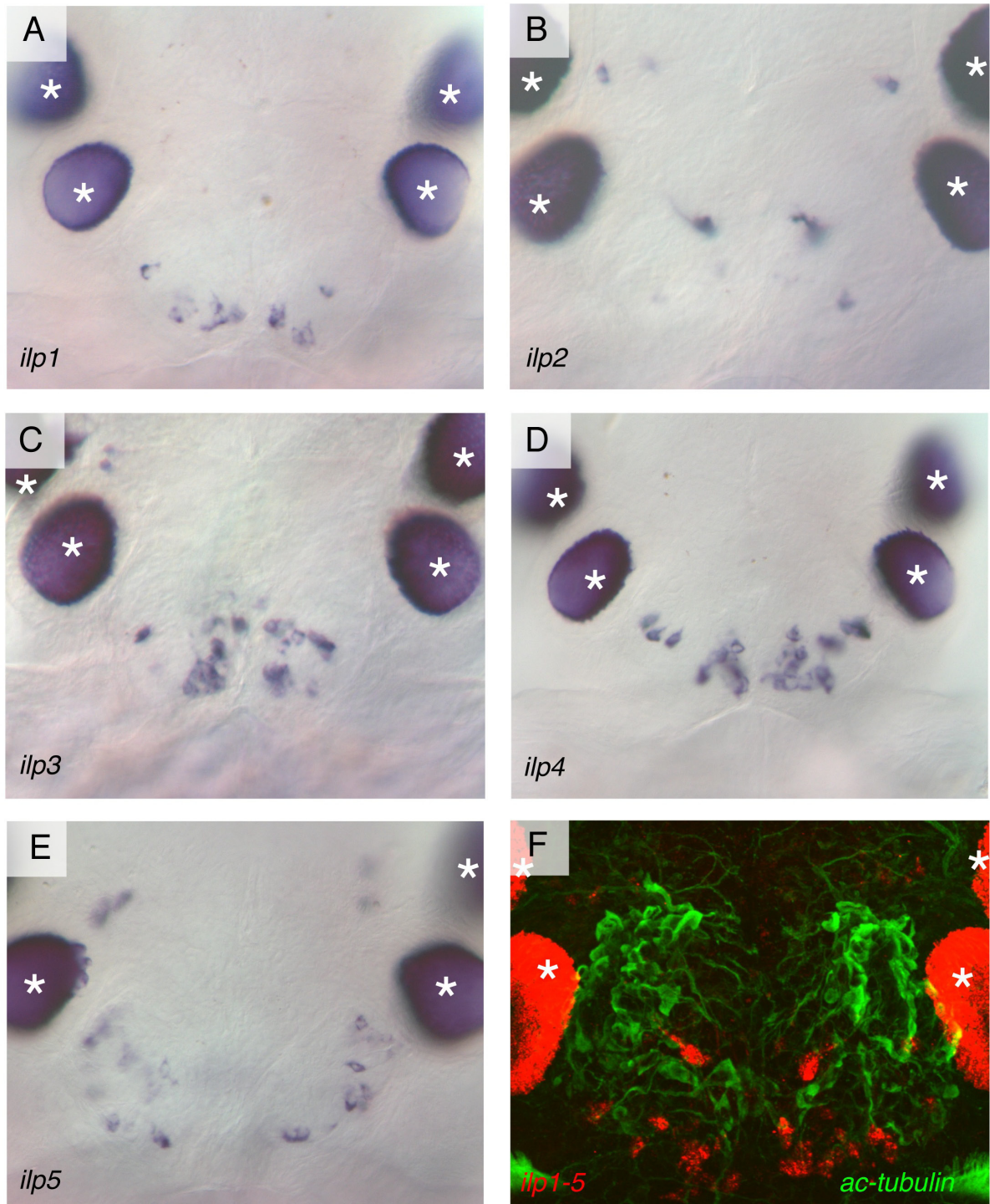


**Figure 11: Expression of insulin-like peptides in atokous worms**

In-situ Hybridization of *Platynereis* insulin-like peptides in the brains of atokous worms. (A-E) Expression patterns of *ilp1*- *ilp5* in clusters of cells in the dorsal part of the brain. (F) Z-projection of confocal sections through the adult brain. In-situ Hybridization demarcates insulinergic cells (red) located within a bilateral cluster of neurons. Axonal scaffold is visualized with FITC-coupled antibody against acetylated-tubulin (green).

Dorsal views (anterior to the top); white asterisk: adult eye.



#### 2.1.1.5. Insulin-like peptide expressing cells are located within clusters of axons that are detected by anti-acetylated tubulin antibody

As shown in the previous section, *Platynereis* insulin-like peptides are expressed in the posterior lobes of the adult brain. Next, I wanted to correlate the expression of insulin-like peptides with the axonal scaffold in the brain. For this reason, I performed in-situ Hybridization with pooled dig-labeled riboprobes for the different *Platynereis* insulin-like peptides and counterstained the axonal scaffold with FITC-coupled anti-acetylated tubulin antibody. I found that the posterior lobes are highlighted as paired structures by anti-acetylated tubulin staining and that insulin-like peptide expressing cells are located in these clusters of axons (Figure 11F). This implies that insulin-like peptides might be produced by neurons in *Platynereis*. To investigate this further, I wanted to characterize the neurosecretory centers of atokous worms by expression analysis of marker genes (section 2.1.2).

#### 2.1.2. Characterization of neurosecretory centers of atokous worms

In insects and molluscs, mainly neurosecretory cells produce insulin-like peptides and I wanted to explore whether this is also the case in *Platynereis dumerilii*. Hence, an intermediate goal of my project was to identify neurosecretory centers in *Platynereis* to correlate them to insulin-like peptide expression. Autoradiographic analyses revealed several regions of the adult brain that contain neurosecretory cells in atokous worms (Mueller 1973). In trochophore larvae, neurosecretory cells of the central brain were identified by combined expression of the marker genes *synaptotagmin* (*syt*) and *prohormone convertase 2* (*pc2*) (Tessmar-Raible et. al., 2007). Similarly, I used a modified in-situ Hybridization protocol to determine the expression of *syt* and *pc2* in atokous worms to identify the neurosecretory centers of the adult brain. Moreover, I studied the expression of *Platynereis nk2.1* in atokous worms, a gene that is expressed in the neurosecretory cells of the trochophore larval brain (Tessmar-Raible et. al., 2007).

#### 2.1.2.1. *Platynereis dumerilii pc2* is prominently expressed in the posterior brain lobes in atokous worms

In vertebrates, prohormone convertase 1/3 (PC1/3) and Prohormone convertase 2 (PC2) are expressed in neuronal and endocrine tissues and are involved in posttranslational processing of proproteins and prohormones. Both genes are expressed in pancreatic  $\beta$ -cells and are responsible for the conversion of pro-insulin to mature insulin (Smeekeens et. al., 1991; Neerman-Arbez et. al., 1993). In *Platynereis*, an orthologue of the vertebrate PC2 protein was identified previously and used a marker for neurosecretory cells (Tessmar-Raible et. al., 2007). I analyzed the expression of *pc2* in atokous worms by in-situ Hybridization and found that *pc2* is expressed broadly in the adult brain and in the ventral nervous system (Figure 12A,B). Prominent *pc2* expression is observed in the region of the posterior brain lobes, paired structures that are located in the space between the nuchal organs.

#### 2.1.2.2. Expression pattern of the neuronal marker *syt* in *Platynereis dumerilii* atokous worms

Synaptotagmins are membrane trafficking proteins that function as calcium sensors in the neurotransmitter release in neurons. A *Platynereis synaptotagmin (syt)* was cloned by K. Tessmar and used as a neuronal differentiation marker in trochophore larvae in previous studies (Tessmar-Raible et. al., 2007). I investigated *Platynereis syt* expression in atokous worms by in-situ Hybridization. As a neuronal marker, *syt* is expressed broadly in the adult brain and a particular high density of cells that express *syt* is observed in the posterior brain lobes (Figure 12C). Moreover, *syt* is expressed in neurons of the ventral nervous system (Figure 12D). *Syt* and *phc2* are both expressed in similar patterns in the posterior brain lobes and in the ventral nervous system. The expression of both genes in the posterior brain lobes and the ventral nervous system indicates that these tissues contain neurosecretory cells.

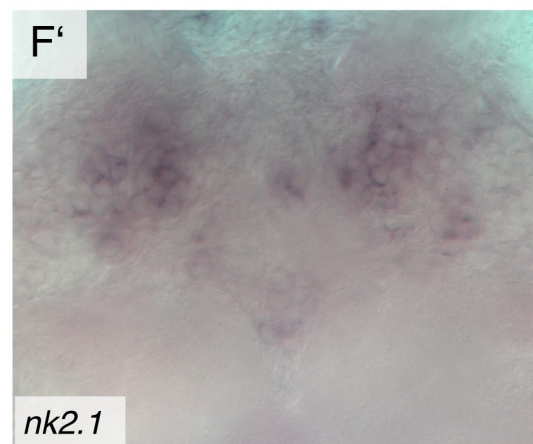
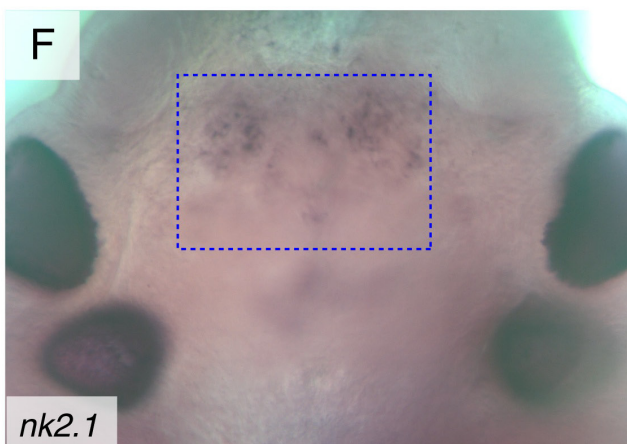
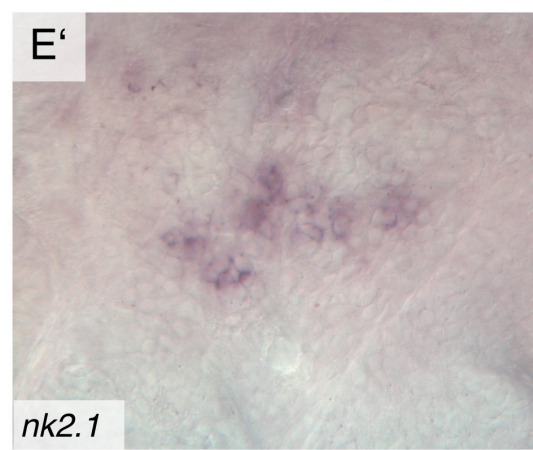
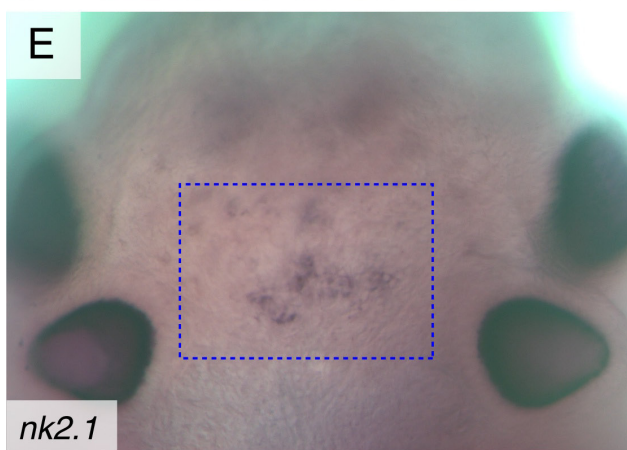
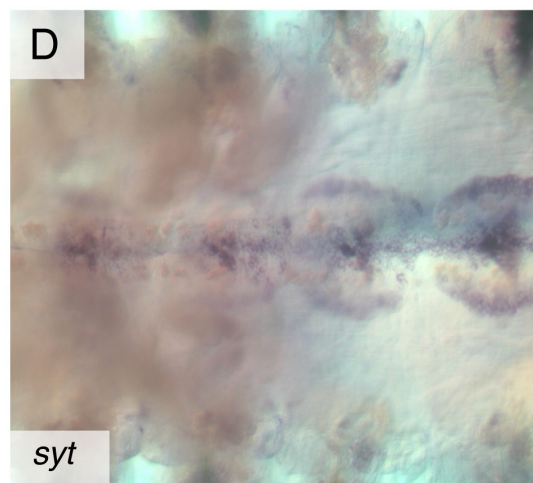
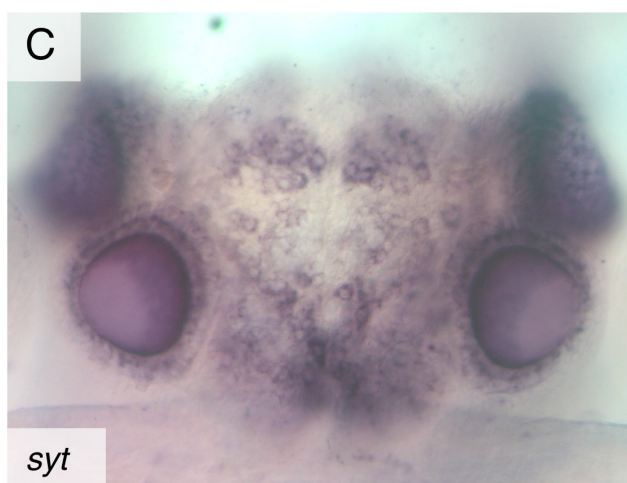
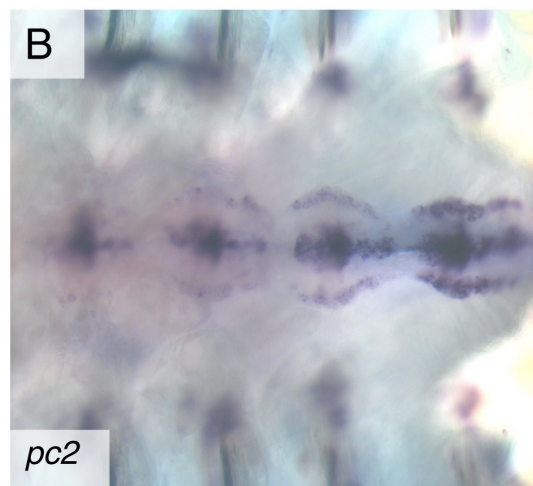
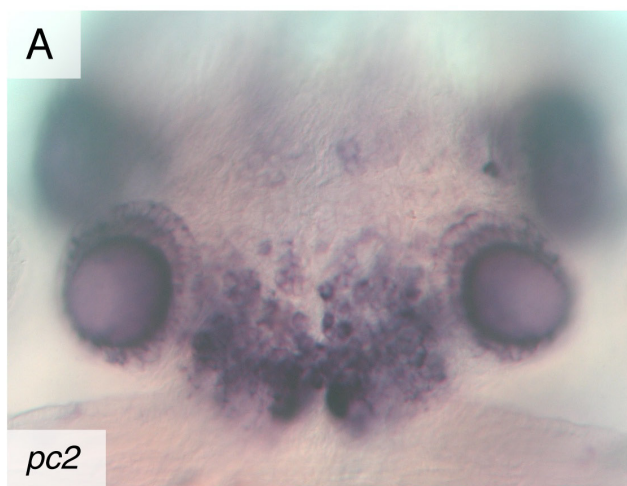


**Figure 12: Neurosecretory centers in atokous worms**

*Pc2* is prominently expressed in the posterior lobes (A) and in the ventral nervous system (B) in atokous worms. The neuronal marker *syt* is broadly expressed in the adult brain (C) and the ventral nervous system (D). Expression pattern analyses revealed two clusters *nk2.1* expressing cells in the brain. A median cluster of cells is located in between the two pairs of adult eyes (E, E') and an anterior cluster is located in the region of the pars intercerebralis (F, F'). Dotted blue rectangles in E and F indicate sections shown in E' and F'. Dorsal views (anterior to the top).

### 2.1.2.3. *Platynereis dumerilii nk2.1* is expressed in a medial cluster of cells and the pars intercerebralis

In vertebrates, the transcription factor *nkx2.1* plays a crucial role in hypothalamus development (Pera et. al., 1998; Sussel et. al., 1999). As a neurosecretory center of the vertebrate brain, various metabolic processes are controlled by the hypothalamus and it has been shown in rat that *igfI*, *igfII* as well as *insulin2* are present in the hypothalamus (Bach et. al., 1991; Lauterio et. al., 1990; Devaskar et. al., 1993). In insects, the pars intercerebralis has been shown to have an analogous function to the vertebrate hypothalamus as a neuroendocrine command center (DeVelasco et. al., 2003, Nässel 2002) and it has been shown to be center of insulin-like peptide expression (Ikeya et. al., 2002). The *Platynereis nkx2.1* orthologue is expressed in neurosecretory cells of the trochophore larvae (Tessmar-Raible et. al., 2007) and I analyzed *nk2.1* expression in adult worms to test for a possible correlation of insulin-like peptides and *nk2.1* expression. *Platynereis nk2.1* is expressed in two major populations in the adult brain. One group of cells is located in the medial brain region between the two pairs of adult eyes and anteriorly (Figure 12E,E'), a second group of *nk2.1* expressing cells is located in a region that was referred to as pars cerebrealis of the adult brain by Müller (1973) (Figure 12F,F').

### 2.1.3. Characterization of *Platynereis dumerilii* orthologues of genes that relate to the function of the vertebrate pancreas

The vertebrate pancreas plays a crucial role in carbohydrate metabolism and is interconnected to the metabolic control centers of the brain that regulate hunger, thirst, sleep, body temperature and circadian cycles (brain-gut axis). In this section, I studied the expression of

genes that are involved in the function of the vertebrate pancreas and brain-gut communication.

#### 2.1.3.1. *Platynereis glut2* is expressed in the region of the infracerebral organ

Glucose-sensing cells play important roles in the control of blood sugar levels. In vertebrates, glucose-sensing cells can be found in the liver, kidney, intestine and pancreatic  $\beta$ -cells. These cells express the glucose transporter *glut2* protein that mediates glucose uptake into the cells (Hogan et. al., 1991). In order to test if a *glut2* orthologue exists in *Platynereis*, I compiled a set of glucose transporter genes from different species and performed and extracted a 600bp fragment of the orthologue of the vertebrate *glut2* gene from transcriptome databases. To investigate if the *Platynereis glut2* gene is correlated to insulinergic cells, I analyzed its expression in atokous worms. *Platynereis glut2* is expressed in a ring- or triangle-like pattern between the posterior pair of adult eyes, in the ventral part of the brain (Figure 13A,A'). In *Platynereis*, this region has been described as the infracerebral organ which is an epithelium surrounding the ventral part of the brain and the dorsal blood vessel (Müller 1973). The infracerebral organ is a neurohemal gland and known as a release site for neuropeptides in annelid species.

#### 2.1.3.2. *Platynereis dumerilii npy* is expressed in distinct cells in the medio-dorsal part of the brain and ventral nervous system

Members of the neuropeptide Y family have a function in brain-gut communication and thereby, influencing feeding behavior, metabolism and reproduction across species (Nässel & Wegener, 2011, for review). In vertebrates, Neuropeptide Y (*npv*) is expressed mainly in the brain whereas *pyy* and pancreatic polypeptide (*pp*) are expressed in endocrine cells of the gut and pancreatic islets of Langerhans, respectively (Larhammar 1996, for review). The *Drosophila* orthologue *npf* is expressed in the brain, midgut and ventral nervous system of



larvae and adults (Brown et. al., 1999). To investigate a possible correlation of *npv* expressing cells with insulinergic cells in *Platynereis*, I wanted to analyze *npv* expression in adult worms. F. Raible cloned an orthologue of the neuropeptide Y family in *Platynereis*. I performed in-situ Hybridization in atokous worms using antisense riboprobe for the *npv* gene and identified a set of 3-8 *npv* expressing cells in the medio-dorsal part of the brain in between the anterior pair of adult eyes (Figure 13B). Moreover, paired *npv* expressing cells are detected in the ventral nervous system in each segment of adult worms (Figure 13C).

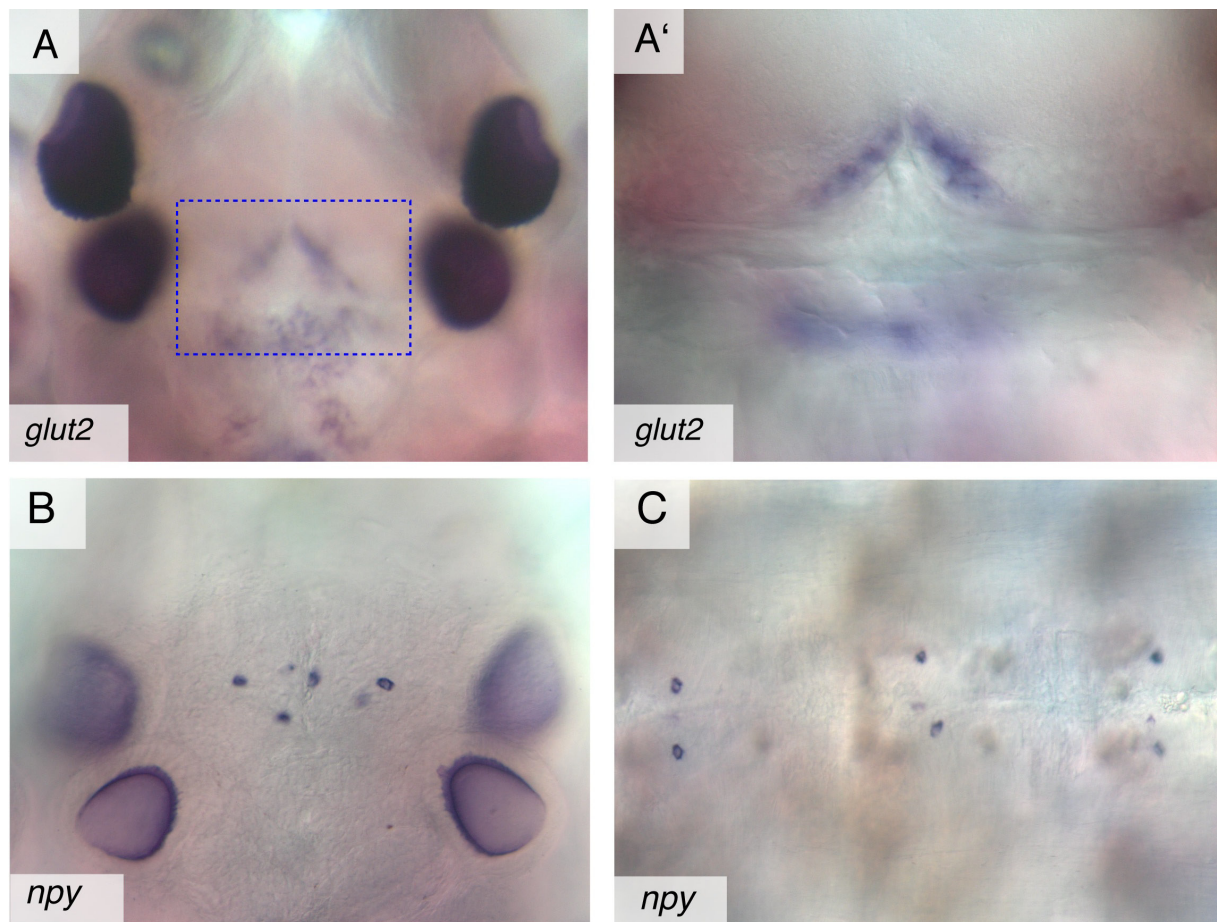


**Figure 13: Expression analyses of genes related to pancreatic functions**

(A,A') The *Platynereis* orthologue of the vertebrate *glut2* is expressed in the region of the infracerebral gland located between the posterior pair of adult eyes. *Platynereis glut2* is detected in the epithelium of the posterior-ventral part of the brain and in cells adjacent to the dorsal blood vessel. (B) *Platynereis npv* is found in cells located between the anterior pair of adult eyes and in pairs of cells in each segment in the ventral nervous system (C).

Dorsal views (anterior to the top); Dotted blue rectangle in A indicates section shown in A'.

## 2.2. Regulation of insulin-like peptides in *Platynereis dumerilii*

### 2.2.1. Characterization of potential upstream factors of *Platynereis* insulin-like peptides

A goal of my project was to explore how insulin-like peptide transcription is regulated in *Platynereis*. In vertebrates, the transcriptional regulation of the insulin gene has been extensively studied and transcription factors that bind the insulin enhancer are well characterized. In a candidate-driven approach, I compiled a set of known vertebrate insulin regulators and examined the expression of their orthologues in *Platynereis*. Subsequently, I compared their expression patterns to that of insulin-like peptides in *Platynereis* to identify potentially conserved regulators of insulin-like peptide expression.

#### 2.2.1.1. *Platynereis dumerilii* *lMaf* is expressed in insulinergic cell-types during early development

##### 2.2.1.1.1. Identification of a large Maf gene in *Platynereis dumerilii*

Transcription factors that belong to the Maf protein family play important roles in pancreatic  $\beta$ -cell differentiation and insulin transcription in vertebrates. The Maf-family is divided into two subgroups, the small Maf proteins and large Maf proteins. Large Maf proteins have a basic-leucine zipper DNA binding motif and a N-terminal transactivation domain. Small Maf proteins lack the transactivation domain. In vertebrates, large Maf proteins comprise MafA, MafB, Nrl and c-Maf and vertebrate small Maf proteins are MafK, MafG, and MafF. Small Maf proteins are expressed in various tissues and are known as repressors of transcription. In mouse and human, MafB plays an important role in pancreatic  $\beta$ -cell differentiation whereas MafA was shown to be a direct regulator of insulin expression by binding to its promoter and activating insulin gene transcription. In most invertebrate species, the Maf-family consists of a single large Maf protein and a single small Maf protein. The *Drosophila* large Maf protein traffic jam (tj) was shown to be involved in gonad morphogenesis (Li et. al., 2003) but no role for tj in insulinergic cells has been reported.

In *Platynereis*, I identified one large Maf (*lMaf*) gene and one small Maf (*sMaf*) gene by BLAST search of *Platynereis* transcriptome libraries with a set of large and small Maf family members from different species. The sequence that I obtained by PCR using specific primers for the large Maf gene was 600bp in length and I performed 5' and 3' RACE-PCR to get its full-length sequence. *Platynereis lMaf* is a single exon gene of 306aa in length and is phylogenetically closely related to *Drosophila* tj and lophotrochozoan large Maf candidate proteins (Figure 14).

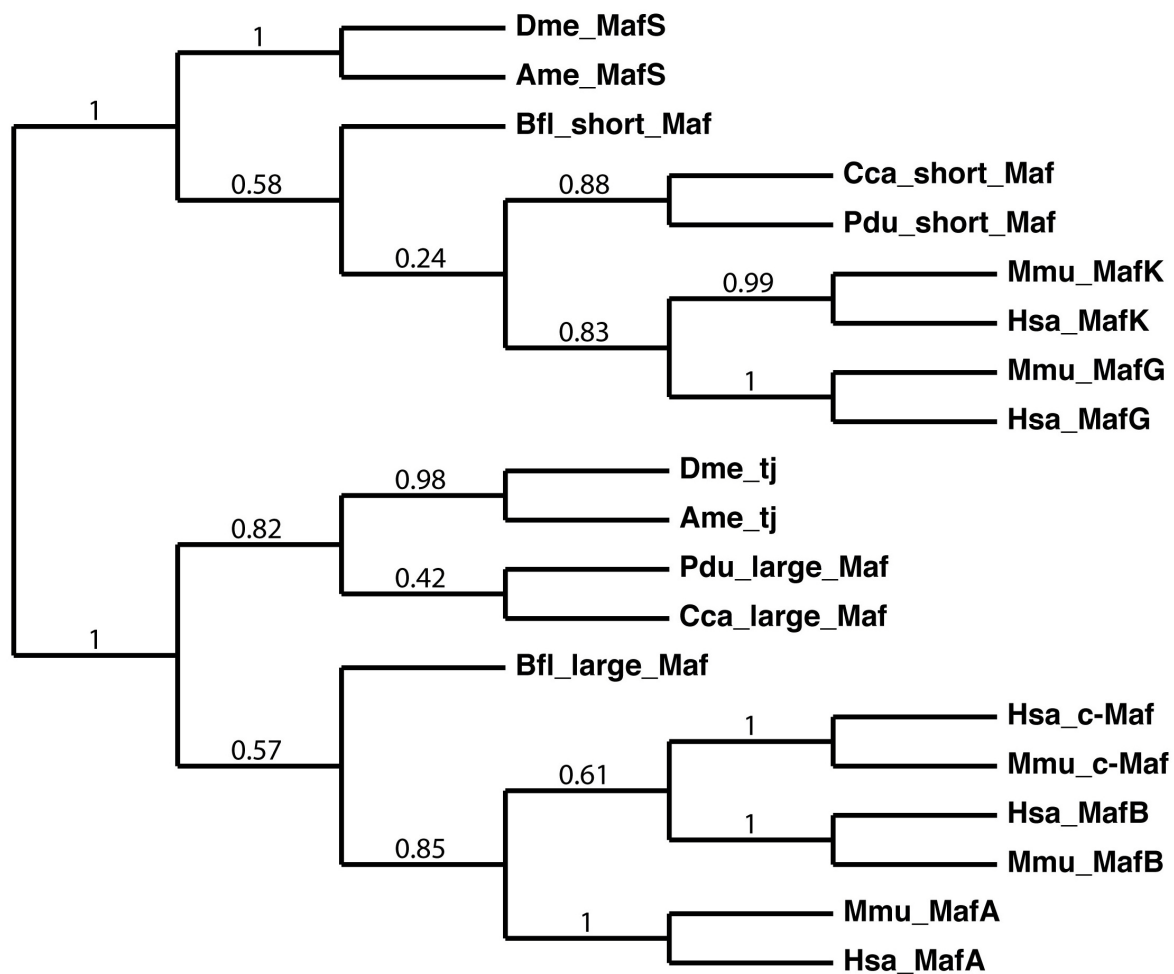


**Figure 14: Phylogenetic analyses of *Platynereis* Maf genes**

Maximum-likelihood phylogenetic tree of Maf proteins in different species. *Platynereis* (*Pdu*) small Maf (*sMaf*) and large Maf (*lMaf*) candidates group together with Lophotrochozoan candidates from *Capitella teleata* (*capitata*) (*Cca*). Invertebrates have a single small Maf and a single large Maf representative, whereas the vertebrate Maf-family consists of several proteins for the two classes.

*Hsa*: *Homo sapiens*; *Mmu*: *Mus musculus*; *Bfl*: *Branchiostoma floridae*; *Ame*: *Apis mellifera*; *Dme*: *Drosophila melanogaster*.



#### 2.2.1.1.2. *Platynereis dumerilii lMaf* is expressed in the larval and postlarval brain

To investigate the expression of *lMaf*, I performed in-situ Hybridization in larval and postlarval stages. I started to analyze *Platynereis lMaf* expression by performing in-situ Hybridization in 48hpf trochophore larvae. *lMaf* mRNA is expressed in eight cells of the larval brain (Figure 15A-F). One pair of *lMaf* expressing cells is located in the center of the larval brain directly below the apical tuft. Another pair of *lMaf* expressing cells is located 4-6 cell diameters ventro-lateral of the apical tuft in the medial larval brain region. A third cluster of four cells resembling a semi-circle, expresses *lMaf* mRNA in the dorsal-medial part of the brain of the 48hpf trochophore larvae.

Next, I performed expression analysis of *lMaf* mRNA in atokous worms. *lMaf* is detected in a cluster of cells which is located in the medio-dorsal region of the posterior part of the adult brain and in two cells that are located between the posterior pair of adult eyes (Figure 15G,G'). Weak expression of *lMaf* is detectable in the adult eyes, too. *Platynereis lMaf* is present in larval and postlarval stages and is expressed in the brain and adult eyes.

#### 2.2.1.1.3. *lMaf* is expressed in insulinergic cells of the trochophore larva

*Platynereis lMaf* and *ilp2*, *ilp3* and *ilp5* are expressed in the brain of 48hpf trochophore larvae and may have overlaps in their expression patterns (compare sections 2.2.1.1.2. and 2.1.1.3.). To determine if the expression patterns of *lMaf* and *ilp2*, *ilp3* and *ilp5* correlate in the larval brain, I established a two-color staining in-situ Hybridization protocol. I applied Dig-labeled antisense riboprobes for *ilp2*, *ilp3* and *ilp5* and a fluorescein-labeled antisense riboprobe for *lMaf* to the in-situ procedure. *Ilp2*, *ilp3* and *ilp5* are expressed in subsets of cells in the larval brain as described above (Figure 16A,D,G,J). The two-color stainings demonstrate that expression of insulin-like peptides correlates with that of *lMaf*. *Ilp2* and *lMaf* are both expressed in one to two cells in the center of the brain whereas only *lMaf* is expressed in additional dorso-medial cells (Figure 16A-C). *Ilp3* and *lMaf* are both expressed in a cluster of dorso-medial cells, but only *lMaf* is expressed in the center of the brain in these two color in-situ stainings (Figure 16D-F). *Ilp5* and large Maf are co-expressed in cells in the center of the

larval brain, a dorsal pair of cells and a bilateral pair of cells located ventro-lateral of the apical tuft (Figure 16G-L).

*Platynereis lMaf* expression overlaps with the expression patterns of *ilp2*, *ilp3* and *ilp5* in 48hpf trochophore larvae. Moreover, two-color in-situ stainings suggest that *lMaf* is generally expressed in insulineric cells of 48hpf trochophore larvae.

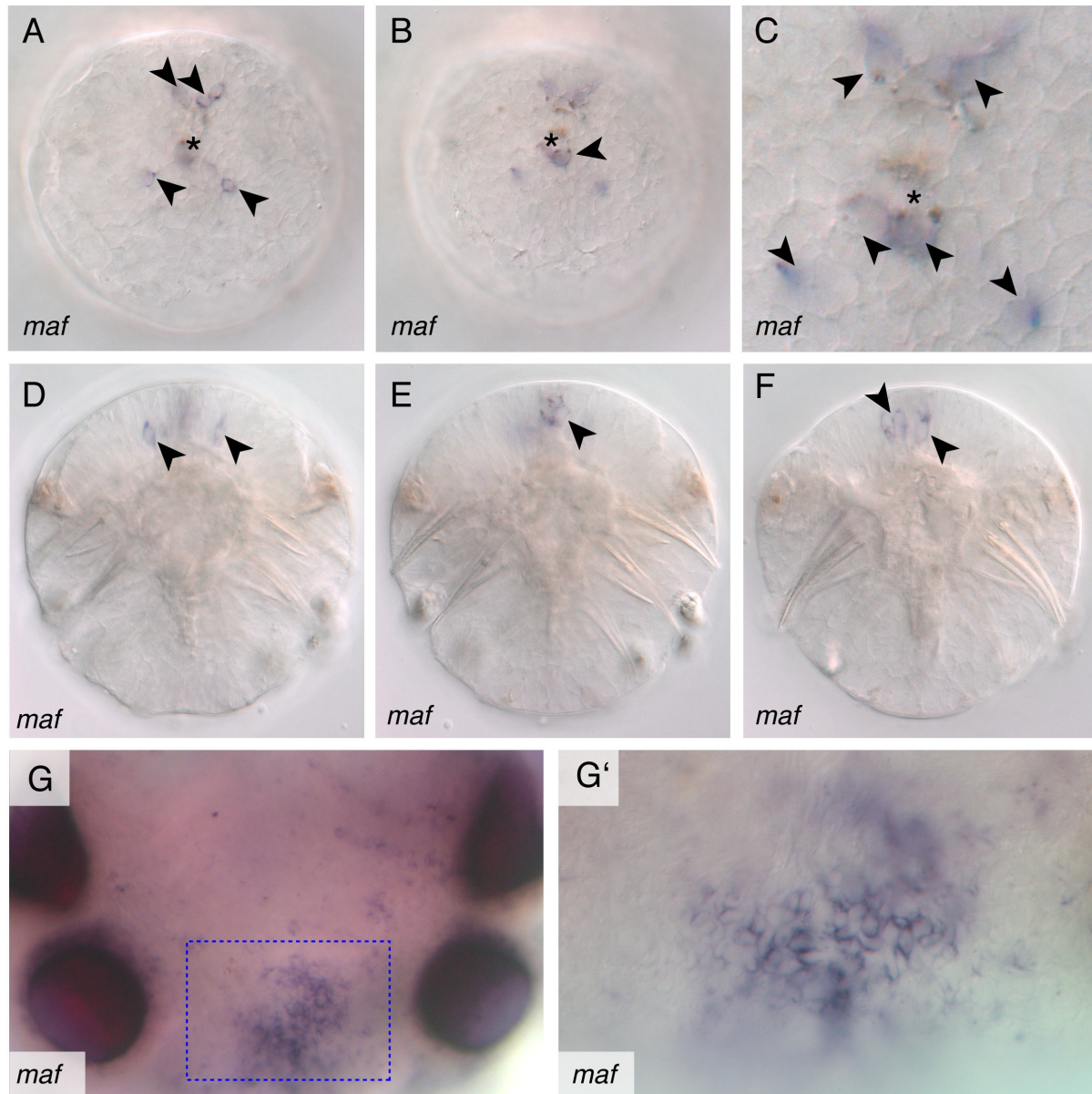


**Figure 15: Expression of *lMaf* in larval and postlarval stages**

In-situ Hybridization of *Platynereis lMaf* at 48hpf (A-F) and in atokous worms (G,G'). In trochophore larvae, *lMaf* is expressed in a bilateral pair of cells located ventro-lateral of the apical tuft (A, C, D), a cluster of cells in the medial-dorsal brain (A, C, F) and a cell in the central brain, below the apical tuft (B, C, E). In atokous worms, *lMaf* is detected in a medio-dorsal region of the posterior part of the brain (G, G').

A-C: apical views (dorsal up); D-F: dorsal views (anterior to the top); G,G': dorsal views (anterior to the top); Black arrowheads indicate expression; black asterisk: apical tuft; Dotted blue rectangle in G indicates section shown in G'.

#### 2.2.1.1.4. *lMaf* and insulin-like peptide 2 are not co-expressed in atokous worms

As shown in section 2.2.1.1.2., *Platynereis lMaf* is expressed in two cells that are located between the posterior pair of adult eyes. This expression pattern resembles that of *ilp2*, which is prominently expressed in two cells located between the posterior pair of adult eyes (see section 2.1.1.4.). Thus, I wanted to test if *lMaf* and *ilp2* are co-expressed in these cells of the adult brain. I performed double in-situ stainings with pooled riboprobes for both of the genes and single in-situ stainings for each gene. If *lMaf* and *ilp2* are co-expressed in the pair of cells between the posterior pair of adult eyes, only two cells should be detectable in this region in a double in-situ for pooled *lMaf* and *ilp2* riboprobes. As shown in Figure 17, the single in-situ stainings show the expected expression patterns of the two genes. In the double in-situ staining, two distinct pairs of cells are detected showing that *ilp2* and *lMaf* are expressed in different cells and there is no co-expression of the two genes in atokous worms (Figure 17). These results indicate that *Platynereis lMaf* is not a regulator of *ilp2* expression in atokous worms.

#### 2.2.1.1.5. Transient expression of a reporter construct recapitulates endogenous *lMaf* expression in the central larval brain

As shown above (section 2.2.1.1.3.), *Platynereis lMaf* is associated with insulin-like peptide expression in trochophore larvae. To investigate expression of *lMaf* during *Platynereis* development in vivo, I generated a reporter construct consisting of 3.6kbp of *lMaf* upstream genomic region fused to egfp as a reporter gene. I injected the reporter construct pTol2{maf::egfp}<sup>FRKT1208</sup> along with synthetic tol2 transposase mRNA into zygotes. Observations during early development of injected embryos revealed that the *lMaf* reporter construct is expressed as early as 6hpf. As shown in Figure 18, *lMaf* reporter recapitulates the endogenous *lMaf* expression at 55hpf in cells that are located in the center of the larval brain. Later in development, egfp expression is detected in cells of the dorso-lateral and dorso-medial part of the head.



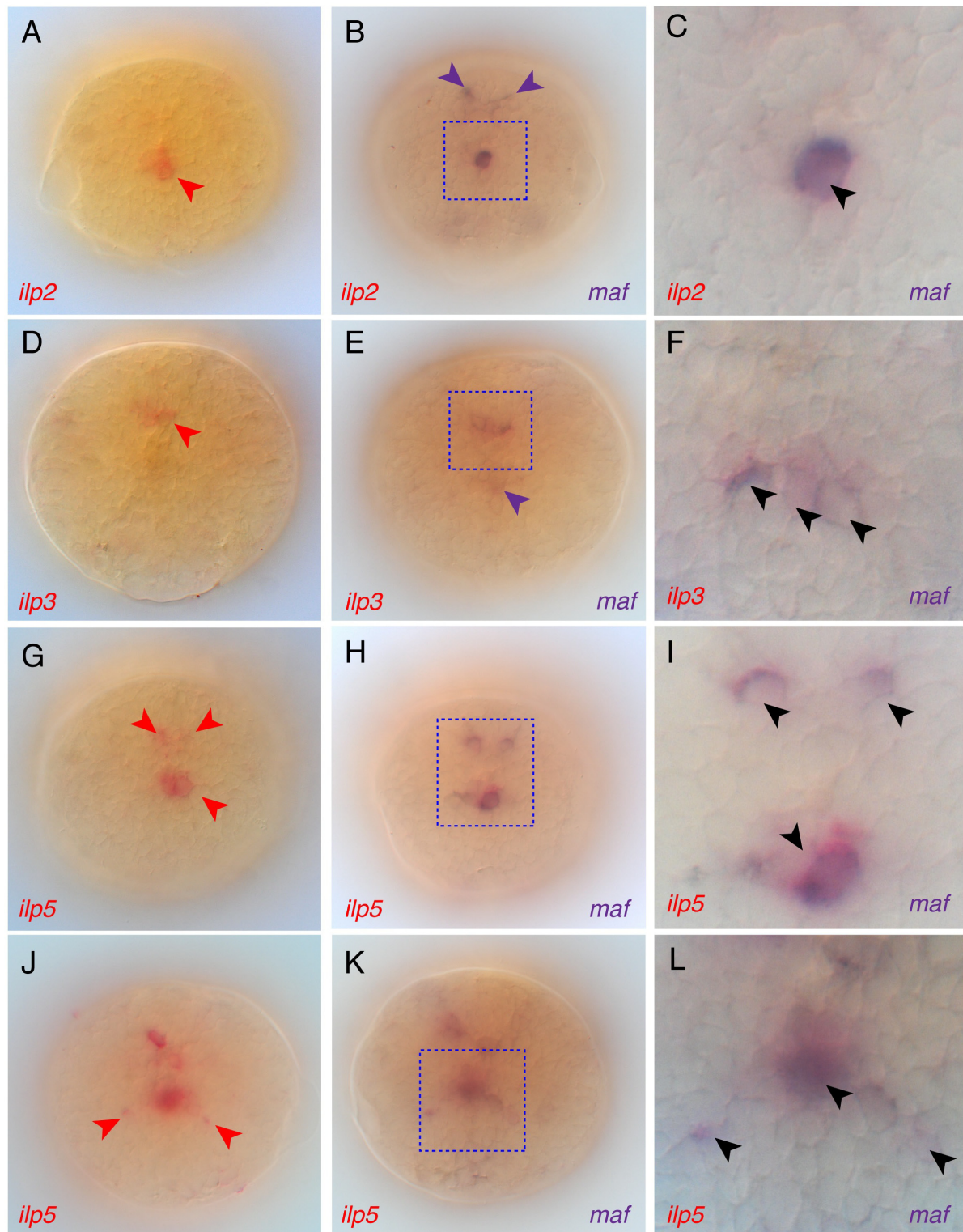


**Figure 16: Co-expression analyses of *IMaf* and insulin-like peptides in trochophore larvae**

Two-color in-situ stainings of *IMaf* (blue) and insulin-like peptides (red) at 48hpf. (A-C) Co-stainings revealed co-expression of *ilp2* and *IMaf* in a cell of the central brain. (D-F) Co-expression of *ilp3* and *IMaf* in the medial-dorsal brain. (G-L) Two-color stainings of *ilp5* and *IMaf* in several clusters of cells in the larval brain. *Ilp5* and *LMaf* are co-expressed in the center of the brain, a medial-dorsal cluster of cells (G-I) and a bilateral pair of cells located ventro-lateral of the apical tuft. Red arrowheads indicate insulin-like peptide expression; purple arrowheads indicate *IMaf* expression; black arrowheads indicate co-expression; Dotted blue rectangles shown in B, E, H, K indicate regions shown in C, F, I, L; apical views (dorsal to the top).

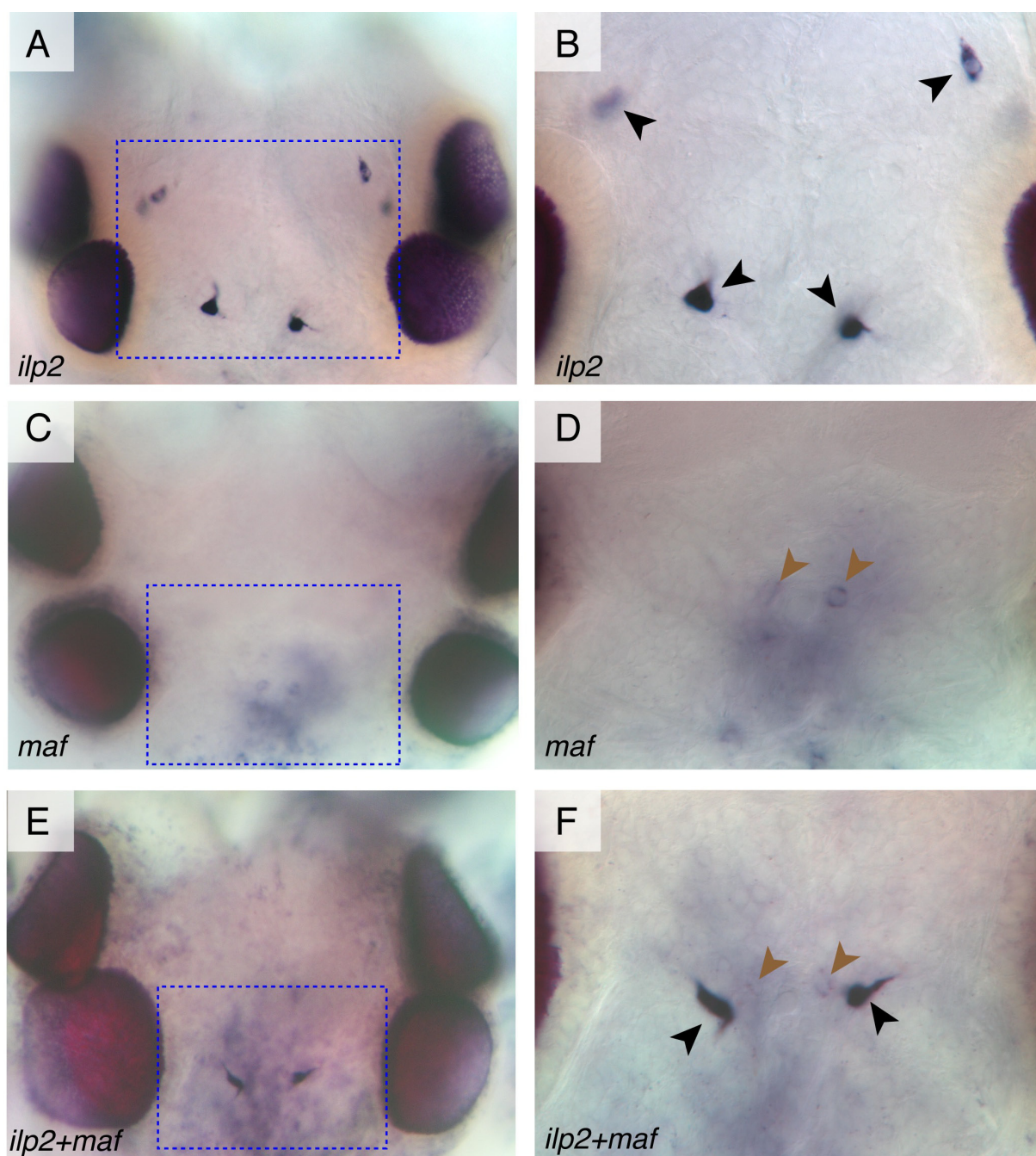


**Figure 17: Double-staining analyses of *lMaf* and *ilp2* in atokous worms**

Comparison of single and double in-situ stainings for *lMaf* and *ilp2* revealed that *ilp2* and *lMaf* are expressed in distinct cells of the adult brain. Single in-situ stainings for *ilp2* (A,B; black arrowheads) and *lMaf* (C,D; brown arrowheads), compared to double in-situ staining for both genes (E,F). Black arrowheads indicate *ilp2* expression; brown arrowheads indicate *lMaf* expression; Dotted blue rectangles shown in A, C and E indicate regions shown in B, D and F. dorsal views (anterior to the top).



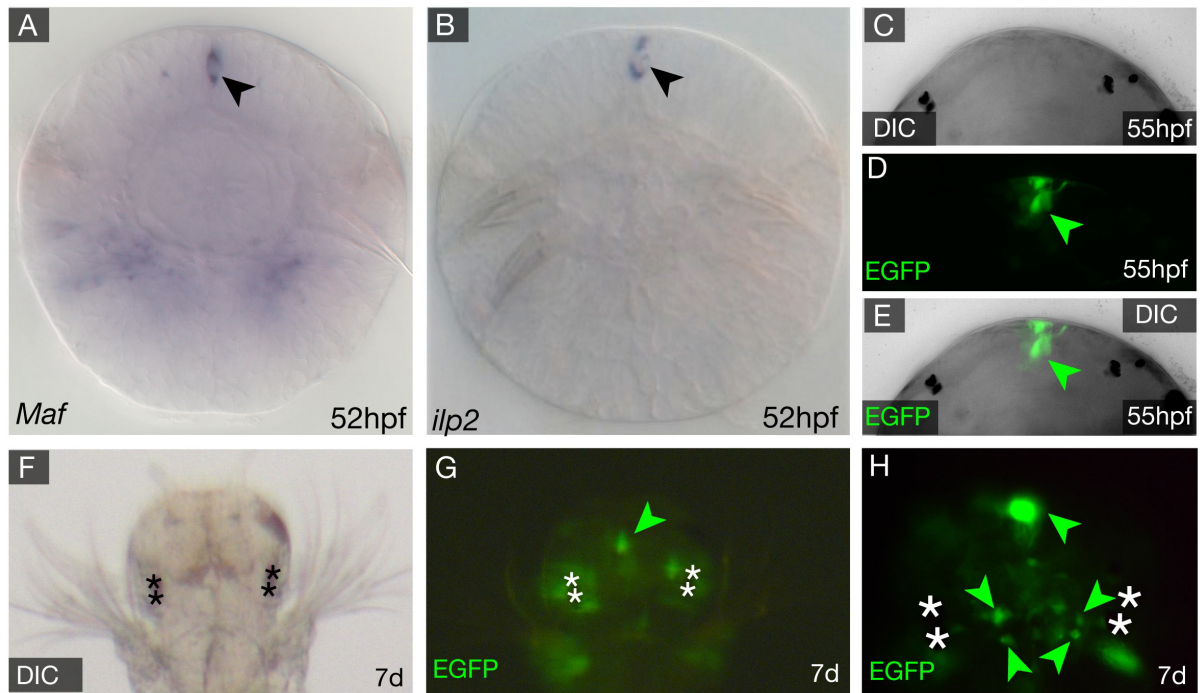


**Figure 18: *IMaf* reporter expression in larval stages**

Expression analyses revealed that *IMaf* and *ilp2* are co-expressed in the central larval brain (A, B; black arrowheads). As a possible marker for insulinergic cells, a reporter construct for *IMaf* was generated. A 3.6kbp upstream element of *IMaf* fused to *egfp* coding sequence revealed robust EGFP expression in the central larval brain (C-E). After 7 days of development, EGFP (green arrowheads) expression is detected in medial-dorsal and dorso-lateral regions of the brain in injected animals (F-H). White asterisks: adult eyes.

#### 2.2.1.1.6. Knockdown of *IMaf* expression reveals inconclusive data

In-situ Hybridization revealed that expression patterns of *IMaf* and insulin-like peptides correlate in trochophore larvae (section 2.2.1.1.3.). Since *IMaf* proteins play important roles in insulin expression (MafA) and in insulinergic cell differentiation (MafB) in vertebrates, I examined if a knockdown of *IMaf* expression has an effect on insulin-like peptide expression in *Platynereis*. To interfere with *Platynereis IMaf*, Morpholino antisense oligos (MASO) were designed that cover the transcription start site and block *IMaf* translation. I injected *IMaf* MASO into zygotes in a concentration of 500μM. Injected embryos and larvae developed normally and did not show any specific phenotype or developmental delay. After 48hpf, injected embryos were fixed and in-situ Hybridizations with riboprobes against *ilp2* were performed. *Ilp2* was chosen as target gene for historic reasons. In an initial experiment using n=12 *IMaf* MASO injected individuals, I found in 80% of the larvae a strong reduction of *ilp2* expression or even absence of expression. In contrast, 100% of the injected control animals as

well as non-injected controls showed *ilp2* expression. However, I did not observe this effect on *ilp2* expression in the following experiments. Therefore, the results from the MASO knockdown experiments have to be considered as inconclusive.

#### 2.2.1.2. *Platynereis dumerilii* *pax6* expression is associated to *ilp2* in atokous worms

*Pax6/eyeless* is a conserved regulator of insulin expression in vertebrates and invertebrates. It has been shown that vertebrate *pax6* activates insulin transcription in pancreatic  $\beta$ -cells and that its *Drosophila* orthologue *eyeless* regulates expression of *dilp5* (Clements et. al., 2008). In this study, I tested if *pax6* correlates with insulin-like peptide expression in *Platynereis*. A *Platynereis* orthologue of *pax6* has been identified and it is expressed in the developing ventral nervous system and the developing brain (Arendt et. al., 2002). To test for a correlation of *pax6* and insulin-like peptides in larval stages, I performed two-color in-situ Hybridization of insulin-like peptides and *pax6* in 48hpf trochophore larvae. In the larval brain, *pax6* is expressed broadly in paired ventro-lateral domains whereas insulin-like peptides are detected in the more central part of the brain. No overlap in the expression of *pax6* and insulin-like peptides was observed in trochophore larvae (Figure 19).

So far, *Platynereis pax6* expression has only been studied in trochophore larvae due to the lack of in-situ protocols for postlarval stages. Using an optimized in-situ Hybridization protocol, I analyzed *pax6* expression in atokous worms and correlated its expression to that of insulin-like peptides. In the adult brain, *pax6* is expressed in two distinct cells that are located in between the posterior pair of adult eyes, in bilateral clusters comprising two cells each between the anterior pair of adult eyes and in clusters of cells located in the pars intercerebralis (Figure 19A-D). The pair of *pax6*-positive cells between the posterior adult eyes is located in a region where *ilp2* expression was observed (see section 2.1.1.4.). To test if of *pax6* and *ilp2* are both expressed in these cells, I performed in-situ double-stainings for *ilp2* and *pax6* (Figure 20). If the two genes are co-expressed, only one pair of cells should appear in the double-stainings. In deed, *pax6* and *ilp2* appear to be co-expressed in the two cells between the posterior pair of eyes (Figure 20E,F).

Two-color and double in-situ stainings revealed that *pax6* and insulin-like peptides are not correlated in trochophore stages, but *pax6* and *ilp2* are co-expressed in a pair of cells in the adult brain.

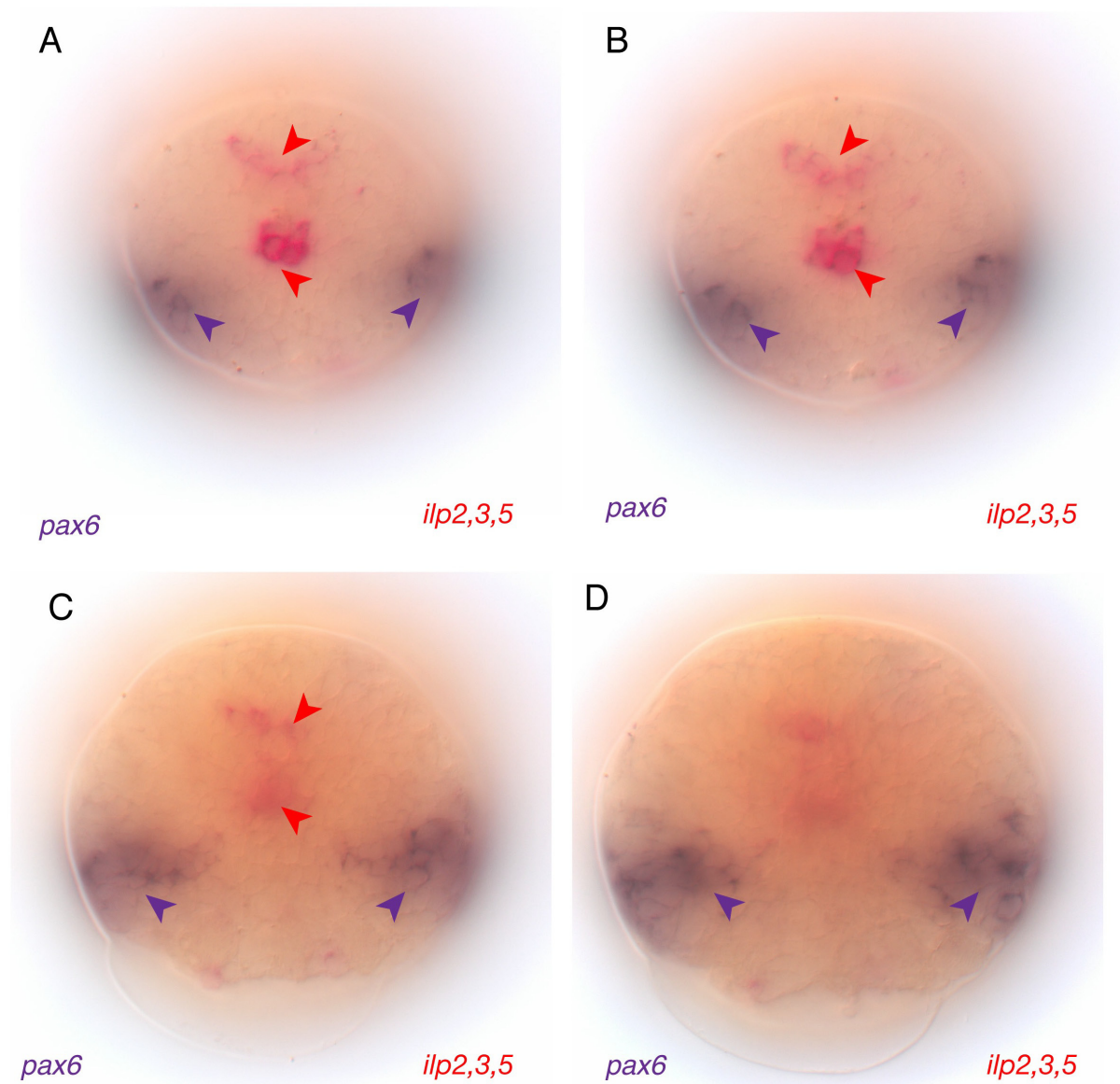


**Figure 19: Expression analyses of *pax6* and insulin-like peptides in trochophore larvae**

Two-color in-situ stainings of *pax6* and pooled riboprobes for *ilp2*, *ilp3* and *ilp5* reveal that *pax6* is not co-expressed with ilps in trochophore larvae (A-D). *Pax6* (purple arrowheads) is detected in ventrolateral domains of the brain whereas ilps (red arrowheads) are detected in central and dorsal brain regions. Apical views (dorsal to the top)



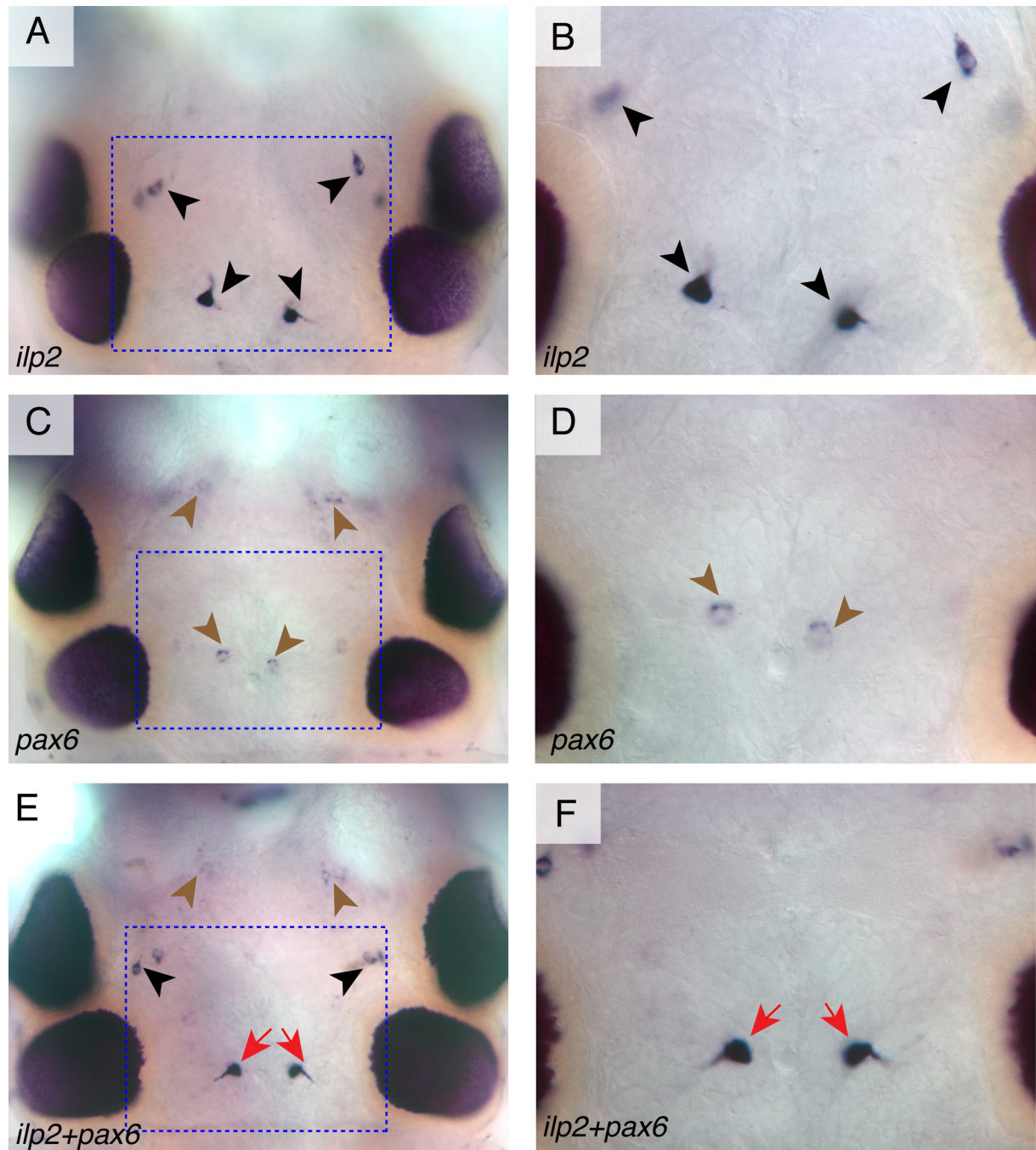


**Figure 20: Double-staining analyses of *pax6* and *ilp2* in atokous worms**

Comparisons of single in-situ stainings and double in-situ stainings reveal that *pax6* and *ilp2* are co-expressed in the brains of atokous worms. (A,B) Expression of *ilp2* is detected in bilateral pair of cells between anterior and posterior pairs of adult eyes (black arrowheads). (C,D) Expression of *pax6* is detected in a pair of cells between the posterior pair of adult eyes and in a bilateral cluster of cells in the anterior part of the brain, in the region of the mushroom bodies (brown arrowheads). (E,F) Double staining of *pax6* and *ilp2* demonstrate co-expression of *ilp2* and *pax6* in the pair of cells in between the posterior pair of adult eyes (red arrows). Dorsal views (anterior to the top); Dotted blue rectangles in A, C and E indicate sections shown in B, D and F.

### 2.2.1.3. *Platynereis dumerilii* insulin-like peptides are not co-expressed with *xlox*

The gene *pdx1* (*ipf1*) is known as a key factor for pancreas development and as a crucial activator of insulin gene transcription in vertebrates. In conventional protostome model species like *Drosophila melanogaster* and *Caenorhabditis elegans*, no orthologue of *pdx1* (*ipf1*) is present. In contrast, orthologues of *pdx1* (*ipf1*) were identified in lophotrochozoan species like *Platynereis dumerilii* and *Neanthes virens* and their expression patterns have been characterized (Hui et. al., 2008; Kulakova et. al., 2007). In *Platynereis*, the *pdx1* (*ipf1*) orthologue *xlox* is expressed in cells of the medial ventral plate in 50hpf trochophore larvae and in late nectochaete juveniles after 5 days of development it is found distinct cell clusters in prospective midgut (Hui et. al., 2008). In addition, weak *xlox* expression was observed in bilateral lobes of the brain in late nectochaete stages. I performed in-situ Hybridization of *xlox* in larval and postlarval stages and compared its expression to that of *Platynereis* insulin-like peptides. As *Platynereis xlox* and insulin-like peptides are detected in different tissues in trochophore larvae, *xlox* might not be a regulator of insulin-like peptide expression in *Platynereis*. Temporal expression of *xlox* in the brain lobes in nectochaete stages also does not correlate to insulinergic cells. No *xlox* expression is observed in atokous worms. These results imply that *xlox* is not a regulator of insulin-like peptide expression in *Platynereis*.

### 2.2.1.4. *Platynereis dumerilii* *islet* gene is prominently expressed in the posterior lobes and the nuchal organ

The vertebrate *Islet1* gene is known to bind the insulin enhancer and activate insulin transcription in pancreatic  $\beta$ -cells. The two vertebrate islet genes, *islet1* and *islet2*, play a crucial role in motorneuron differentiation. A similar function in motorneuron differentiation has been reported for the *Drosophila* orthologue islet (Thor et. al., 1997). In *Platynereis*, a single orthologue of islet was cloned (Denes et. al., 2007) and I performed expression analyses in atokous worms to determine if the *Platynereis* islet gene is associated with insulin-like peptide expression. I found that *islet* is expressed in bilateral clusters of cells in the anterior part of the brain and in the posterior lobes (Figure 21A). Moreover, islet is expressed prominently in the nuchal organ. As shown in Figure 21B, *Platynereis* insulin-like

peptides are expressed in the islet-positive region. The overlap of *Platynereis* islet gene expression with that of insulin-like peptides in the posterior brain lobes might be an indication for a conserved function of *islet* as regulator of insulin expression.

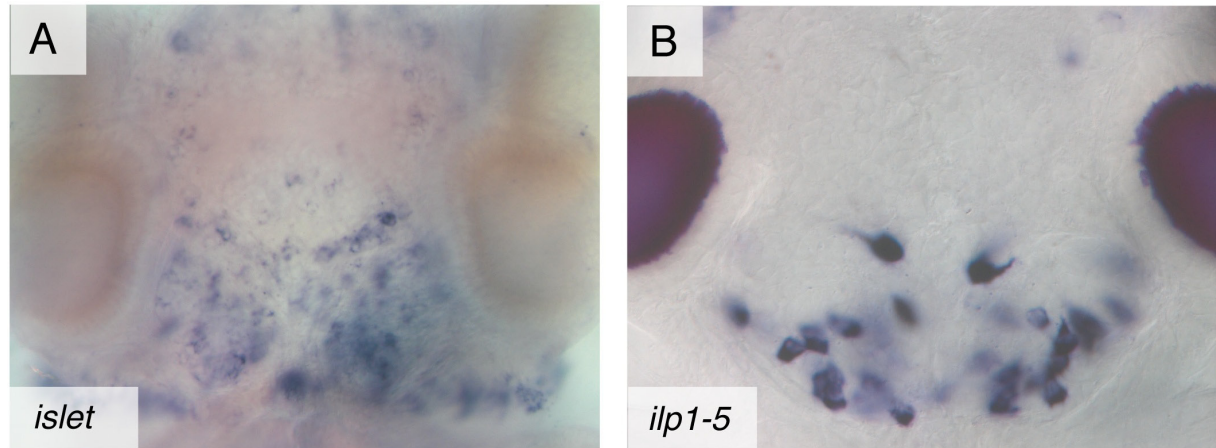


**Figure 21: *islet* gene expression**

(A) *Platynereis islet* gene is expressed prominently in the posterior lobes of the brain and the nuchal organs. The posterior lobes are the center of insulin-like peptide expression in *Platynereis* (B). Dorsal views (anterior to the top). Animal shown in A is from an inbred strain lacking the eye pigment (red-eye strain).

### 2.2.2. Elevated expression levels of insulin-like peptide mRNA after food intake in *Platynereis dumerilii*

In vertebrates, levels of insulin transcripts are elevated in response to food intake in the pancreatic  $\beta$ -cell. In this study, I wanted to test if food intake has a similar effect on the expression levels of insulin-like peptides in *Platynereis* as reported for vertebrates. Therefore, I determined and compared the expression levels of insulin-like peptides of fed animals and non-fed animals. Atokous worms were kept separated from each other for seven days without feeding and subsequently divided into two groups. One group of animals was fed with a mixture of algae, spinach and fish food whereas the other group did not receive any food. Eight hours after feeding, levels of insulin-like peptide mRNA from head samples were determined by qRT-PCR and compared between the two groups. Levels of *ilp1*, *ilp2* and *ilp4* are significantly elevated in the group of animals that were fed compared to the non-fed control whereas levels of *ilp3* and *ilp5* were not significantly changed (Figure 22A-E).

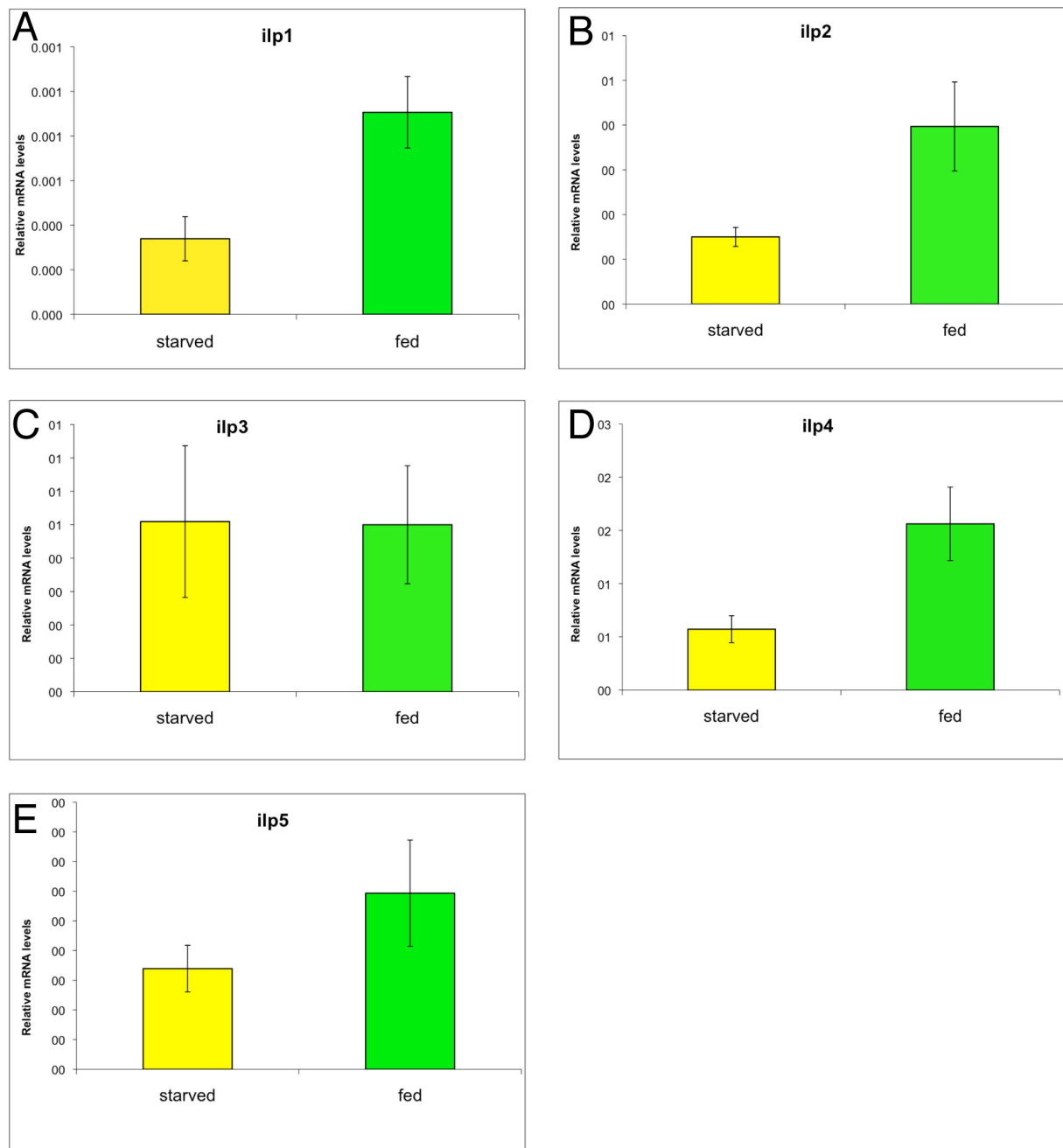


**Figure 22: Food-dependent expression of insulin-like peptides**

Starvation assay performed on juvenile worms. Expression levels of insulin-like peptides were determined in a group of animals 8 hours after feeding (green) and a non-fed control group (yellow). Levels of *ilp1*, *ilp2* and *ilp4* were significantly higher after feeding compared to the starved control (A, B, D). Levels of *ilp3* and *ilp5* were not altered after food intake compared to the control. Dataset consists of 6 biological samples with 2 technical replicates each; *rps9* was chosen as reference gene to determine relative expression levels.

### 2.2.3. Circadian expression of insulin-like peptides in *Platynereis dumerilii*

In vertebrates, pancreatic insulin metabolism and the circadian clock are tightly interconnected and it has been suggested that this is an ancestral feature to integrate physiological processes and circadian behavior. Moreover, pancreatic  $\beta$ -cells possess their own circadian clock (Marcheva et. al., 2010). In this study, I investigated if such an interconnection between insulin-like peptide expression and the circadian clock might exist in *Platynereis*.

#### 2.2.3.1. *Platynereis dumerilii* ilps are expressed in a 24h rhythm

To investigate fluctuations in the expression levels of *Platynereis* insulin-like peptides during the day, I performed qRT-PCR experiments at 6 different time-points during a 24-hour period in a normal light-dark regime. I found that a peak of insulin-like peptide expression levels is in the early morning at 6 a.m. (Figure 23). This is the time-point when the light is just switched on after 8 hours of darkness. In the course of the day, the expression levels of insulin-like peptides are significantly lower than at 6 a.m. and for *ilp1*, *ilp2*, *ilp3* and *ilp4* no additional peak of expression is observed in the light-dark cycle (Figure 23A-D). In contrast, *ilp5* expression has another peak of expression at 6 p.m. in the evening (Figure 23E).

#### 2.2.3.2. *Platynereis dumerilii* ilps keep their expression rhythm in the dark

Next, I wanted to investigate if fluctuations of insulin-like expression levels are still preserved after a period of constant darkness. After 48 hours kept in complete darkness, atokous worms were sampled over a 24-hour time period at 6 different time-points and expression levels of insulin-like peptides were determined by qRT-PCR. The temporal expression patterns of insulin-like peptides over 24-hour period show a peak of expression in the morning (Figure 24). Subsequently, expression levels of *ilp1*, *ilp2*, *ilp3* and *ilp4* decrease and no further peak of expression is detected (Figure 24A-D). In contrast, *ilp5* has an additional peak of

expression in the morning (Figure 24E). Hence, a rhythmic expression of insulin-like peptides is preserved in worms that were kept under constant darkness for 48 hours.

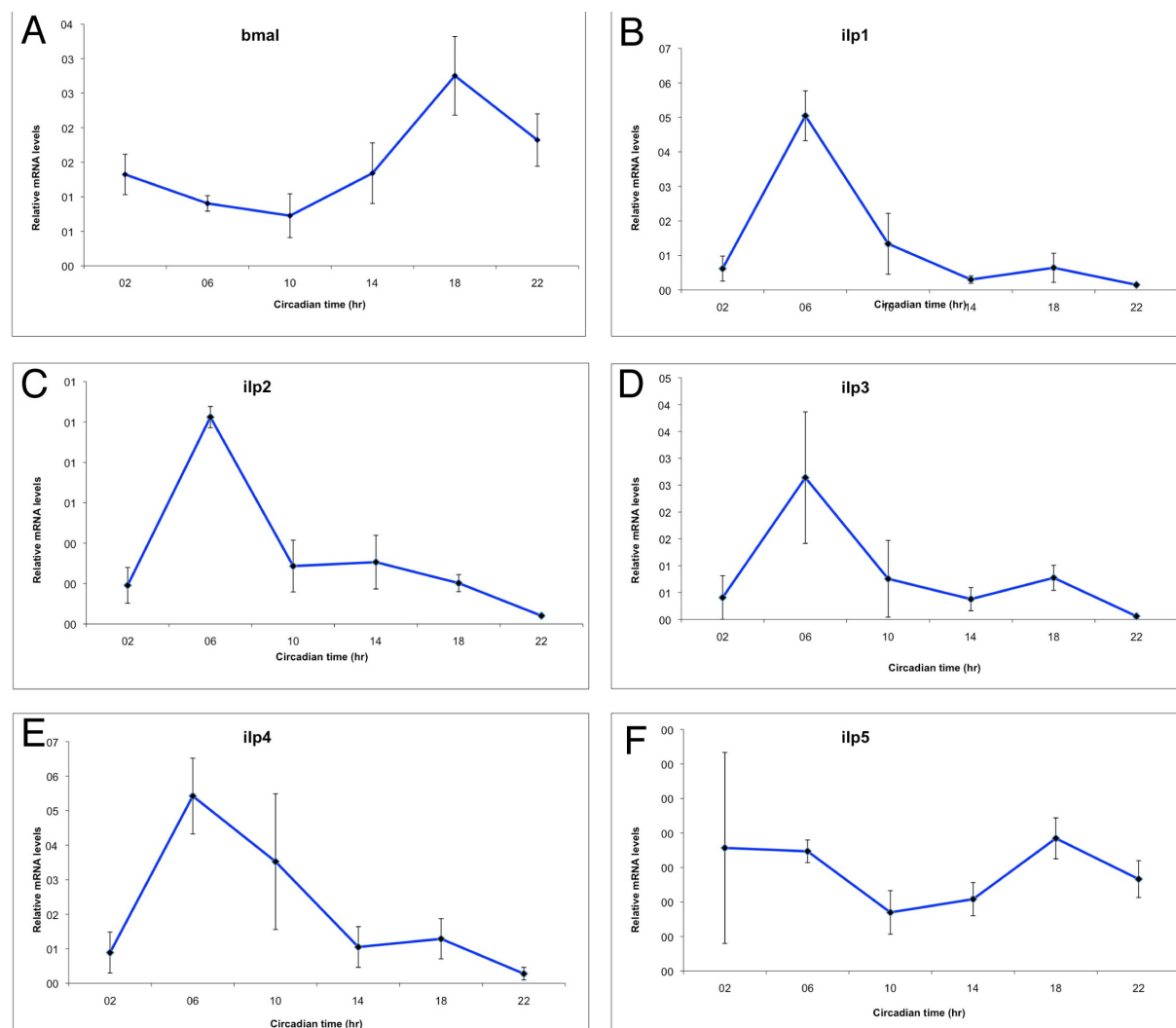


**Figure 23: Circadian expression of insulin-like peptides**

Relative expression levels of insulin-like peptides were determined by qRT-PCR during a 24-hours time-period in a light-dark cycle in 4-hour-intervals at 2am, 6am, 10am, 2pm, 6pm and 10pm. *Bmal*, a component of the circadian clock with a known rhythmic expression behavior, was selected as control and shows normal expression curve with a maximum in the evening and a minimum around noon (A). *Ilp1*, *ilp2*, *ilp3* and *ilp4* have their peaks of expression in the early morning at 6am, when light was switched on after 8h of darkness (B-E). In the course of the light period, expression levels of *ilp1*, *ilp2*, *ilp3* and *ilp4* decrease and their curves stay flat until 2am. No additional peak of expression is observed for *ilp1*, *ilp2*, *ilp3* and *ilp4*. (F) Compared to 10am and 2pm, *ilp5* expression levels are elevated in the early morning between 2am/6am and in the evening at 6pm. Dataset consists of 4 biological samples and 2 technical replicates each; *rps9* was chosen as reference gene to determine relative expression levels;



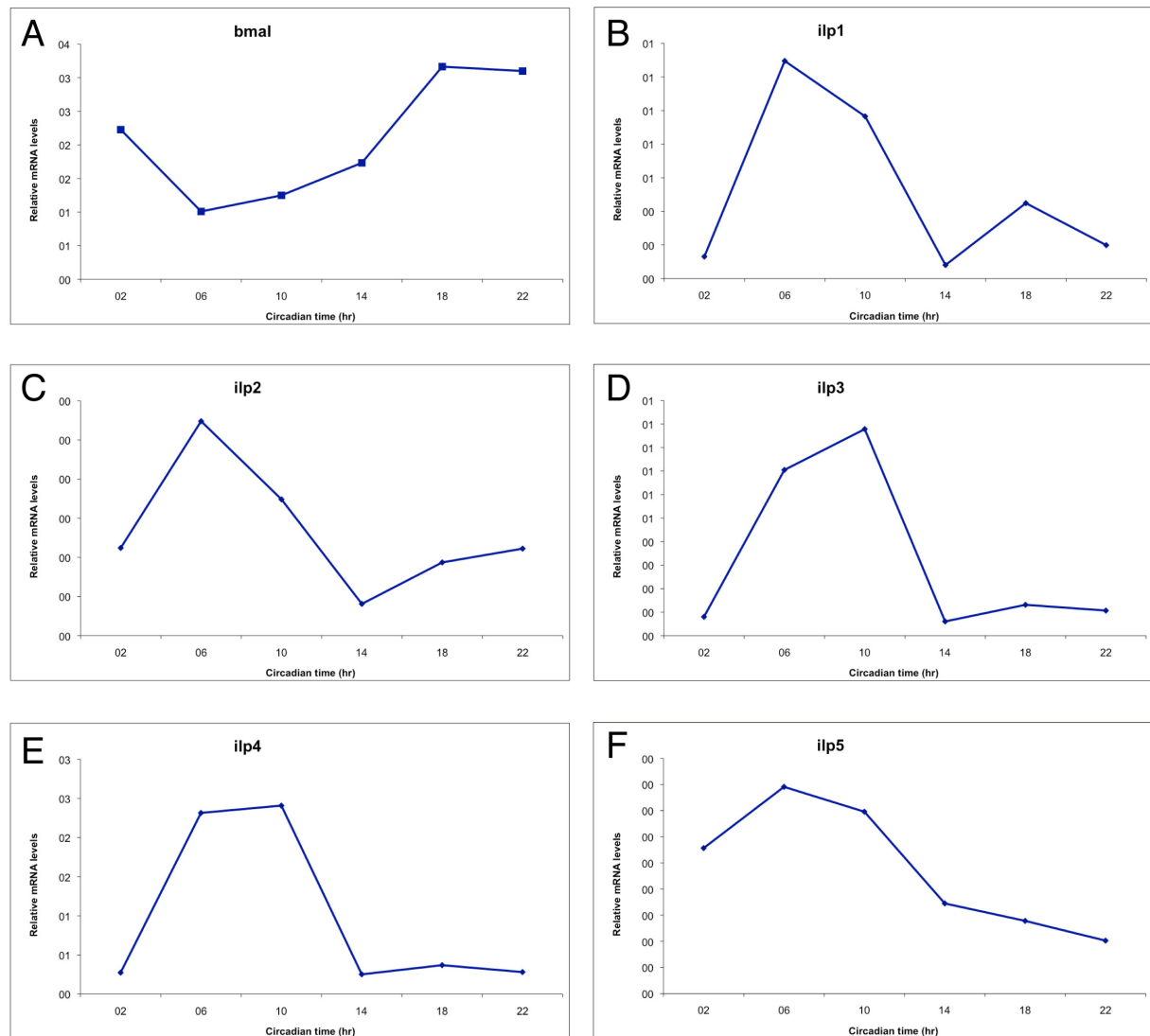


**Figure 24: Relative expression of insulin-like peptides under constant darkness**

Relative expression levels of insulin-like peptide mRNA were determined during a 24-hours time-period under constant darkness in 4-hour intervals at 2am, 6am, 10am, 2pm, 6pm and 10pm. The clock component *bmal* was chosen as control gene and shows a normal expression behavior (A). (B-F) Relative expression levels of insulin-like peptides. All insulin-like peptides show high relative expression levels in the early morning that decrease during the course of the day. *Ilp1* (B) and *ilp2* (C) show a smaller peak of expression in the late afternoon, whereas other insulin-like peptides have only a single peak of expression (D, E, F). Dataset consists of 2 biological samples with 2 technical replicates each; *rps9* was chosen as reference gene to determine relative expression levels.

### 2.2.3.3. Insulin-like peptides are expressed in a constant number of cells during the day

In the previous section (2.2.3.1.), daily fluctuations of *Platynereis* insulin-like peptide levels were observed. To examine if these temporal fluctuations of insulin-like peptide expression levels are due a changing number of cells that express insulin-like peptides during the day, I performed in-situ stainings for insulin-like peptides on heads of atokous worms at two different time-points. In-situ stainings were performed with samples at 6am (high levels of ilp-expression) and 6pm (low levels of ilp-expression), respectively. No difference in the number of cells was observed when counting insulin-like peptide expressing cells at the peak of insulin-like peptide (6am) expression and comparing to the number of cells at minimal expression levels (6pm). This implies that fluctuations in insulin-like peptide expression levels are not due to changing numbers of ilp-expressing cells.

## 2.3. Establishing transgenesis in *Platynereis dumerilii*

### 2.3.1. Transposase activity in *Platynereis dumerilii*

In order to generate suitable reporter constructs for transgenesis in *Platynereis*, three different transposon systems that have been proven to be useful in a broad range of animals were selected and tested in this study. Two of the systems tested in this study belong to the Tc1/mariner superfamily of transposable elements, the Minos transposon and the Mos1 transposon. Minos transposable element has been first identified in *Drosophila hydei* (Franz and Savakis, 1991), Mos1 transposon was first isolated from *Drosophila mauritiana*. The third transposon tested in this study, was the hAT/Tol2 element from the medaka fish *Oryzias latipes*. Target vectors for all three transposon systems were re-engineered to carry compatible I-SceI meganuclease restriction sites that allowed to introduce I-SceI-flanked reporter constructs without further modifications.



### 2.3.1.1. Minos Transposase mediates genomic integration of reporter constructs in *Platynereis dumerilii*

Firstly, I wanted to investigate if the Minos transposon is an appropriate system to establish transgenesis in *Platynereis*. A. Pavlopoulos has previously demonstrated that Minos transposase injected as mRNA into *Platynereis* zygotes is converted into an active enzyme that is capable to excise a reporter construct from a donor vector. For this purpose, he used a PCR-based approach as it was shown before for the crustacean *Parhyale hawaiiensis* (Pavlopoulos et. al., 2005).

To test if Minos transposase integrates a reporter construct into the *Platynereis* genome, I performed microinjections of the pMi{tuba::egfp}<sup>FRKT555</sup> reporter construct along with synthetic Minos mRNA into *Platynereis* zygotes. F.Raible generated the construct pMi{tuba::egfp}<sup>FRKT555</sup> and K.Tessmar showed that it recapitulates faithfully the early endogenous expression of tuba, a gene expressed in ciliated cells of *Platynereis* larvae (Figure 25A). Injected larvae were screened for reporter expression between 24h and 48h after injection and after five days of development. At five days of development, in 12% of the surviving larvae the complete endogenous tuba expression was recapitulated by egfp expression. To investigate if the tuba::egfp reporter construct was integrated into the *Platynereis* genome, 6 animals were tail-clipped after two month of development and genomic DNA was extracted from the clipped tails. Genomic Southern hybridization with a radiolabeled egfp probe revealed specific signals in 3 out of the 6 tested animals and 1-3 integrations of tuba::egfp per genome were detected (Figure 25B).

To examine flanking genomic regions of integration sites, I performed Thermal-Asymmetric-Interlaced PCR (TAIL-PCR). As shown for Arabidopsis (Liu et al., 1995) TAIL-PCR is an effective tool to amplify genomic sequences adjacent to insertion sites of genes from a minimal amount of starting material. Nested specific primers for TAIL-PCR that anneal to the Minos terminal repeats were designed and two specific amplicons of 500bp and 150bp in size for the right terminal repeat were obtained (Figure 25C). Sequencing of both amplicons revealed two independent integration events and in both cases the reporter plasmid was not cut precisely at the ends of the terminal repeat. Instead, in one case the last 10 nucleotides of the terminal repeat were absent and in the other case the cleavage of the reporter was shifted by 13 nucleotides into the donor sequence. Integrations of Minos occur randomly in the genome, but a TA dinucleotide is used for insertion (Franz et. al., 1994; Metaxakis et.al., 2005). The TA dinucleotide is duplicated upon integration, which leads to a characteristic TA

signature located at insertion sites of the Minos transposon. The TA signature was present in one of the TAIL-PCR amplicons whereas the other fragment had an AA dinucleotide at the insertion site.

To test if a transgene can be detected from minimal amounts of starting material, an egfp-specific PCR on the 6 pMi{tuba::egfp}<sup>FRKT555</sup>-injected individuals that were included in the Southern hybridization was performed. In accord with the results from the Southern hybridization, an egfp fragment was amplified from those individuals that were tested positive for genomic integrations of tuba::egfp (Figure 25 D).

Tail-clipped individuals regenerated their tails and were used for breeding. After breeding of pMi{tuba::egfp}<sup>FRKT555</sup>-injected animals, their offspring was screened for tuba::egfp expression but no egfp expression was observed in about 50 batches.

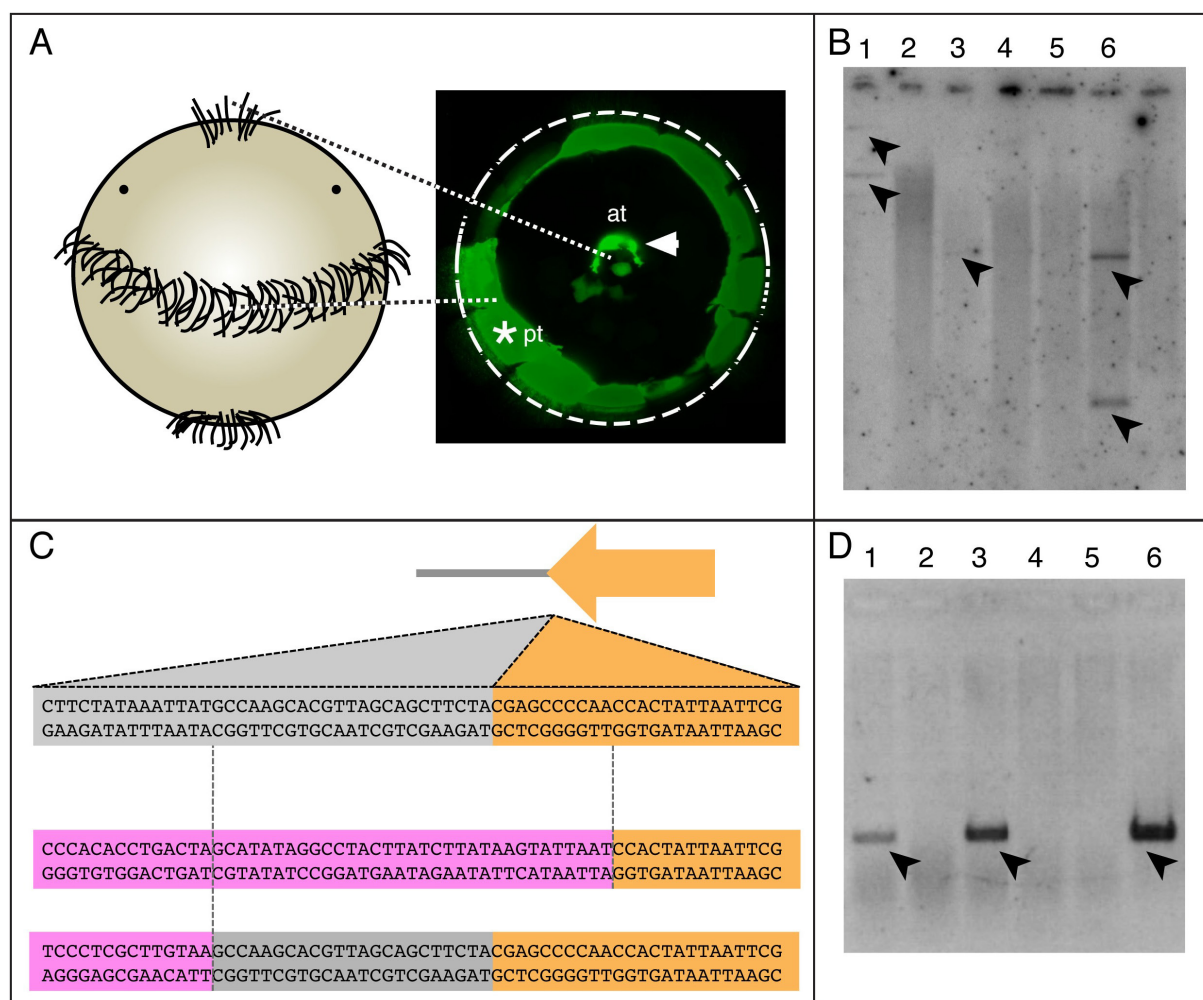


**Figure 25: Genomic integrations of Minos-derived reporter constructs**

(A) Fluorescent reporter construct driving EGFP expression in ciliated cells of trochophore larvae (fluorescence image by K. Tessmar-Raible; apical view). (B) Southern blot revealed genomic integrations of Minos-derived reporter constructs in 3 out of 6 tested animals (black arrowheads). (C) Sequencing of genomic insertion sites revealed that excision of the reporter from the donor vector occurred imprecisely, resulting in integrated reporter constructs that lack the end of their terminal

repeats or have retained vector sequence in their genomic insertion sites. TR sequences are labeled in orange, vector sequences in grey and genomic sequences are labeled in purple. (D) PCR-amplification of *egfp* sequence as an assay to test for genomic insertions of reporter constructs (black arrowheads). Genomic DNA used in (B) and (D) derived from the same 6 individuals.

### 2.3.1.2. Transient Expression of reporter constructs using *tol2* Transposase

Secondly, I wanted to explore if the *tol2* transposon system is a suitable tool for transgenesis in *Platynereis*. I wanted to assess if injected *tol2* mRNA is efficiently converted into an active transposase enzyme in living animals. I used a PCR-based approach to test the *tol2*-dependent excision of a reporter construct from a donor vector. Primers that match vector-specific sequences outside the *tol2* terminal repeats were designed (Figure 26A). I expected that if the co-injected transposase mRNA led to the enzymatically active transposase, these primers should amplify a distinct, small donor fragment of about 200bp in length in an mRNA-dependent fashion. Four hours after zygotes were injected with pTol2{rps9::egfp}<sup>FRKT868</sup> with and without synthetic *tol2* transposase mRNA, PCR was performed on pooled embryos. The PCR fragment of expected size was obtained only from embryos that were co-injected with pTol2{rps9::egfp}<sup>FRKT868</sup> along with *tol2* mRNA and not from embryos that were injected with pTol2{rps9::egfp}<sup>FRKT868</sup> only (Figure 26 B). Sequencing of the PCR fragment revealed that on both ends of the terminal repeats the vector was cut precisely and that both ends of the donor were joined after excision (Figure 26A).

Next, I wanted to investigate if the presence of *tol2* transposase mRNA in the injection solution has an effect on the expression of the ubiquitously expressed reporter construct pTol2{rps9::egfp}<sup>FRKT868</sup>. Zygotes were injected with a) pTol2{rps9::egfp}<sup>FRKT868</sup> along with *tol2* mRNA and b) with pTol2{rps9::egfp}<sup>FRKT868</sup> only. Compared to individuals injected without *tol2* mRNA, animals that were injected along with *tol2* mRNA showed a strongly enhanced *egfp* expression three days after injection (Figure 26 C,D).

After 7 days of development, 18% of the animals that were injected with p{Tol2rps9::egfp}<sup>FRKT868</sup> and *tol2* transposase showed ubiquitous *egfp* expression. In individuals ubiquitous *egfp* expression persisted throughout lifetime (Figure 26E,F). To determine if *tol2* transposase mediated genomic integrations of pTol2{rps9::egfp}<sup>FRKT868</sup>, genomic Southern hybridization with radiolabeled *egfp* as a probe was performed. Southern

hybridization revealed specific signals in two out of four tested individuals indicating that *rps9::egfp* was integrated into the *Platynereis* genome (Figure 26G).

To assess if the reporter construct was cleaved and integrated precisely at the end of its terminal repeats and to examine the genomic insertion site, I performed TAIL-PCR on individuals injected with *pTol2{rps9::egfp}<sup>FRKT868</sup>* and *tol2* mRNA. Nested specific TAIL primers that match to regions between the *tol2* terminal repeats and the I-SceI cloning site of the reporter construct were designed. A fragment of 400bp in length from the left terminal repeat was amplified by TAIL-PCR and sequenced (Figure 26H). The sequence of the fragment revealed that the reporter construct was cleaved precisely at the end of the terminal repeat and was integrated into the *Platynereis* genome.

Although reporter expression in individuals was observed throughout lifetime, no reporter expression was found in the offspring of in total 168 injected individuals. To determine if the *egfp* gene is present in the offspring, *egfp*-specific PCR was performed. In one out of 8 batches tested in the PCR the *egfp* fragment was detected indicating that the reporter construct is inherited to the next generation (Figure 26I).

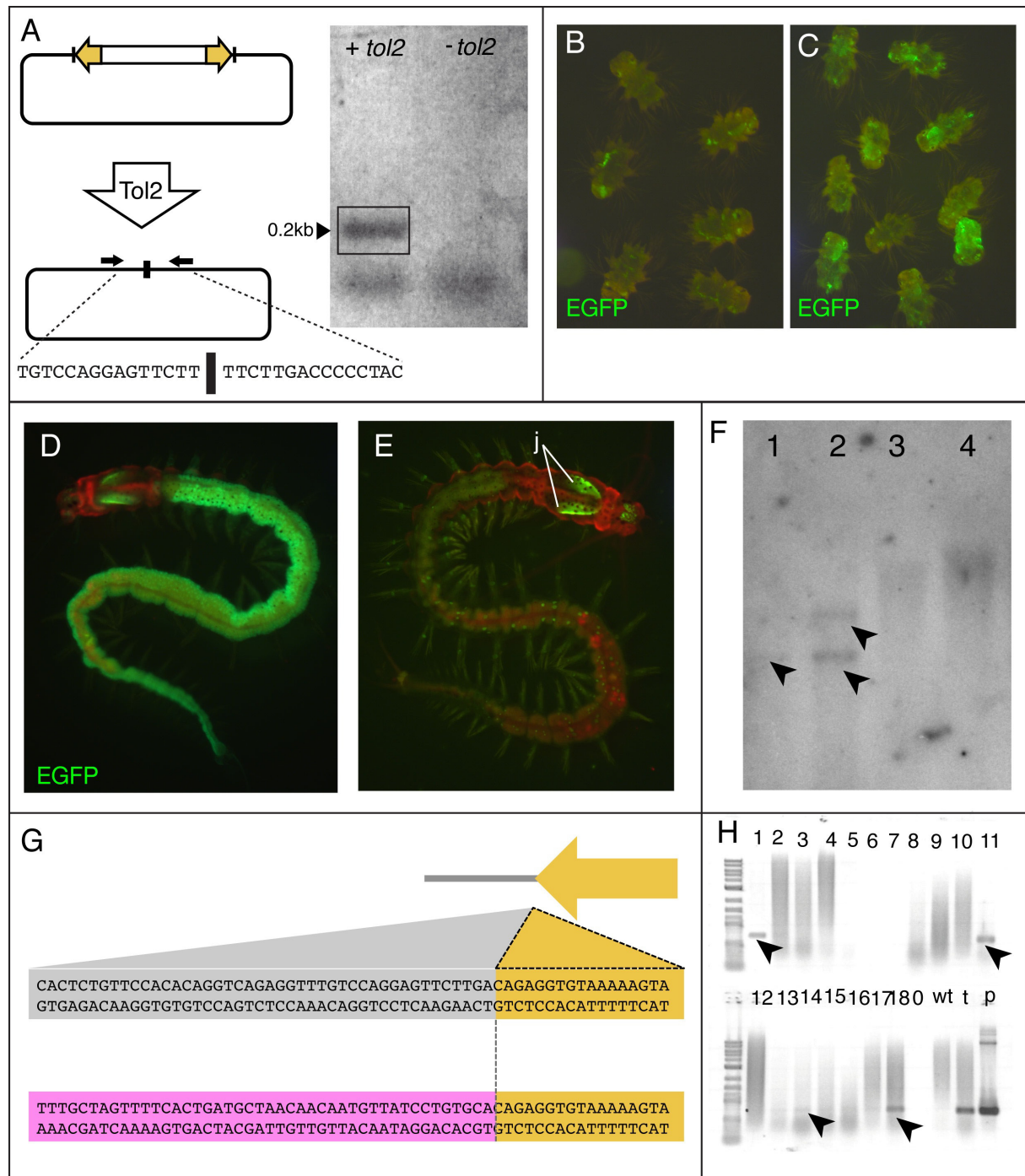


**Figure 26: Tol2 transposase activity and F<sub>0</sub> transgenesis of a Tol2-based ubiquitous fluorescent reporter construct delivered by microinjection.**

(A) Tol2 transposase mediates the excision of the reporter construct from the donor vector. PCR using vector-specific primers (arrows) yields a 200bp PCR fragment specifically from embryos co-injected with *tol2* transposase mRNA (left lane) compared to controls (right lane). Sequencing of two subcloned PCR fragments revealed precise cleavage of the reporter construct at the Tol2 TR (bottom). (B-E) Tol2 transposase causes long-lasting reporter activity; pTol2{rps9::egfp}<sup>frkt868</sup>-injected animals co-injected with *tol2* mRNA (B) show significantly stronger Egfp fluorescence (green arrow) than those without transposase (C) (ae: autofluorescence around the adult eyes). Egfp expression (green arrows) two months after injection with pTol2{rps9::egfp}<sup>frkt868</sup> along with *tol2* mRNA (D) compared to a non-injected animal (E). Note autofluorescent signal of the jaws (j) as well as the iridophore pigments (p) in both the head and trunk. (F) Detection of genomic insertions of Tol-derived reporter constructs in 2 out of 4 tested animals by southern Hybridization with radiolabeled probe for egfp. Sequencing of subcloned

TAIL-PCR fragments revealed precise cleavage at the end of the Tol2 TR (yellow) and insertion into a genomic locus (purple) of Tol2-derived reporter construct (G). (H) PCR-amplification of egfp fragment from injected individuals (lanes 9-18) and their offspring (lanes 1-8) indicate presence of the reporter construct. PCR-controls: 0: water control; wt: wildtype genomic DNA; t: EGFP transgenic DNA; p: EGFP plasmid.

### 2.3.1.3. Heritable genomic integrations and expression of reporter constructs using Mos1 transposase

The third transposon system I studied in *Platynereis* was the Mos1 transposon. Similar to minos and tol2 transposase, enzymatic activity of Mos1 transposase in *Platynereis* was determined using a PCR strategy. The excision assay with PCR primers that anneal to donor vector sequences outside the Mos1 terminal repeats revealed that Mos1 is converted into an active enzyme in *Platynereis* and sequencing of five different amplicons revealed that cleavage of mos1 transposase is less precise than for tol2. Typically, amplicons were lacking donor specific sequences directly adjacent to one of the terminal repeats and retained fragments of the terminal repeat flanking the other side of the reporter construct (Figure 27A-C). In all amplicons, the TA signature characteristic for Mos1 was present.

Reporter construct pMos{rps9::egfp}<sup>FRKT1074</sup> was used to test if the presence of Mos1 transposase enhances egfp expression. In contrast to tol2 transposase, animals that were co-injected with pMos{rps9::egfp}<sup>FRKT1074</sup> and Mos1 transposase showed no significant increased of egfp expression after 3 days compared to animals that were injected with pMos{rps9::egfp}<sup>FRKT1074</sup> only (Figure 27D,E). After 7 days of development, 5% of the surviving larvae that were injected with pMos{rps9::egfp}<sup>FRKT1074</sup> showed ubiquitous egfp expression.

Since the PCR excision assay revealed that Mos1 transposase cleaved out the reporter construct unprecisely from the donor, I wanted to assess if Mos1 transposase integrates a reporter construct into the *Platynereis* genome and if the Mos1 terminal repeats were cut precisely at their ends. Therefore, I performed TAIL-PCR with nested specific primers that bind the Mos1 terminal repeats. A 1kb fragment of the right terminal repeat of the Mos1 transposon was obtained by TAIL-PCR and sequenced (Figure 27 F). The last 71bp of the Mos1 terminal repeat were absent and the sequence continued with *Platynereis* genomic DNA. This finding was in line with the data from the PCR excision assay, indicating that Mos1 transposase cleaves not precisely at the end of the Mos terminal repeats. Moreover, at

the genomic insertion site of the reporter construct, the characteristic TA dinucleotide was present.

Notwithstanding the unprecise cleavage and reduced efficiency compared to *tol2* and *minos* transposases, however, *Mos1*-mediated transgenes are both heritable and functional in the next generations.



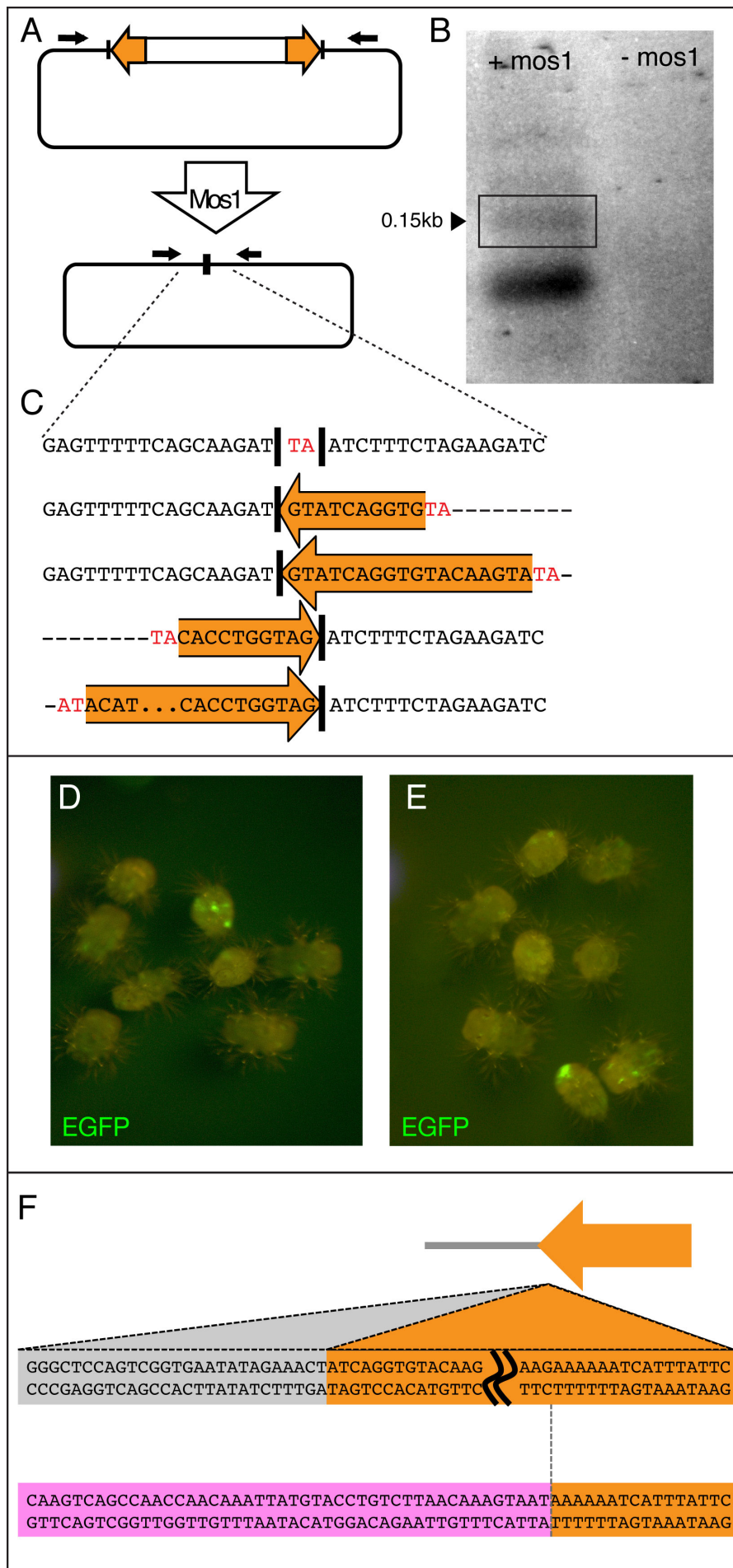




**Figure 27: Mos1 transposase activity and genomic insertions of Mos1-based reporter constructs** (A) Mos1 transposase mediates the excision of the reporter construct from the donor vector. PCR using vector-specific primers (arrows) yields a 150bp PCR fragment specifically from embryos co-injected with *mos1* transposase mRNA (left lane) compared to controls (right lane) (B). Sequencing of five subcloned PCR amplicons revealed occasionally, fragments of the left or the right IR are retained in the donor vector indicating imprecise cleavage of the reporter construct (C). The characteristic TA dinucleotide observed at the cleavage sites is shown in red, retained portions of IR are labeled in orange. Individuals that were injected with reporter plasmid pMos{rps9::egfp} along with synthetic *mos1* transposase mRNA showed no significant increased EGFP expression compared to individuals injected only with reporter plasmid after 3 days of development (D,E). Sequencing of a subcloned TAIL-PCR fragment of a genomic insertion site revealed that the reporter construct lacks part of its terminal repeat (TR), derived from unprecise cleavage of the Mos1 transposase enzyme (F). TR sequences are labeled in orange, vector sequences in grey and genomic sequences are labeled in purple.

### 2.3.2. Generation of stable transgenic reporter lines in *Platynereis dumerilii*

#### 2.3.2.1. A transgenic reporter line for *alpha-tubulin* demarcates ciliated cells of the prototroch

In this study, I established the first transgenic reporter line in *Platynereis* by a transposon-based approach. The reporter construct pMos{tuba::egfp}<sup>FRKT707</sup> was delivered along with synthetic Mos1 transposase mRNA into *Platynereis* zygotes by microinjection.

Out of 409 injected zygotes 176 larvae hatched and 28 individuals were raised until maturity. Transgenic offspring was obtained from two injected individuals. One transgenic batch died after two days of development, the other transgenic batch survived and was subsequently used for further analysis (Figure 28A,B). Southern hybridization of genomic DNA from transgenic individuals of three generations with radiolabeled *egfp* as a probe revealed that the reporter line carries a single integration of the *tuba::egfp* reporter construct which is stably inherited into the next generation and does not re-mobilize on its own (Figure 28C).

In trochophore larvae at 24 hours of development, endogenous *tuba* is prominently expressed in the prototroch, and also shows a specific expression in the cells of the apical ciliary tuft (Figure 28D). In *tuba::egfp* transgenic trochophore larvae, I observed a robust pattern of *egfp* mRNA expression that precisely matched the localization of *tuba* mRNA in both the prototroch and the apical tuft, establishing that the required regulatory regions are included in the reporter construct (Figure 28E). Consistently, live imaging revealed Egfp fluorescence in the same, highly stereotyped pattern (Figure 28F). However, in contrast to endogenous *tuba*

mRNA, *egfp* mRNA is not observed in the metatroch rings, and expression in the prototroch diminishes over the course of metatrochophore development (Figure 28G,H). Moreover, endogenous *tuba* is expressed consistently in the paratroch rings during development from nectochaete larvae to 4-5 segmented errant juveniles (Figure 29A-E), whereas no *egfp* expression is detected in later stages of development of *tuba::egfp* transgenic animals.

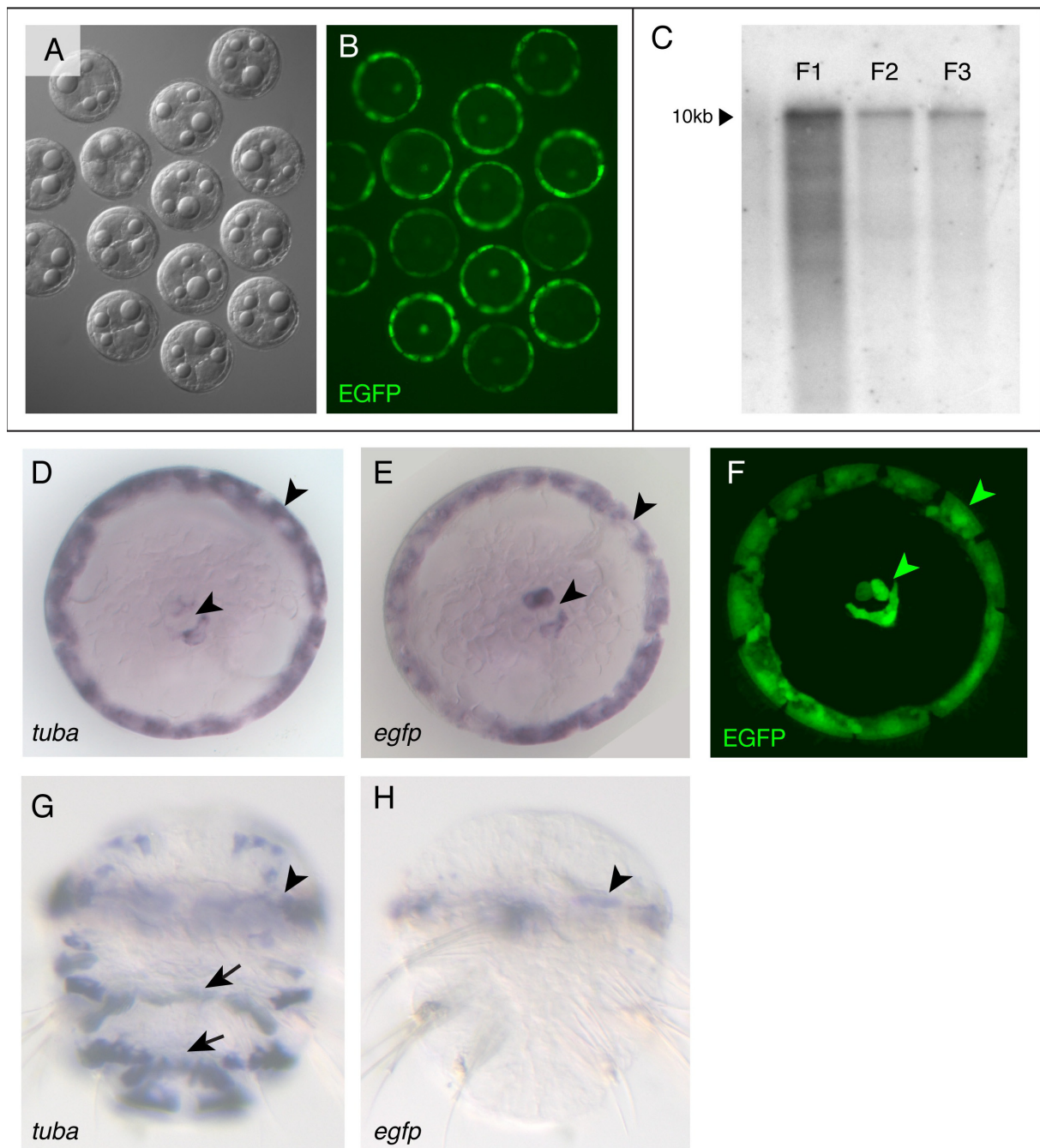


**Figure 28: Stable expression and inheritance of a ciliated cell-specific reporter construct using Mos1-based transgenesis.**

(A,B) Stereotypical expression of  $\text{pMos}\{\text{tuba}::\text{egfp}\}^{\text{frkt707}}$  in transgenic 24h trochophore larvae (A: brightfield image, B: fluorescence image). (C) Stable inheritance of reporter construct. Southern blot of digested genomic DNA reveals a single genomic integration (black arrowhead) of the reporter

construct that is transmitted through three filial generations (F<sub>1</sub>-F<sub>3</sub>). (D) Early endogenous tuba expression in the prototroch (pt) and apical tuft (at) is faithfully recapitulated by Egfp expression in transgenic individuals (E: RNA; F: fluorescence) at 24hpf. (G, H) Discrepancy between expression of *tuba* and *egfp* at 60h of development. Endogenous *tuba* expression (G) is observed in both prototroch (arrowheads) and metatroch (arrow), whereas *egfp* expression (H) is only retained in the prototroch (arrowhead) after 60h of development. A, B, D, E, F: apical views (dorsal to the top), G, H: ventral views (anterior to the top).

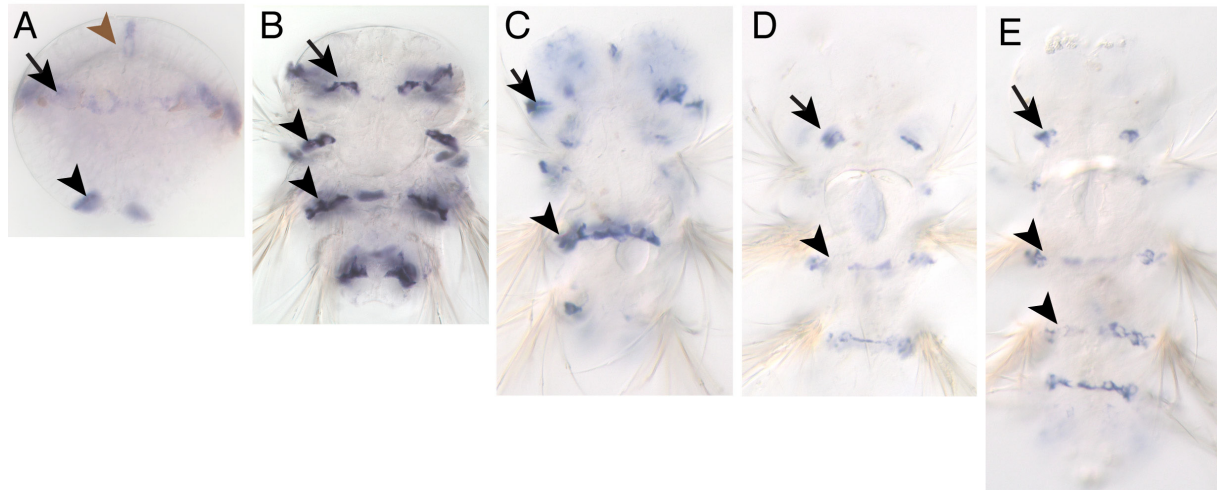


**Figure 29: Expression of *alpha-tubulin* during development**

Expression of *alpha-tubulin* (*tuba*) is detected in the apical tuft (brown arrowhead), the prototroch (black arrow) and the telotroch (black arrowhead) at 24h post fertilization (A). (B-E) During development, tuba expression persists in the prototroch (black arrows) and is expressed in the metatroch rings (black arrowheads) that are added upon elongation of the nectochaete and juvenile animals. Ventral views (anterior to the top)

### 2.3.2.2 phiC31 integrase is active in *Platynereis dumerilii*

The phiC31 integrase has been developed as a tool to cause efficient and site-specific genomic integrations of reporter constructs in model species like *Drosophila melanogaster* (Groth et. al., 2004; Bischof et. al., 2007). The bacteriophage phiC31 encodes for an integrase that mediates sequence-specific recombination between attP and attB sites. Genetically modified individuals that carry an attP site in their genome as a landing platform have been generated. Site-specific integration of a reporter that carries an attB site into the attP site is then mediated by the integrase that is co-delivered along the reporter.

To further optimize transgenesis in *Platynereis*, I tested if the phiC31 integrase system is capable to recombine two plasmids that carry attP and attB sites in *Platynereis* in vivo (Figure 30A). Therefore, the two plasmids (pMos{5'attP-tuba::egfp}<sup>FRKT1031</sup>, pJet{5'attB-rps9::egfp})

were co-injected along with synthetic phiC31 integrase mRNA. Four hours after injection, embryos were collected and PCR-screened for recombination events. Successful recombination events should result in PCR products of about 350bp in length (Figure 30B). Bands of expected size on agarose gel indicate that the phiC31 integrase is active in *Platynereis* and is capable to recombine two plasmids in vivo.

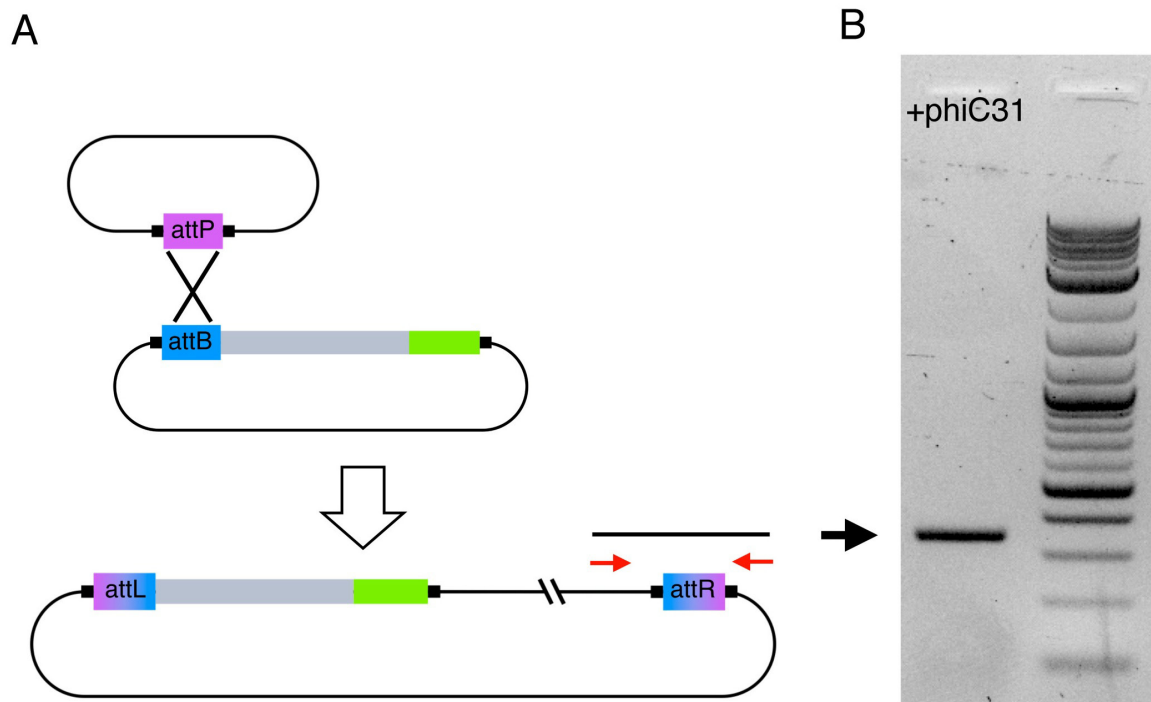


**Figure 30: phi C31 integrase is capable to recombine two plasmids in vivo**  
**(A)** Recombination of a plasmid carrying an attP-site and a reporter plasmid carrying an attB-site is mediated by the phi C31 integrase. **(B)** Successful recombination is monitored by a 350bp PCR

### 2.3.2.3. A transgenic reporter line for *r-opsin* revealed previously uncharacterized photoreceptor cells in *Platynereis dumerilii*

In this study, I generated a transgenic fluorescent reporter line for *r-opsin*, a characteristic marker rhabdomeric photoreceptor cells. To generate the *r-opsin* transgenic line, I used a reporter construct that was established by V. Babu Rajan. A recombineering approach was used to insert a cassette containing egfp-coding sequence into a previously identified bacterial artificial chromosome carrying the *Platynereis r-opsin* locus. A 8kB piece of the

recombineered locus was then amplified and cloned into the modified Mos1 target vector to give rise to the reporter construct pMos{r-opsin::egfp}<sup>FRKT890</sup>.

I injected about 360 zygotes with the pMos{r-opsin::egfp}<sup>FRKT890</sup> reporter construct along with synthetic Mos1 mRNA. 224 larvae hatched and among 44 individuals that had living offspring, I identified one transgenic founder individual that gave rise to the transgenic r-opsin::egfp line. Subsequently, V. Badu Rajan analyzed the transgenic *r-opsin* strain for reporter expression. K. Tessmar and F. Raible observed that EGFP expression in r-opsin::egfp transgenic larvae could be traced from 2 days onwards in the adult eye primordia. After two weeks of development, endogenous *r-opsin* mRNA is expressed prominently in the adult eyes and their neuronal projections connecting the adult eyes towards the medial brain (Figure 31A). Moreover, endogenous *r-opsin* expression is detected in bilateral patches of cells anterior to the adult eyes that were termed as frontal lateral eyelets. I used confocal microscopy to determine in vivo expression pattern of EGFP in two weeks-old r-opsin::egfp transgenic animals. In these animals, I observed robust expression of EGFP that recapitulates precisely the endogenous *r-opsin* expression in the adult eyes including their neuronal projections as well as in the frontal lateral eyelets (Figure 31B). In *r-opsin* transgenic animals, EGFP is consistently expressed in adult eyes and their neuronal projections throughout lifetime. In contrast, EGFP expression in the frontal lateral eyelets diminishes over the course of development and I did not observe EGFP expression in these cells in juvenile worms that had more than 21 segments.

In addition to EGFP expression in cephalic photoreceptors, V. Babu Rajan discovered that the transgenic reporter line also expresses EGFP in cells that are located in the upper lip of the notopod of the parapodia and in cells located on the ventral side of the trunk in the ventral midline and on the parapodial basis in *r-opsin* transgenic worms (Backfisch et. al., 2013). Both of these cell-types have neuronal projections that innervate the ventral nervous system. Endogenous *r-opsin* expression in these newly identified photoreceptors was confirmed by Whole-mount in situ Hybridization by V. Babu Rajan. By analyzing *r-opsin* transgenic individuals, I found that the first EGFP expressing parapodial cells appear in 11-segmented transgenic juvenile worms and that EGFP expression in cells on the ventral side of the trunk appears in 17-segmented transgenic worms. Expression of EGFP in both newly identified photoreceptor cell-types is persistent in r-opsin::egfp transgenic animals throughout lifetime (Figure 31C-F).



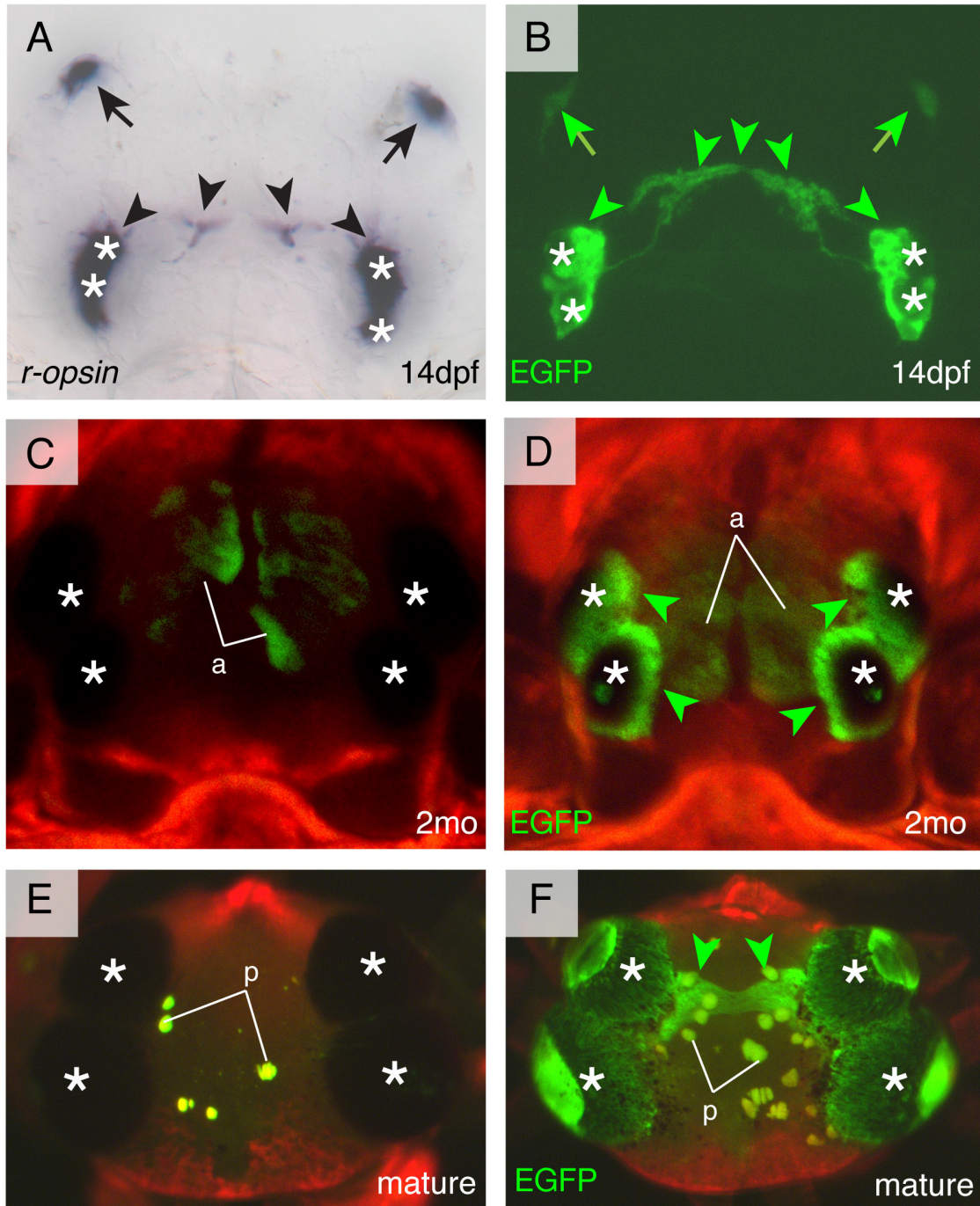


**Figure 31: Stable transgenic expression of an *r-opsin* fluorescent reporter in cephalic photoreceptors**

(A) *R-opsin* mRNA is detected in adult eyes (white asterisks), their neuronal projections (black arrowheads) and the frontal lateral eyelets (black arrows). (B) EGFP expression of a transgenic reporter strain recapitulates endogenous *r-opsin* expression pattern. *R-opsin* transgenic juvenile worms (C) and mature individuals (E) revealed robust EGFP expression throughout lifetime. Note autofluorescent pigments in the head of non-transgenic individuals (a, p). A-D: dorsal views (anterior to the top); E, F: frontal views (dorsal to the top)

### 2.3.3. Molecular specification of non-cephalic photoreceptors

The *r-opsin* transgenic strain that was generated in this study, led to the discovery of previously uncharacterized non-cephalic photoreceptors in *Platynereis dumerilii* (section 2.3.2.3.). To address whether these non-cephalic photoreceptors resemble other non-cephalic photoreceptors like the amphioxus Hesse organ or cephalic eyes in terms of gene-expression, I investigated their molecular specification. For this, I performed whole-mount double in-situ Hybridization after a newly established protocol in atokous worms and 8-days posterior-tail regenerate worms with a set of candidate genes.

#### 2.3.3.1. *Dachshund* correlates with *r-opsin* expression in cells of the ventral trunk

*Platynereis dachshund* (*dach*) was previously reported for its expression in the mushroom bodies in juvenile worms (Tomer et al, 2010). By whole-mount in-situ Hybridization of atokous worms, I identified additional domains of *dach* expression in the adult eyes and the ventral nerve cord (Figure 32A,B). Moreover, in 8-day-old posterior tail regenerated worms *dach* is expressed in the regenerated segments (Figure 32C,C'). It is expressed broadly in the ventral nerve cord and in at least one cell in the anterior part of each regenerating notopod. Transcripts of *dach* are also detectable in cells that could be parapodial ganglia cells judged by their localisation (Winchell et. al. 2010).

To compare the expression pattern of *dach* and *r-opsin* mRNA, I established a new two-color whole-mount in-situ Hybridization protocol based on NBT-BCIP and FastRed staining reactions.

A majority of *r-opsin* expressing cells co-express *dach* gene in the ventral trunk cells. Figure 32D shows co-expression of *r-opsin* mRNA and *dach* mRNA in a cell located in the ventral midline of the adult trunk. In the head, both, *r-opsin* and *dach* correlate in the adult eyes (Figure 32E). In regenerated parapodia, close to 90% of the analyzed cases, an *r-opsin* cell is immediately neighbored by a basally adjacent *dach*-positive cell Figure 32F). In contrast, *dach* expression is not detectable in adult parapodia (Backfisch et. al., 2013).

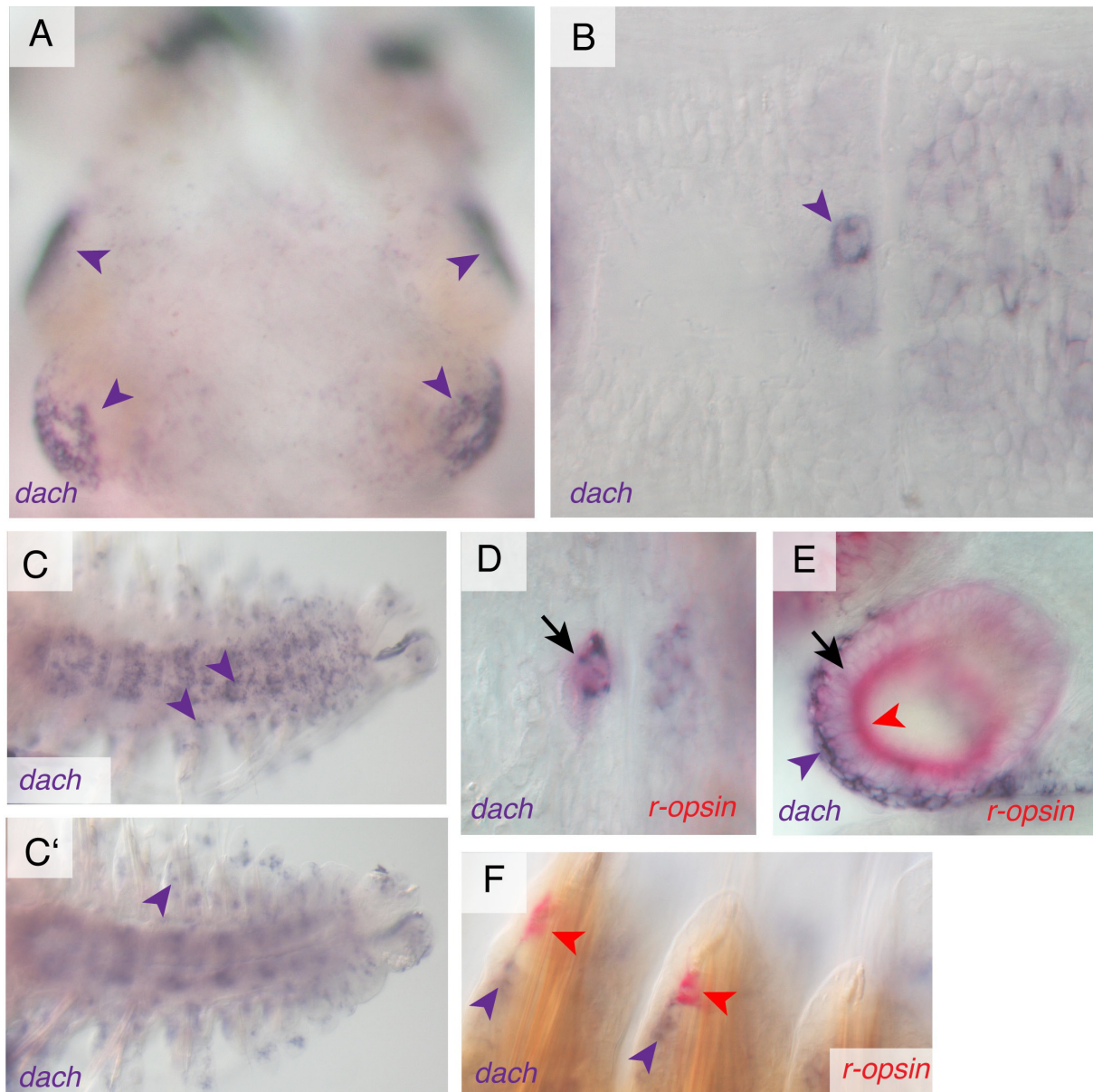


**Figure 32: Expression analyses of dachshund in atokous worms reveal correlations with *r-opsin* in ventral non-cephalic photoreceptors**

(A-C') Expression analyses of *dachshund* (*dach*) in atokous worms. *Dach* is expressed in the adult eyes (A) and cells on the ventral side of the trunk (B). In 8-days posterior regenerated individuals, *dach* is expressed broadly in the ventral nervous system and the parapodial ganglia (C). Moreover, *dach* is detected in cells at the anterior basis of the parapodia of 8-days posterior regenerated worms (C'). Two-color stainings revealed co-expression of *dach* and *r-opsin* in cells of the ventral trunk (D) and the adult eyes (E). In 8-days posterior regenerated segments, *r-opsin* expressing cells are neighbored by *dach*-positive cells (F). A, E: dorsal views; B-D,F: ventral views; arrowheads indicate expression; black arrows indicate co-expression.



### 2.3.3.2. Correlating *pax6* and *r-opsin* expression

#### 2.3.3.2.1. *Pax6* and *r-opsin* are co-expressed in the frontal lateral eyelets of juvenile worms

Firstly, I investigated a possible correlation of *r-opsin* and *pax6* expression in cephalic Photoreceptors. As shown above, cephalic *r-opsin* expression is detected in adult eyes and in the frontal lateral eyelets. It has been shown that *Platynereis* adult eyes develop via a *pax6*-independent mechanism that uses *So/Six* genes but *Platynereis* larval eyes express *pax6* (Arendt et. al., 2002). From the previous studies, it remains unclear if the frontolateral eyelets are remnants of the larval eye, or if larval eyes are reduced after the second day of development.

To investigate *pax6* and *r-opsin* expression synchronously in the frontolateral eyelets, I performed two-color fluorescent in-situ Hybridization in 14-days-old errant juveniles after established protocols. *Pax6* is broadly expressed in ventro-lateral domains of the brain and expression analyses revealed that *pax6* and *r-opsin* are co-expressed in the frontolateral eyelets (Figure 33 A-F) (Backfisch et. al., 2013).

#### 2.3.3.2.2. No correlation of *pax6* and *r-opsin* in atokous worms

Secondly, I examined the expression pattern of *pax6* in the trunk of atokous worms and correlated *pax6* expression to *r-opsin* positive cells. *Pax6* expressing cells that are dispersed over the adult ventral trunk were identified but no correlation to *r-opsin* expression is found in these cells (Figure 34A). Moreover, *pax6* is not expressed in the parapodial notopod of adult segments. In 8-day-old posterior tail regenerated worms, *pax6* expression is detected in longitudinal columns along the regenerating ventral nervous system and in single cells located at the posterior basis of the regenerating parapodial notopod (Figure 34 B,B'). In contrast, *r-opsin* expressing cells are located in the anterior upper lip of each of the regenerating notopods and dispersed on the ventral side of the regenerated segments. No co-expression of *pax6* and *r-opsin* has been observed in posterior tail regenerated worms (Figure 34 C,D,D') (Backfisch et. al., 2013).

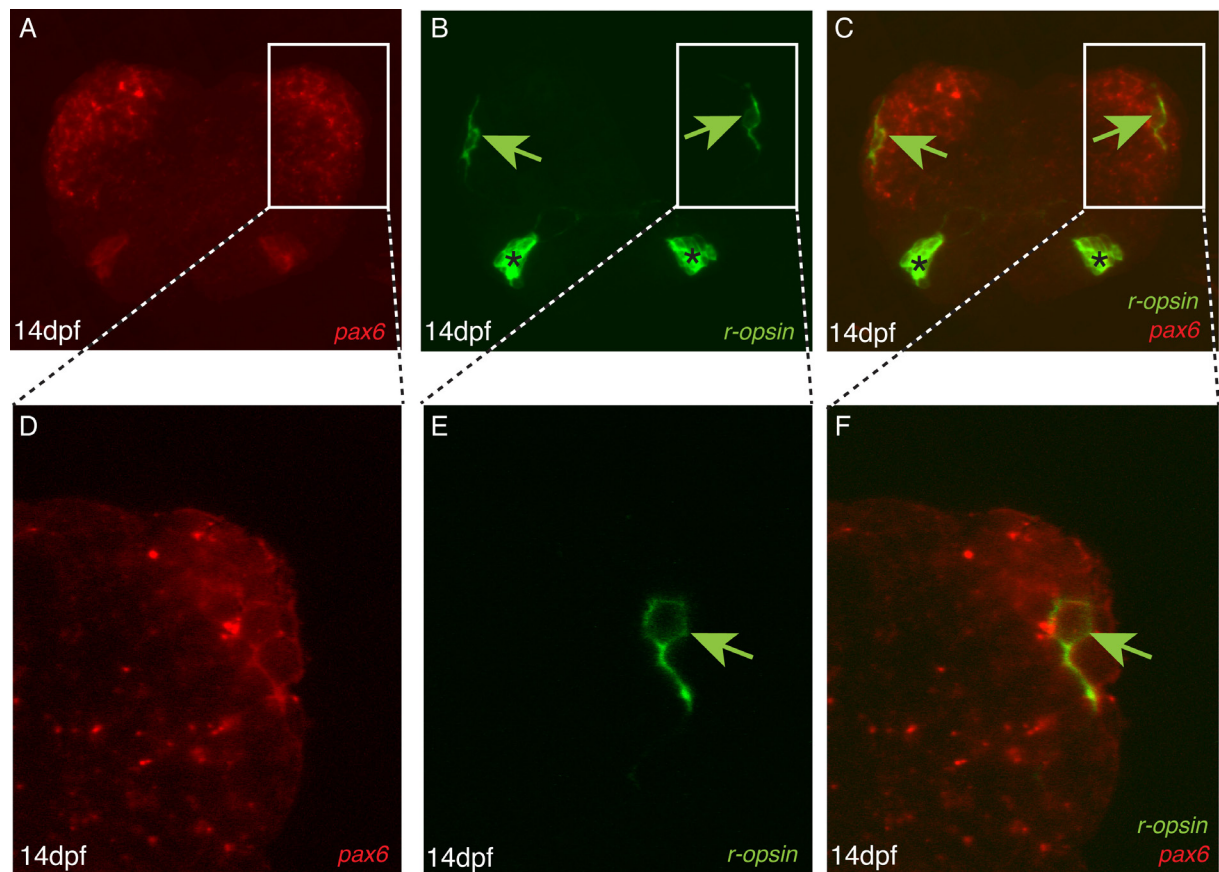


**Figure 33: Co-expression of *r-opsin* and *pax6* in frontal lateral islets**

Fused stacks (z-projections) of confocal images on double-fluorescent WMISH. (A,C,D,F) *pax6* expression detected in red; (B,C,E,F) *r-opsin* expression detected in green. (D-F) larger views of areas boxed in panels A-C. Green arrows point at frontolateral eyelet PRCs, asterisks mark the adult eyes. All panels are dorsal views, anterior to the top.

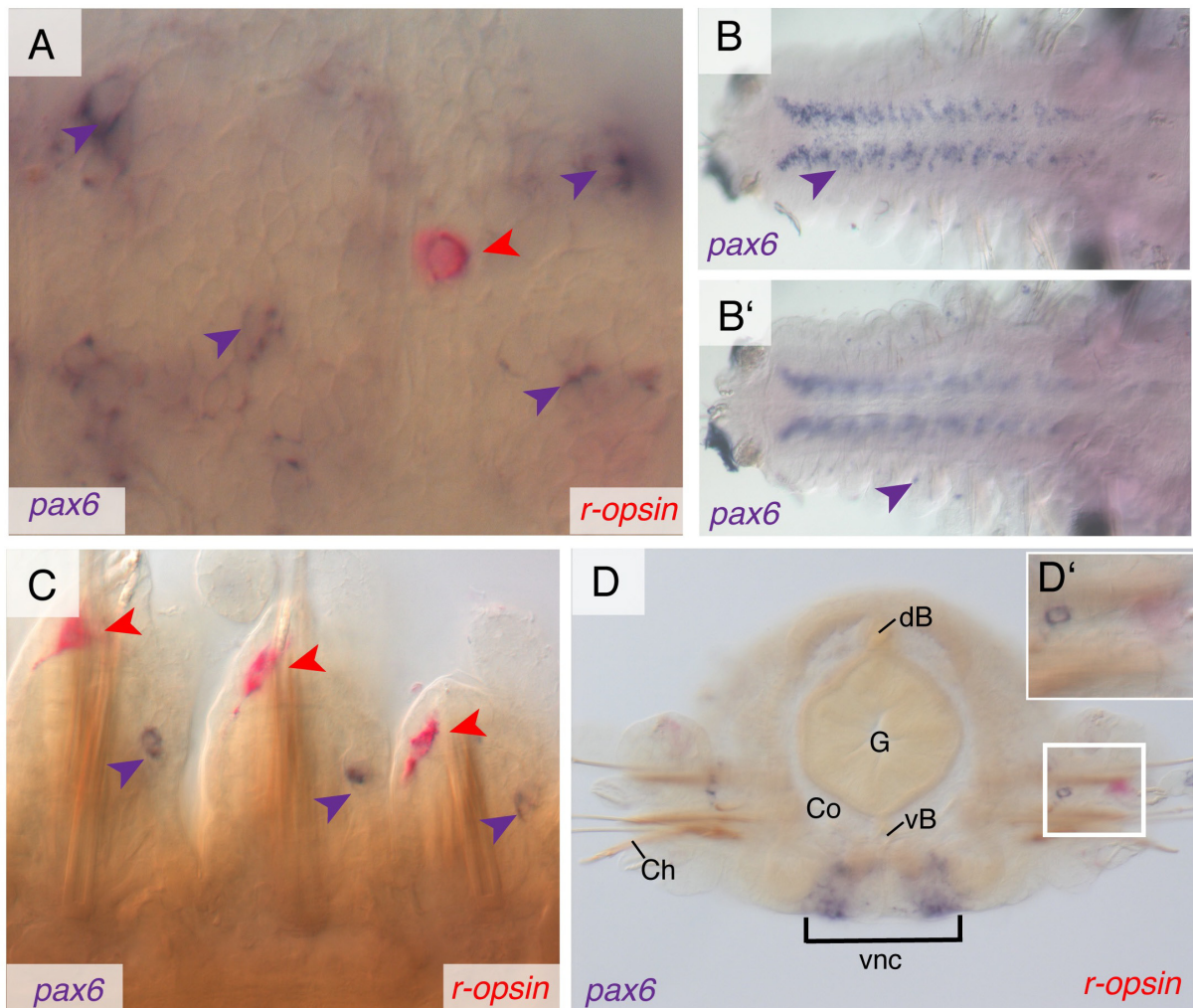


**Figure 34: Expression analyses of *pax6* in atokous worms reveal *pax6*-independent non-cephalic photoreceptors**

Two-color stainings show distinct cells *pax6* and *r-opsin* expressing cells in the ventral trunk (A). In 8-days posterior regenerated worms, *pax6* is expressed in longitudinal columns along the regenerating ventral nervous system and in single cells located at the posterior basis of the regenerating parapodial notopod (B, B'). Two color stainings in posterior regenerated individuals revealed that *r-opsin* expressing cells are distinct from *pax6* expressing cells (C, D, D').

A-C: ventral views; D,D': frontal view; dB: dorsal blood vessel; vb: ventral blood vessel; g: gut; Co: coelom; Ch: chaete; vnc: ventral nerve cord; white rectangle indicates in D indicates region shown in D'.

### 2.3.3.3. *G(q)* is present in photoreceptor cells

To assess if *r-opsin* positive cells function as photoreceptors, I cloned the *Platynereis* orthologue of *G(q)* a specific G alpha subunit that is required for signal transduction in *r-opsin*-based Photoreceptors and commonly associated with these cells (Figure 35A).

In atokous worms, expression the pattern of *r-opsin* and *g(q)* match perfectly in all cells that were observed. *G(g)* and *r-opsin* are co-expressed in the adult eyes, the cells of the ventral trunk, parapodial notopod and in 8-day-old posterior tail regenerated worm segments (Figure 35B-E). The tight correlation of *r-opsin* and *g(q)* expression supports the hypothesis that *r-opsin* positive cells function as photoreceptors in *Platynereis* (Backfisch et. al., 2013).

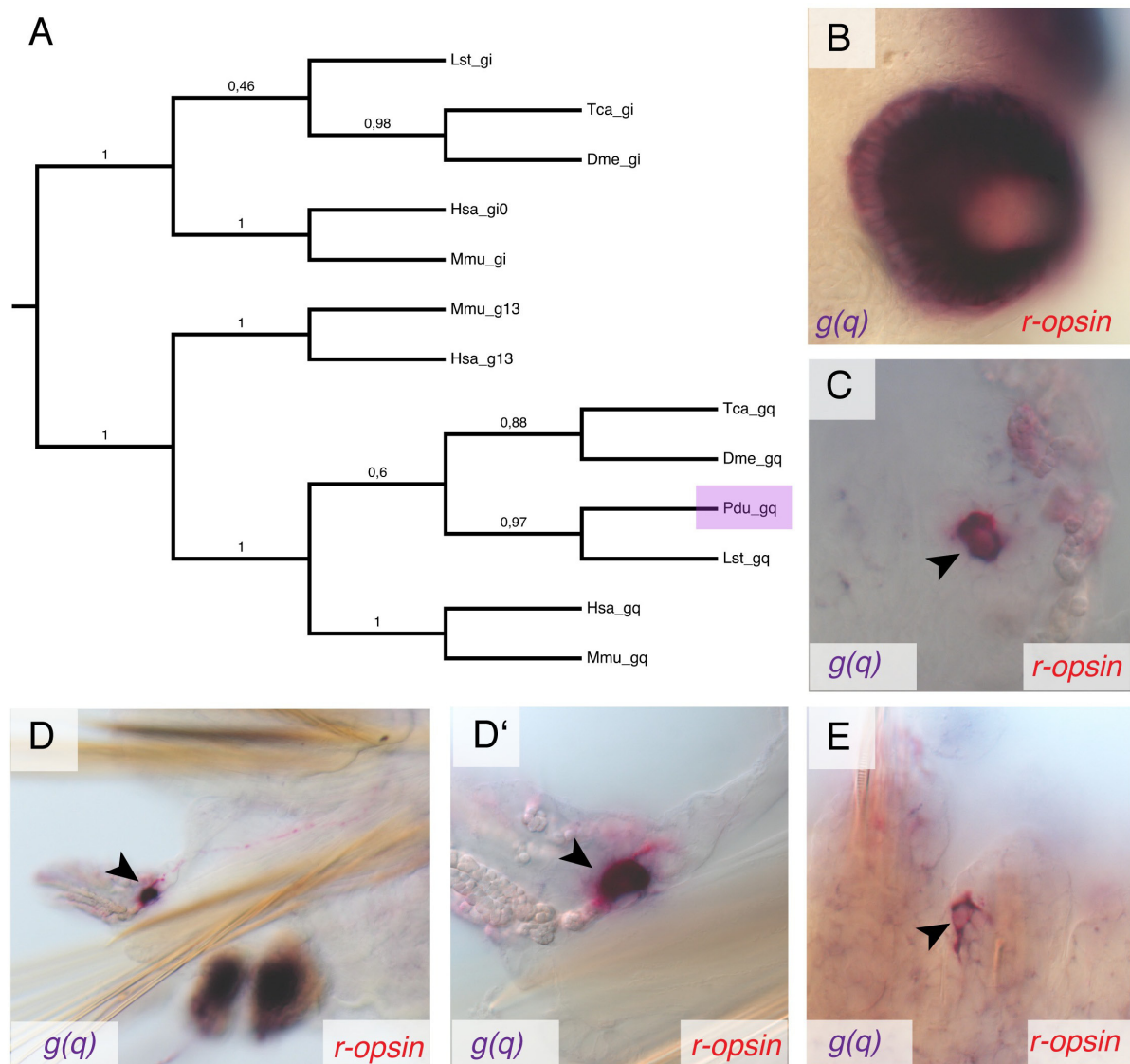


**Figure 35: *Platynereis g(q)* demarcates photoreceptor cells**

(A) An orthologue of the G-alpha subunit q (*g(q)*) was identified in *Platynereis* (purple rectangle). Two-color stainings revealed co-expression of *g(q)* and *r-opsin* in the adult eyes (B) and non-cephalic

photoreceptors of the ventral trunk (C) and the parapodia (D, D'). (E) Co-expression of *r-opsin* and *g(q)* in parapodial cells of 8-days posterior regenerated worms.  
B: dorsal view; C, E: ventral views; D,D': frontal views of sections through segments.

#### 2.3.3.4. *brn3* is detected in *r-opsin* neighboring cells

The *brn3* family members of POU domain transcription factors are involved in the development of sensory neurons in vertebrates (Xiang et. al., 1995). In *Platynereis*, a single orthologue of the *brn3* family was identified and cloned previously by K. Tessmar-Raible. Firstly, I examined *brn3* expression in atokous worms and detected *brn3* positive cells that are located in the upper lip of the parapodial notopod (Figure 36A). Secondly, in 8-day-old posterior tail regenerated individuals *brn3* expression is detected in longitudinal patches of cells along the ventral nerve cord and in the parapodial ganglia of the newly formed segments (Figure 36B). Moreover, *brn3* expression is detected in distinct cells in the developing parapodia.

Co-expression analyses by two color in-situ stainings revealed that in adult parapodia a *brn3* expressing cell is directly adjacent to the *r-opsin* expressing cell of the upper lip of the notopod (Figure 36C). In regenerating parapodia, the first *r-opsin* expressing cells are accompanied by a *brn3* expressing cell (Figure 36D) (Backfisch et. al., 2013).

#### 2.3.3.5. *pax2/5/8* is expressed in regenerated tails

I cloned the *Platynereis* paired box gene *pax2/5/8*, the orthologue of the vertebrate *pax2*, *pax5*, *pax8* proteins and the *Drosophila sv/spa* to investigate its expression in atokous and 8-day-old tail posterior regenerated worms. *Pax2/5/8* was detected only in the regenerated segments and not in adult body parts by in-situ Hybridization. *Pax2/5/8* is expressed broadly in the epithelial cell layer of the regenerated part, most prominently in the dorsal and the parapodial epithelia (Figure 36E).

Two-color in-situ stainings revealed that the *r-opsin* expressing cells are located adjacent to the *pax2/5/8*-positive domains in the regenerated segments (Figure 36F). Around 80% of the observed *r-opsin* positive cells are found directly adjacent to the *pax2/5/8* expression domains (Backfisch et. al., 2013).



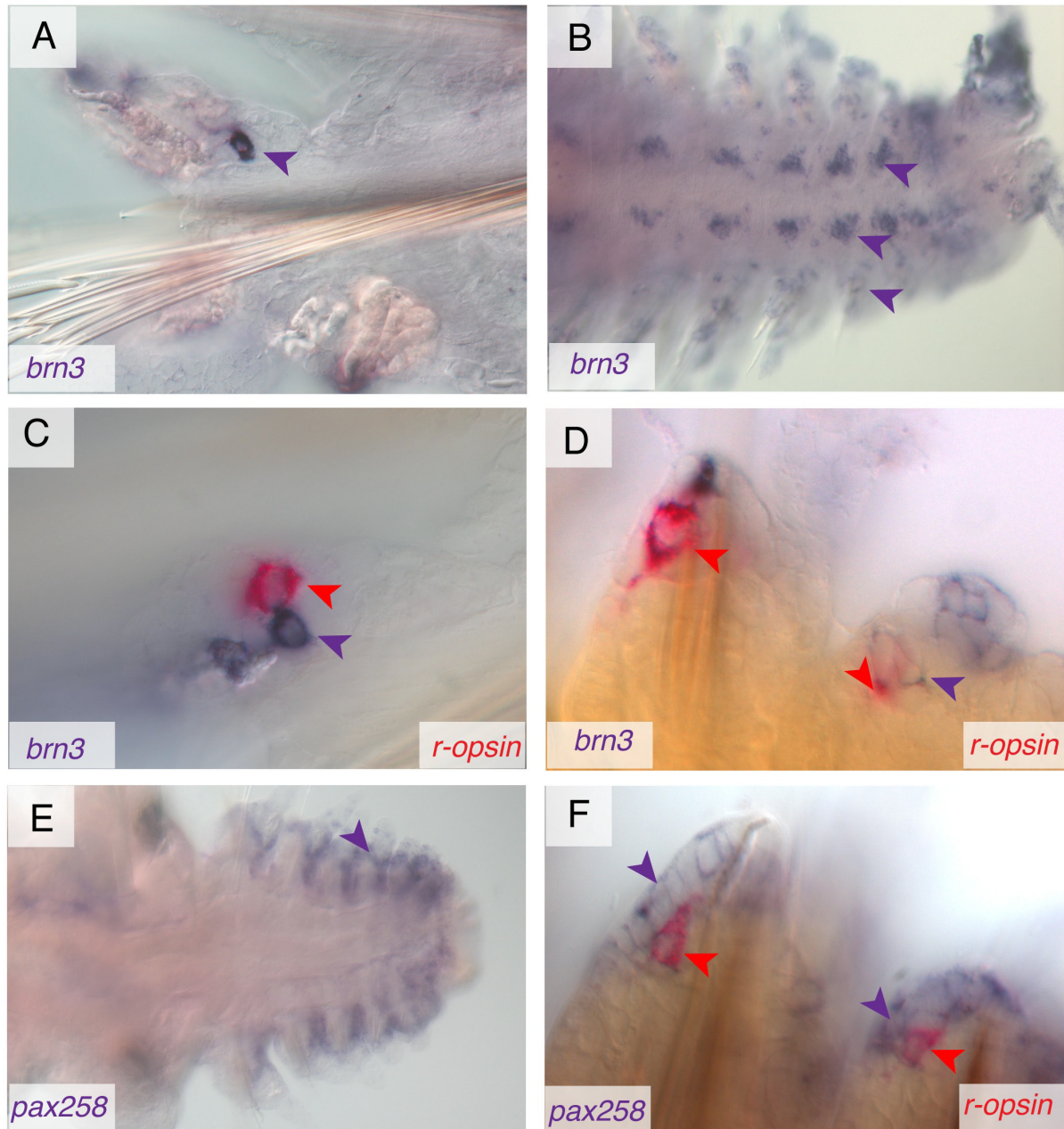


**Figure 36: Expression of *brn3* and *pax2/5/8* in cells adjacent to non-cephalic photoreceptors**

Expression analyses of in atokous worms revealed *brn3* expressing cells in adult parapodia and cells located in the developing ventral nervous system, parapodial ganglia and parapodia in 8-days posterior regenerated worms (A, B). Two-color staining show *brn3* expressing cells in the adult (C) and developing (D) parapodia that are immediately neighboring an *r-opsin* expressing cell. *Pax2/5/8* is expressed broadly in the dorsal epithelium of 8-days posterior regenerates (E). Two color stainings show an *r-opsin* expressing cell directly adjacent to the *pax2/5/8*-positive region in the regenerated part of an animal (F). A, C: frontal views of sections through segments; B, D, E, F: ventral views





### 3. Discussion

#### 3.1. Expanding the molecular toolkit to study cell types in *Platynereis* larvae and at postlarval stages

*Platynereis dumerilii* has emerged as a key reference species for annelids and has made significant contributions to the fields of evolutionary and developmental biology (Fischer and Dorresteijn 2004; Fischer et. al., 2010). However, methods to study cell types over a longer period of time during development were not available in *Platynereis* until now. In this study, I have developed robust protocols for transient transgenesis and established the first transgenic reporter strains in *Platynereis*. Moreover, I have optimized in-situ Hybridization protocols to study gene-expression patterns at postlarval stages and established two-color in-situ staining procedure to investigate co-expression of genes.

##### 3.1.1. The tol2 transposon is a powerful tool for transient transgenic approaches in *Platynereis dumerilii*

Transient transgenic approaches are widely used to generate transgenic organisms. For instance, zygotic microinjections of linearized reporter constructs result in robust reporter gene-expression and have become a standard methodology for transgenic approaches in sea urchin (Franks et. al., 1990; Franks et. al., 1988; Arnone et. al., 1997; Rast et. al., 2003) and in the cephalochordate amphioxus, circular reporter plasmids are injected to generate transgenic animals (Yu et. al., 2004). In contrast to stable transgenic strains that are screened for reporter expression and germline transmission of the transgene in subsequent generations, transient transgenic animals are directly analyzed for reporter in F<sub>0</sub>. Transient transgenic approaches using fluorescent reporter constructs allow analyzing a high number of animals in a short period of time, but requiring high throughput delivery methods for the transgene in early developmental stages and efficient expression systems that yield complete expression patterns of reporter constructs. I developed an efficient microinjection protocol for *Platynereis* zygotes as a diploma student (Backfisch diploma thesis; Backfisch et.al, 2013). This microinjection protocol allows injection of up to 230 zygotes in an injection session of around one hour. Based on this microinjection protocol, I explored the use of the Tol2 transposable element

that originates from the medaka fish *Oryzias latipes* in *Platynereis*. In this study, I used a Tol2-derived vector construct to drive ubiquitous expression of EGFP under the control of cis-regulatory elements of the ribosomal gene *rps9* in larval and postlarval stages. Injected zygotes gave rise to fully fluorescent adult worms, establishing the Tol2 transposable element as a powerful tool for transient transgenic approaches in *Platynereis*. Moreover, I tested Tol2-derived fluorescent reporter constructs that drive EGFP expression in ciliated cells of trochophore larvae (*alpha-tubulin* reporter), in the center of the larval brain (*lMaf* reporter) and in photoreceptor cells (*r-opsin* reporter). Around 20% of the zygotes that were injected with fluorescent reporter constructs, yielded complete or almost complete endogenous expression patterns of their target genes. Moreover, robust reporter gene expression is persistent throughout the lifetime of the animals. Excision assays and sequencing of genomic insertion sites of Tol2 reporter constructs revealed that the Tol2 transposable element is cleaved precisely at the end of the terminal repeats and integrated into the *Platynereis* genome. This means that Tol2 transposase mRNA is translated into an active enzyme in *Platynereis*.

### 3.1.1.1. Evidence for silencing of tol2 reporter constructs in the next generation

Although tol2-derived transgenic individuals show robust expression of the reporter gene EGFP throughout lifetime, no expression of EGFP was observed in the offspring of injected animals, even when mature animals were screened for fluorescence before breeding. However, genomic integrations of reporter constructs were detected in injected animals and *egfp* sequence was amplified from genomic DNA of offspring derived from injected parents. This discrepancy between fluorescence in the two generations might reflect a permanent silencing of the reporter, possibly by a mechanism residing in the germline, which is known to be able to detect transposons in other species (Sijen et. al., 2003). Alternatively, the discrepancy could be explained by insertions of tandem repeats of the reporter into the *Platynereis* genome. It has been shown that tandem repeats of transgenes are often recognized and silenced in animals and plants (van der Krol, 1990, Dorer, 1994, Garrick 1998). Whether tol2 reporter constructs are integrated in tandem repeats in *Platynereis* remains to be elucidated.

In this study, I demonstrated that Tol2-derived fluorescent reporter constructs are suitable tools for transient transgenic applications in *Platynereis*. Tol2-derived fluorescent reporter constructs enable to trace cells throughout development and individuals can be screened and analyzed directly in F<sub>0</sub>. Because of the low levels of mosaicism, the robust transient transgenic technology using the Tol2 system will be particularly useful for assessing the functionality of cis-regulatory elements.

### 3.1.2. Establishing of the first stable transgenic strains in *Platynereis* using the Mos1 transposable element

Stable transgenic strains have been established in plants as well as in several vertebrate and invertebrate model organisms and have paved the way for various discoveries and applications in cell biology, molecular biology and biochemistry. However, in *Platynereis* or other annelids, stable transgenic strains were not established.

In this study, I generated the first stable transgenic reporter lines in *Platynereis dumerilii* using the Tc1/mariner-type element Mos1 that was initially isolated in *Drosophila mauritiana*. Mos1-derived vectors that carry fluorescent reporter constructs flanked on both sides by Mos1 terminal repeats were injected along with synthetic Mos1 transposase mRNA into *Platynereis* zygotes. I demonstrated that Mos1 transposase mRNA is translated into a functional protein in injected individuals, excises the transgene from the vector and mediates its genomic integration. Integrated reporter constructs are stably transmitted and are expressed in subsequent generations of transgenic founders. The integrated reporter constructs are not silenced or re-mobilized in the *Platynereis* genome. Excision assay revealed that cleavages of Mos1 transposase occur imprecisely on both ends of the terminal repeats. Notwithstanding, reporter constructs that were imprecisely cleaved are integrated into the *Platynereis* genome as shown for the transgenic alpha-tubulin reporter line. This transgenic strain carries a single integration of the tuba::egfp reporter construct which is lacking a part of its right terminal repeat and has additional vector-derived sequences on its left terminal repeat. Imprecise insertions for Mos1 were also reported in other species, like *Drosophila mauritiana* (Bryan et. al., 1990) and yeast (Yang et. al., 2006) and it was shown that incomplete Mos1 transposable elements are capable to transpose in *Drosophila simulans* (Ogura et. al., 2003). The genomic target site for the Mos1 transposable element is a TA dinucleotide, which is duplicated upon

genomic insertion (Ketting et. al., 1998; van Luenen et. al., 1994). This characteristic TA dinucleotide signature was also found at genomic insertion sites of reporter constructs in *Platynereis* and is evidence for transposition events of functional Mos1-transposase. Moreover, TA dinucleotide footprints are also present in the donor vector after excision of reporter constructs in *Platynereis*. Similar footprints have been reported for the human hmar1 transposable element that leaves a characteristic TTA/TAA trinucleotide footprint in the donor vector upon excision (Miskey et. al., 2007). These remaining footprints are derived from double-strand break repair caused by the excision of the transposable element.

### 3.1.2.1. Possible reasons for the discrepancy of endogenous and EGFP expression in the *alpha-tubulin* transgenic reporter strain

To generate the first stable transgenic reporter line in *Platynereis*, I used a fluorescent reporter construct that drives EGFP expression under the control of cis-regulatory elements of an *alpha-tubulin* gene that is specifically expressed in the ciliated cells of larval and postlarval stages. The transgenic reporter line carries a single genomic integration of the reporter construct and recapitulates precisely the early endogenous expression of *alpha-tubulin* in early trochophore stages. However, later in development, the reporter expression is shut down whereas the endogenous *alpha-tubulin* expression persists in errant juveniles even after three weeks of development. An explanation underlying the discrepancy of endogenous *alpha-tubulin* expression and reporter gene expression is, that the *alpha-tubulin* upstream element that was used to generate the reporter construct is able to drive EGFP expression only during early development. Enhancer elements that are essential to drive EGFP expression in later stages are absent from the cloned *alpha-tubulin* reporter. An alternative explanation for the discrepancy of endogenous mRNA and EGFP expression is that position effects might occur at the genomic integration site that shut down EGFP expression in later stages of development. Position effects describe the variation of transgene expression depending on the genomic region of insertion (Weiler et. al., 1995; Allshire et. al., 1994; Heinikoff et. al., 1992). To address whether EGFP expression in the *alpha-tubulin* transgenic line is restricted to early developmental stages because of an incomplete enhancer or because of position effects, a second *alpha-tubulin* transgenic reporter line should be generated. In the course of this study, I obtained transgenic offspring from a second founder animal, but the embryos died after two days of development.

The methodology to generate stable transgenic reporter lines using the Mos1 system, fills a critical gap in the toolkit currently available for *Platynereis*. Stable transgenic strains are an invaluable tool to characterize and functionally study labeled cell types throughout the lifetime of the animal. This includes the further use of transgenic strains as cell type markers, or the generation of reporters for cellular substructures or signaling. Moreover, the generation of stable transgenic lines will allow ablation and isolation of cell types to investigate cell function and to determine the transcriptome of labeled cells.

### 3.1.3. phi C31 integrase system as a potential improvement in transgenic technology

In this study, I pioneered the use of the phi C31 system in *Platynereis dumerilii*. The phi C31 system is derived from the bacteriophage phi C31 and is based on an integrase enzyme that mediates recombination of attB- and attP-sites, two short nucleotide sequences that are recognized by the integrase. The ability of the phi C31 integrase to recombine attB- and attP-sites, allows the site-directed insertion of a transgene carrying an attB-site into the host genome that carries an attP site. To explore the use of phi C31 integrase system in *Platynereis*, I modified the *alpha-tubulin* reporter and the *rps9* reporter by introducing attP- and attB-sites, respectively. I co-injected the two modified plasmids along with integrase mRNA into zygotes and demonstrated that the phi C31 integrase is capable to recombine the two plasmids in vivo. Based on these results, I have tried to generate a transgenic reporter line that carries a genomic attP-site, which can be used as landing site for transgenes that carry an attB site. For this, I tried to integrate the modified *alpha-tubulin* reporter construct that carries an attP-site in a Mos1-derived transgenesis vector into the *Platynereis* genome, but so far I did not obtain transgenic offspring of injected animals.

The phi C31 integrase system is known as a highly efficient tool to generate site-specific genomic insertions of transgenes in *Drosophila melanogaster*. As shown by Groth et. al. (2004), injections of attB-containing plasmids along with phi C31 integrase mRNA into fly embryos that carry attP-landing sites in their genomes, yield up to 55% of fertile adults producing transgenic offspring. A transgenic strain that carries such an attP-landing site in the genome, could improve the efficiency of transgenic technology in *Platynereis*. Moreover, establishing the phi C31 integrase system will help to exclude position effects that occur at

genomic insertion sites of transgenes. Such a position effect might restrict EGFP expression of the *alpha-tubulin* reporter strain to early trochophore stages as discussed in previous section (section 4.1.2.1.).

### 3.1.4. Optimized in-situ Hybridization protocols allow studying and comparisons of gene expression patterns at postlarval stages in *Platynereis dumerilii*

So far, analyses of gene expression patterns by in-situ Hybridization have been restricted to larval stages and posterior-regenerated worms in *Platynereis*, due to the lack of robust staining protocols for postlarval stages. I have developed an optimized in-situ Hybridization protocol that allows studying gene-expression patterns at postlarval stages. In addition, I established a two-color in-situ staining procedure that I have used for co-expression analyses in larval and postlarval stages during my work. Analyses of gene-expression patterns and co-expression analyses in the adult brain and trunk revealed new insights into the regulation of insulin-like peptides and the molecular specification of non-cephalic photoreceptors. The newly developed in-situ staining techniques provide extension of the molecular toolkit and will help to address questions in physiology, evolutionary biology and chronobiology at postlarval stages in *Platynereis*.

## 3.2. Molecular analyses reveal new insights into the neurosecretory centers of the adult *Platynereis* brain

Gene expression analyses revealed that neurosecretory markers are highly expressed in the posterior brain lobes in adult worms, which are located behind the posterior pair of adult eyes, in between the nuchal organs. The posterior lobes express particularly high levels of *prohormone convertase 2*, a gene that is specifically expressed in neuroendocrine cells and the neuronal marker gene *synaptotagmin*. Autoradiographic studies in adult *Platynereis* brain revealed that neurosecretory cells might be located in the posterior lobes, but further analyses focused on neurosecretory cells located elsewhere in the brain (Müller, 1973). In *Nereis diversicolor*, another annelid species, endocrine activity of a brain region located between and

behind the posterior pair of adult eyes promoting oogenesis and regeneration was described by Golding (1977). The finding that the posterior brain lobes express high levels of neurosecretory markers, provide new insights into their function as neuroendocrine centers in *Platynereis*. In line with this, *Platynereis* insulin-like peptides are expressed in the posterior lobes. Likewise, this family of peptide-hormones is generally expressed in neurosecretory cells in the brain of invertebrates. The posterior lobes of the adult brain have not been investigated explicitly in *Platynereis*, but their function as neurosecretory centers demonstrated in this study, makes them interesting for further studies.

### 3.3. New insights into the regulation of insulin-like peptides in *Platynereis dumerilii*

A main focus of this work was to explore the regulation of *Platynereis* insulin-like peptides. 5 different insulin-like peptides have been identified and their expression patterns were correlated to that of genes known regulate insulin transcription in vertebrates. Moreover, an influence of food intake and the circadian clock on insulin-like peptide expression levels has been observed in this study.

#### 3.3.1. Phylogenetic analyses of the *Platynereis* insulin-like peptides

In this study, 5 different insulin-like peptides have been identified in *Platynereis*. Amino acid sequence alignments revealed that *Platynereis* insulin-like peptides have extended C-termini unlike vertebrate insulin and *Lymnaea stagnalis* insulin-like peptides. In this aspect, *Platynereis* insulin-like peptides resemble the vertebrate insulin-like growth factors *igf1* and *igf2*. Phylogenetic comparison with different human insulin-family members demonstrated that *Platynereis* and *Lymnaea stagnalis* insulin-like peptides do not split into peptides that are closer related to insulin, igf's or relaxin. These findings are in line with the current view that protostome insulin-related peptides are in general referred to as insulin-like peptides and no distinction is made into insulin, igf's or relaxin. Outside vertebrates, distinct peptides that resemble an igf and insulin have been identified in tunicates, leading to the assumption that the split of insulin-like peptides into insulin-like growth factor and insulin may have occurred in protochordates (McRory and Sherwood, 1997). The relaxin sub-family may have split from



insulin and igf's during vertebrate evolution, since an invertebrate *relaxin* has not been identified to date (Wilkinson & Bathgate, 2007, for review). Among *Platynereis* insulin-like peptides, the most distantly related peptide seems to be *ilp2* and interestingly its gene-structure is also the most deviating with large introns and a locus of around 30kbp in length. The loci of *Platynereis ilp1*, *ilp3* and *ilp4* are located in a cluster of 30kbp total in length and sequence alignments showed that *ilp3* and *ilp4* show strong sequence similarities, implying that these two genes arose upon gene duplication. *Platynereis* insulin-like peptides share sequence similarities among each other and group together in a phylogenetic tree. Possible functions of the different *Platynereis* insulin-like peptides cannot be derived from phylogenetic analyses.

### 3.3.2. Expression analyses in larval and postlarval stages indicate that *Platynereis* insulin-like peptides are differentially regulated and have diverse functions

Expression patterns of the 5 *Platynereis* insulin-like peptides have been analyzed in larval and at postlarval stages by in-situ Hybridization. All *Platynereis* insulin-like-peptides are expressed in the larval and adult brains and have individual expression patterns. During larval development, *ilp2*, *ilp3* and *ilp5* are expressed in subsets of cells located in the central region of the larval brain. Later in development, expression of insulin-like peptides is observed in cells of the dorsal part of the brain and in adult worms, they are mainly expressed in the posterior brain lobes. The individual expression patterns and the different temporal expression of the *Platynereis* insulin-like peptides suggest that they are differential regulated. This assumption is supported by the observation that *pax6* is co-expressed with *ilp2* but not with other insulin-like peptides. As in other species, the different *Platynereis* insulin-like peptides will have distinct functions in growth, metabolism and reproduction and are therefore individually regulated. The function for each of the *Platynereis* insulin-like peptides needs to be elucidated.

### 3.3.3. Assessing the regulatory code of insulineric cells in *Platynereis dumerilii*

#### 3.3.3.1. Expression analyses suggest a function of *Platynereis lMaf* in insulineric cell types during larval development

A single *Platynereis* orthologue of the vertebrate *MafA* and *MafB* gene has been identified, its expression pattern was analyzed in larval and postlarval stages and compared to expression patterns of insulin-like peptide by in-situ Hybridization. In trochophore larvae, *lMaf* mRNA is co-expressed with *ilp2*, *ilp3* and *ilp5*, which are the three insulin-like peptides expressed at this developmental stage. In contrast, no co-expression of *lMaf* and insulin-like peptides was observed in atokous worms. The finding that *Platynereis lMaf* is co-expressed with insulin-like peptides only in larval stages suggests that *lMaf* could have a role in the development of insulineric cells, similar to the function of *MafB* in the differentiation of pancreatic  $\beta$ -cells in mouse and humans (Nishimura et. al., 2006; Artner et. al., 2006, Hang et. al., 2011). As it is not detectable in insulineric cells of atokous worms, *Platynereis lMaf* is rather not a direct regulator of insulin-like peptide expression as shown for its orthologue *MafA* in vertebrates (Olbröt et. al., 2002). To investigate if a knockdown of *Platynereis lMaf* has an effect on insulin-like peptide expression, I performed translational knockdown experiments using Morpholino antisense oligos against *Platynereis lMaf*. However, these experiments remained inconclusive. Initially, a pilot knockdown experiment revealed a decreased *ilp2* expression, but in the following experiments this could not be reproduced. An explanation could be that the region covered by the Morpholino oligo is polymorphic and that different alleles of *lMaf* exist in the different *Platynereis* strains. In this case, genotyping assays could help to identify a suitable *Platynereis* inbred strain to perform knockdown experiments for *lMaf*. Moreover, I cloned and tested an *lMaf* fluorescent reporter construct and found that the EGFP expression recapitulates the endogenous *lMaf* expression in the central larval brain. In this study, *Platynereis lMaf* has shown to be co-expressed with insulin-like peptides in trochophore larvae and a function of *lMaf* in differentiation of insulineric cells was suggested. The function of *Platynereis lMaf* still needs to be elucidated more accurately. Novel tools like targeted gene-knockout experiments that are currently being established in *Platynereis*, will help to analyze the role of *lMaf*.

### 3.3.3.2. Evidence for a conserved function of *Platynereis pax6* as a regulator of *ilp2* expression in atokous worms

The transcription factor *Pax6/Eyless* has been shown to be a direct regulator of insulin gene transcription in vertebrate and insect species, and hence it has been hypothesized that *pax6/eyeless* has a conserved function as an insulin regulator across species (Clements et. al., 2008). In this study, I found that *pax6* and insulin-like peptides are not co-expressed in trochophore stages, but *pax6* and *ilp2* are co-expressed in the brain of atokous worms in a bilateral pair of cells located in between the posterior pair of adult eyes. These findings suggest that *Platynereis pax6* could bind an enhancer element of *ilp2*, which activates *ilp2* expression at postlarval stage. Certainly, further experiments to investigate if *Platynereis pax6* is a regulator of *ilp2* are necessary. Notably, the finding that *pax6* and *ilp2* are co-expressed in *Platynereis* as a lophotrochozoan species, contribute a complementary set of data that support the hypothesis that *pax6* is a conserved regulator of insulin transcription in the bilaterian animals.

### 3.3.3.3. Indication for a function of *Platynereis islet* in sensory cells

The vertebrate *islet* gene is known to bind the insulin enhancer and activate insulin transcription. The *Platynereis islet* orthologue is broadly expressed in the posterior brain lobes and detected in the nuchal organs, structures that contain sensory cells. Hence, it might be that *Platynereis islet* gene is expressed in secretory cell-types. The correlation of *islet* gene-expression and insulin-like peptide expression in the posterior lobes suggests that *islet* could be regulator of insulin-like peptides in *Platynereis*. It would be very interesting to examine the function of *Platynereis islet* more in detail, in particular its possible role in sensory cells as suggested in this study.

#### 3.3.3.4. *Platynereis xlox* is not a regulator of insulin-like peptides in *Platynereis*

*Pdx1/ipf1*, a key gene for pancreatic  $\beta$ -cell development and insulin transcription in vertebrates is not present in the conventional protostomian model organisms *Drosophila melanogaster* and *C. elegans*, but an orthologue (*xlox*) has been found in the lophotrochozoan *Platynereis* (Hui et. al., 2008). In this study, I investigated if *Platynereis xlox* might have a conserved function as regulator of insulin transcription or during insulinergetic cell-type differentiation as its vertebrate orthologue. This is not the case, since insulin-like peptides are expressed in the brain and *xlox* is found in clusters of cells in the gut and ventral nervous system in trochophore larvae. Weak *xlox* expression is transiently detected in cerebral ganglia of nectochaete, but does not correlate with insulin expression. Hence, a function of *pdx1/ipf1/xlox* in insulinergetic cell-types is not conserved between vertebrates and *Platynereis*. Orthologues of *xlox* have been identified in other lophotrochozoan species as well and a conserved role for *xlox* in anterior-posterior gut patterning, gut morphogenesis and a possible function in the ventral neuroectoderm has been discussed (Samadi et. al., 2010; Fröblius et. al., 2006; Kulakova et. al., 2008, Brooke et. al., 1998; Holland et. al., 2001). Based on these studies in related lophotrochozoan species and its expression pattern, I suggest that *xlox* has a similar function in gut morphogenesis in *Platynereis*. Its function in the ventral neuroectoderm needs to be elucidated.

#### 3.3.4. Evidence for circadian clock-controlled expression of *Platynereis* insulin-like peptides

Components of the *Platynereis* circadian clock have been identified and their expression has been analyzed in trochophore larvae (Arendt et. al., 2004) and in atokous worms (J. Zantke, unpublished). *Platynereis bmal*, a component of the circadian clock, is expressed in the dorsal larval brain in a similar region where I detected the expression of insulin-like peptides. Moreover, when J. Zantke analyzed clock gene expression in atokous worms, she found that clock genes are expressed in the posterior brain lobes, which have been described as the centers of *Platynereis* insulin-like peptide expression. The overlap of expression patterns of clock genes and insulin-like peptides overlap imply that a correlation of the circadian clock and insulin-like peptides exists in *Platynereis*. In vertebrates, a tight interconnection of the

circadian clock and metabolic processes that involve insulin has been observed. The coupling of the circadian clock and glucose metabolism allows synchronization of these important systems. As an example, the pancreatic  $\beta$ -cells possess their own and self-sustained peripheral clock which allows cyclic insulin-secretion (Marcheva et.al., 2010). In order to integrate circadian processes with glucose metabolism, the pancreatic clocks are controlled and adjusted by the suprachiasmatic nucleus (SCN). The SCN is the master pacemaker that synchronizes peripheral clocks in the different tissues of the vertebrate body and is located in the hypothalamus. The vertebrate hypothalamus itself has been shown to play a role in glucose homeostasis and insulin sensing (Livingstone et. al., 1995, Yang et. al., 1999). Moreover, hypothalamic insulin expression has been reported in rat (Devaskar et. al., 1993) and fish (Hrytsenko et. al., 2007). It is hypothesized that the coupling of glucose-metabolism and circadian rhythms is an ancient paradigm (Rutter et. al., 1999, for review). The coincidence of clock gene expression and insulin-like peptide expression in the posterior lobes in *Platynereis* found in this study, might reflect an ancestral-type feature to integrate inputs from circadian rhythms and metabolism.

I have investigated a connection of the *Platynereis* circadian clock and insulin-like peptide expression and demonstrated that insulin-like peptide mRNA levels fluctuate during a 24-hour period. The rhythmic expression of insulin-like peptides persists even after two days under constant darkness. In vertebrates, a daily rhythm of insulin content of pancreatic  $\beta$ -cells and insulin secretion has been reported before but so far, a daily rhythm of insulin-like peptide mRNA levels has not been reported, yet. The findings of my study suggest that insulin-like peptide expression is directly under control of the circadian clock in *Platynereis*. Further investigations in other species will help to understand if the coincidence of the centers of the circadian clock and insulin-expression observed in *Platynereis* is a more general feature in bilaterians.

### 3.3.5. Food-dependent expression suggests conserved functions of *Platynereis* insulin-like peptides in glucose metabolism

Insulin and insulin-related peptides have conserved functions in nutrient-metabolism, growth and reproduction across species. In this study, I have investigated if *Platynereis* insulin-like peptides may play role in nutrient-metabolism. I have shown that expression levels of *Platynereis ilp1*, *ilp2* and *ilp3* are up regulated after food intake. This implies that *Platynereis*

*ilp1*, *ilp2* and *ilp3* might play a role in carbohydrate metabolism and their expression may be stimulated by cellular glucose up-take, similar to the expression of insulin in the pancreatic  $\beta$ -cell. Hence, *Platynereis ilp1*, *ilp2* and *ilp3* may have a similar function than the vertebrate pancreatic insulin in lowering blood glucose levels after food-intake (Saltiel & Kahn, 2001). In contrast, expression levels of *ilp4* and *ilp5* are not altered after food-intake, which could mean that their functions resemble more the function of vertebrate insulin-like growth factors or relaxins. Further analyses will help to elucidate the functions of the different *Platynereis* insulin-like peptides.

### 3.4. Expression patterns analyses of *glut2* and insulin-like peptides in atokous worms indicate a possible mechanism of glucose sensing and insulin-secretion in *Platynereis dumerilii*

In *Platynereis*, insulin-like peptides are exclusively expressed by neurosecretory cells of the brain in larvae and in atokous worms. Brain-specific expression of insulin-like peptides is known in other lophotrochozoan species like in the pond snail *Lymnaea stagnalis* and in the sea hare *Aplysia californica*. In *Lymnaea*, insulin-like peptides are expressed by the light-green cells (LGC) of the cerebral ganglia and by the buccal ganglia. In *Aplysia*, the first characterized insulin-like peptide in *Aplysia californica* is exclusively found in the central region of the cerebral ganglia (Floyd et. al., 1999). In both species, insulin-like peptides are delivered by axonal transport to neurohemal release sites where they are secreted into the hemolymph. It is not known, how insulin-like peptides are secreted in *Platynereis* or other annelid species. Based on analyses of gene-expression patterns performed in this study, I would like to propose a possible mechanism of insulin-like peptide secretion and glucose sensing in *Platynereis*. The proximity of insulinergic cells located in the posterior brain lobes and the dorsal blood vessel suggests that a connection between insulin-like peptide production and the blood system may exist in *Platynereis*. The tissue localized between the posterior lobes and the dorsal blood vessel has been described as the infracerebral organ (Müller 1973). A possible function of the infracerebral organ as endocrine gland either in synthesizing or - more likely - in excretion of substances into the blood stream that were delivered from the brain by axonal transport was suggested by Müller and Hofmann (Müller 1973, Hofmann 1976). Moreover, in the annelid *Nephtys*, the infracerebral organ has been described as

neurosecretory gland (Golding 1970). As shown in this study, the *Platynereis* orthologue of *glut2*, a gene expressed in glucose-sensing cells, is expressed in the infracerebral organ. The presence of *glut2* in the infracerebral organ can be best explained by a blood glucose-sensing function of this organ in *Platynereis*.

Hence, a possible mechanism of insulin-like peptide secretion in *Platynereis* might be as follows: *Platynereis* insulin-like peptides are expressed in the posterior brain lobes and delivered to the infracerebral organ. The infracerebral organ located in close proximity to the dorsal blood vessel senses levels of blood glucose and releases insulin-like peptides upon altered blood glucose levels. This would be similar to the mechanism of insulin-like peptide secretion in mollusc species and would resemble the function of the insect PI and CC in blood sugar-sensing and insulin-like peptide expression (Kim et. al., 2004).

### 3.5. Neuronal expression of *Platynereis* insulin-like peptides provide evidence for a neural origin of insulinergetic cells

Insulin-producing cells have been extensively studied in different species, but so far, the origin of these cells is poorly understood and different evolutionary scenarios are being discussed. In bilaterian animals, insulin-like peptides are produced by neurons as well as by endocrine cells of endodermal origin and it is being discussed if they arose from a common ancestor or evolved independently. A current hypothesis is, that a common ancestor of insulinergetic cells existed and this precursor had neuronal status. This hypothesis is in line with the findings that insulinergetic cells of endodermal origin like the vertebrate  $\beta$ -cell, have striking similarities with neurons in terms of development and gene-expression and their physiological and functional properties (Ackermann et. al., 2007; Cerf 2006, Heremans et. al., 2002). Moreover, regulatory conservation of insulin transcription between flies and mammals has been reported (Clements et. al., 2008; Okamoto et. al., 2012). In fact, neuronal insulin-like peptide expression is widespread in all bilaterian branches. In vertebrates, *igfI* and *igfII* are expressed in the central nervous system and it has been reported that insulin is expressed in the brains of rat and fish. In insects, the center of insulin-like peptide expression is located in cells of the pars intercerebralis and in molluscs, insulin-like peptide expression is found in the cerebral ganglia (Ikeya et. al., 2002, Smit 1988). In this study, expression patterns of insulin-like peptides from the annelid *Platynereis* have been characterized and found exclusively in



the brain. These findings in *Platynereis* provide for support the hypothesis, that a potential common ancestor of insulinerbic cells might have been a neuron.

### 3.6. Molecular analyses of non-cephalic photoreceptors in *Platynereis* reveal similarities to the amphioxus Hesse organ

A transgenic fluorescent reporter strain that recapitulates the endogenous expression of *r-opsin*, a characteristic marker for rhabdomeric photoreceptors, helped to discover non-cephalic photoreceptors in *Platynereis* (Backfisch et. al., 2013). These newly identified non-cephalic photoreceptors are found on the ventral side of the trunk in the region of the ventral midline, at the basis of the parapodia and in the notopod of the parapodia (Figure 38). Molecular analysis of these non-cephalic photoreceptors revealed that they differentiate independent of *pax6*, a gene that is involved in eye development in many metazoans, and that they could share a common origin with the amphioxus Hesse organ. The amphioxus Hesse organs express *dachshund* and a majority of the *Platynereis* ventral photoreceptors do expresses *dachshund*. During development, a *dach*-positive cell immediately neighbors the parapodial photoreceptors. A close correlation between *r-opsin* positive cells and expression of the transcription factors *brn3* and *pax2/5/8* has been observed in this study. A *brn3* expressing cell is observed directly adjacent to parapodial photoreceptor cells during early development and in adult parapodia. *Pax2/5/8*, which is detected in the dorsal epithelia of 8-days-posterior regenerates, is expressed next to a parapodial photoreceptor cell. However, in adult parapodia, no *pax2/5/8* is observed. Provided that the non-cephalic photoreceptors are functioning, they should express a suitable G alpha protein for phototransduction. In fact, all observed *r-opsin* positive cells do express the G alpha protein subunit *g(q)*. Presumably, the non-cephalic photoreceptors are functional. Although the co-expression data generated in this study still wait to be extended to other genes, they already provide insight into the “molecular fingerprint” of non-cephalic photoreceptors. At least for the parapodial PRCs, whose stereotypic occurrence facilitates analyses about spatiotemporal expression similarities, we conclude that *r-opsin* cells differentiate from a territory expressing *pax2/5/8*, but not *pax6*, and that they are tightly linked with the expression of *dach* and *brn3* (Backfisch et. al., 2013).

### 3.7. Co-expression of *pax6* and *r-opsin* in frontal lateral eyelets reveal *pax6*-positive photoreceptors in *Platynereis*

It is currently unclear if the *Platynereis* frontal lateral eyelets are relicts of the larval eyes that were described to be gradually reduced after the second day of development (Rhode 1992). The larval eyes are present during trochophore development and do express *pax6* (Arendt et. al., 2002). In this study, I have shown that the *Platynereis* frontal lateral eyelets co-express *r-opsin* and *pax6* in errant juveniles reminiscent of the larval eyes. I monitored EGFP expression in the frontal lateral eyelets in *r-opsin* transgene individuals and found that EGFP is present in the frontal lateral eyelets in worms that have not more than 22 segments. However, another screen performed by V. Babu Rajan, revealed EGFP fluorescence in worms that have up to 40 segments (Backfisch et. al., 2013).

The protocols for transgenic approaches and for in-situ staining methods that were developed in this study, fill a critical gap in the molecular toolkit currently available for *Platynereis dumerilii* and will help to address open biological questions in both developmental and evolutionary biology, as well as chronobiology.

The findings of this study provide new insights into the regulation of insulin-like peptides in *Platynereis* and indicate possibly ancient features of insulin-like peptide transcription, their functions and their interconnection to the circadian clock in bilaterian animals. Moreover, the findings support the hypothesis that insulinergic cells are of neuronal origin.



## 4. Materials and Methods

### 4.1. *Platynereis dumerilii* culture

Animals are raised and bred in laboratory culture at 18°C which is maintained according to Hauenschild & Fischer (Hauenschild C & Fischer A, 1969). The breeding behavior of *Platynereis dumerilii* is dependent on the moonlight, hence animals are kept in culture rooms with artificial moonlight. To ensure continuous availability of embryos and larvae for experiments throughout the lunar cycle, culture rooms with different moon-phases were established.

A laboratory culture with various inbred strains has been established with worms originating from the laboratory culture of Dr. Detlev Arendt at the EMBL in Heidelberg and animals caught in the Mediterranean Sea.

### 4.2. *Platynereis* Whole-Mount in-situ Hybridization

#### 4.2.1. Protocol

A protocol for in-situ Hybridization in *Platynereis* (Tessmar-Raible et. al., 2005) was adopted and modified for this study.

*Platynereis* larval stages were fixed in 4%PFA/2xPTW for two hours at room temperature, juvenile worms were fixed overnight at 4°C or for 6 hours at room temperature. Specimens were washed 3x in 100% Methanol and stored at -20°C in 100% Methanol. After stepwise rehydration in 75%, 50% and 25% of Methanol/1xPTW for 3 minutes each, specimens were washed twice in 1xPTW for 5 minutes and subsequently treated with 100µg/ml ProteinaseK (Merck) in 1xPTW according to the different stages of development as follows:

- 24hpf to 72hpf: 1 minute
- 73hpf to 7dpf: 2 minutes
- 8dpf to 16dpf: 2 minutes 30 seconds
- atokous worms and adult heads: 5 minutes

ProteinaseK treatment was stopped by rinsing specimens twice with 2mg/ml Glycine/1xPTW followed by post-fixation in 4%PFA/1xPTW for 20 minutes. Specimens were washed 5x in

1xPTW for 5 minutes and pre-hybridized in Hybridization-Mix (50% Formamide, 5xSSC, 50µg/ml Heparin, 0.1% Tween20, 5mg/ml torula RNA) for 2 hours at 65°C in a water bath. Hybridization was performed using 2-8ng/µl of Digoxigenin-labeled riboprobe in a final volume of 200µl Hybridization-Mix overnight at 65°C. Specimens were washed twice in 2xSSCT/50%Formamide, once in 2xSSCT and twice in 0.2xSSCT. All washing steps were carried out for 20 minutes and at 65°C. After pre-absorbtion in 5% sheep serum/1xPTW for 2 hours at room temperature specimens were incubated in a 1:2000 dilution Anti-DIG-AP, F<sub>ab</sub> fragments (Roche) in 5% sheep serum/1xPTW overnight at 4°C on a shaker. Optionally, to visualize the axonal scaffold, monoclonal antibody raised against acetylated  $\alpha$ -tubulin (SigmaT6793, Sigma, St. Louis, MO, USA) was added in a 1:250 dilution at this step. Specimens were washed 6x in 1xPTW for 15 minutes and equilibrated twice in Staining-buffer SB (100mM TrisHCl pH 9.5, 100mM NaCl, 50mM MgCl<sub>2</sub>, 0.1% Tween20) for 5 minutes. Staining reaction was performed in PVA-SB (100mM TrisHCl pH 9.5, 100mM NaCl, 50mM MgCl<sub>2</sub>, 0.1% Tween20, 5% Polyvinylalcohol solution) containing the alkaline phosphatase substrates nitro blue tetrazolium chloride (NBT, 4.5µl/ml, Boehringer) and 5-bromo-4-chloro-3-indolyl-phosphate (BCIP, 3.5µl/ml, Boehringer) at room temperature for 2-48 hours in the dark. Polyvinylalcohol was found to enhance the signal-to-noise ratio of stainings, likely due to formazan formation in the alkaline phosphatase reaction () and was introduced in this study to the *Platynereis* in-situ Hybridization protocol. Staining reaction was stopped by washing specimens 3x in 1xPTW, followed by post-fixation in 4%PFA/1xPTW for 20 minutes at room temperature and 3 washes in 1xPTW. When anti-acetylated tubulin antibody was applied to the procedure, Alexa Fluor 488 goat anti-mouse antibody (1069846, Molecular Probes (Invitrogen), Eugene, Oregon, USA) was added to the specimens in a 1:250 dilution in 1xPTW and incubated overnight at 4°C on a shaker. Optionally, to visualize the nuclei, DAPI can be added at this step in a final concentration of 10µg/ml. Specimens were washed 6x with 1xPTW and stored in the anti-photobleaching agent DABCO (Roth, Karlsruhe, Germany) in a concentration of 2.5mg/ml in Glycerol at 4°C protected from light.

#### 4.2.2. Preparation of DIG-labeled antisense-riboprobes

5µg of plasmid were linearized using a suitable restriction enzyme in a total digest volume of 20µl and subsequently analyzed on 1%agarose/1xTAE gel containing sybrsafe DNA dye (Invitrogen) in a 1:10.000 dilution. The linearized template DNA was excised from the gel

and purified in a final elution volume of 40µl ddH<sub>2</sub>O. Transcription reaction (12µl template DNA; 2µl 10x RNA Pol Reaction buffer (New England Biolabs); 2µl NTP/DIG-UTP-Mix (Roche); 2µl ddH<sub>2</sub>O; 1µl RNasin (Fermentas); 1µl Sp6- or T7-RNA Polymerase (both New England Biolabs)) was performed in 200µl thin-walled PCR tubes on a thermal cycler at 37°C for 3 hours. To remove template DNA, 2µl DNase I (Fermentas) were added to the transcription reaction, mixed by pipetting and incubated for 30 min at 37°C. DIG-labeled antisense riboprobe was purified using RNeasy kit RNA cleanup protocol (Qiagen), eluted in 40µl of RNase-free water and 3µl of the RNA were analyzed on 1% agarose/1xTAE gel. 80µl of Hyb-Mix were added to the antisense RNA probe, mixed and stored at -20°C.

#### 4.2.3. Preparation of Polyvinylalcohol stock solution

To prepare 100ml of 10% (w/v) Polyvinylalcohol stock solution, 10g Polyvinylalcohol powder (Sigma Aldrich) were added to approximately 80ml ddH<sub>2</sub>O and heated to 80°C in a water bath on a combined hot-plate magnetic-stirrer device until the Polyvinylalcohol was completely dissolved. Subsequently solution was brought to 100ml with ddH<sub>2</sub>O and stored at room temperature.

#### 4.2.4. Two-color in-situ protocol

Fluorescein-labeled riboprobe was added along with DIG-labeled riboprobe to the specimens and hybridized overnight at 65°C. NBT-BCIP staining reactions for the DIG-labeled riboprobes were performed according to described protocols using anti-DIG-AP F<sub>ab</sub> fragments. Subsequently, specimens were washed once in 1xPTW and incubated for 30min in 0.1M Glycine/HCl (pH2.2)/0.1%Tween. After washing 4x in 1xPTW, specimens were blocked for 1h in 5% sheep serum/1xPTW followed by incubation with anti-Fluorescein-AP F<sub>ab</sub> fragments in a 1:1.000 dilution in 5% sheep serum /1xPTW for 2h. Specimens were washed 4x in 1xPTW for 15min and equilibrated once in 0.1M TrisHCl (pH8.2). Staining reactions were performed using Fast Red tablets (Roche) dissolved in 0.1M TrisHCl (pH8.2) according to manufacturer's recommendations.

Note: Strong riboprobes should be labeled with fluorescein-UTP and weaker probes with DIG-UTP due to the greater sensitivity of DIG-UTP. Staining procedure can be altered and Fast-Red can be stained first, followed by NBT-BCIP staining.

### 4.3. Microinjection

Microinjections of zygotes and 2-cell stage embryos were performed according to a protocol established by B. Backfisch (see diploma thesis B. Backfisch).

Freshly fertilized egg batches were incubated for 45 minutes at 18°C. Zygotes were transferred onto nylon nets and the jelly coat was washed off with 2x 150ml of seawater. To soften the vitellogenin envelope zygotes were treated with Proteinase K (Merck, 50µg/ml final concentration) for 25 seconds in a volume of 30ml and subsequently washed 6x with 150ml of seawater.

Injection stages made of 1.5% Agarose in seawater were adapted from a microinjection protocol in *Parhyale hawaiiensis* and modified for *Platynereis* microinjections by N. Kegel (see diploma thesis N.Kegel). Injection stages were placed into the lid of a petri dish (diameter: 5.5cm) and submerged with seawater. Zygotes were mounted with a pipet onto the injection stage and injected using microcapillaries under a 10x objective. Injection pressure ( $p_i$ ) applied by the microinjector typically ranged between 200-400hpa and compensation pressure ( $p_c$ ) was found to be optimal between 10-14hpa. After injection, embryos were transferred into dishes with fresh seawater and kept at 18°C.

### 4.4. Salt-extraction protocol for genomic DNA

A salt-extraction protocol for genomic DNA was adopted and modified in this study (Aljanabi and Martinez, 1997). The tissue was homogenized in 400µl Homogenization buffer (0.4M NaCl, 10mM Tris-HCl pH 8.0, 0.2mM EDTA), 20µl 10% SDS and 20µl ProteinaseK solution (20mg/ml) at 65°C for 2-3 hours on a Thermomixer. 500µl of 5M NaCl were added to the sample, mixed for 10s on a vortexer and centrifuged for 30 min at 10.000g. The supernatant was transferred to a fresh 2ml tube. To precipitate the DNA, 1 volume of Isopropanol was added, mixed by inverting the tube and incubated at -20°C for 1 hour. After incubation the sample was centrifuged for 20min at 10.000g and the supernatant was removed. To wash the DNA pellet, 1 ml of 80% Ethanol was added followed by centrifugation at 10.000g for 5 min. The Ethanol was removed and the pellet was air-dried for 15 min and subsequently the pellet was resuspended in 50µl of ddH<sub>2</sub>O. Samples were stored at -20°C.



## 4.5. Southern blot and radioactive Hybridization

### 4.5.1. Detection of genomic insertions

#### 4.5.1.1. Blotting of genomic DNA to nylon membrane

Genomic DNA was extracted from tail-clips or whole worms using either the Nucleospin kit or the salt-extraction protocol. 8µg of genomic DNA per sample were digested at 37°C for 16h using HindIII restriction endonuclease (Fermentas) and analyzed on a 0.8% agarose/1xTBE gel. After staining in Ethidium bromide bath (1:10.000 dilution in 1xTBE) for 20min an image of the gel was captured. To denature the DNA double strands, the gel was placed into Denaturing solution (1.5M NaCl, 0.5M NaOH) for 40 min and subsequently transferred to Neutralisation solution (1.5M NaCl, 0.5M Tris-HCl pH 7.4) for 20 min. To transfer DNA fragments to the nylon membrane, a blot was assembled as shown in Figure 37 and placed into a plastic tray (lid of a pipet tip box) containing 250ml of 10xSSC. 10xSSC was soaked through the blot by capillary forces and hereby maximized the amount of DNA fragments transferred to the nylon membrane. After blotting overnight, the blot was disassembled, the DNA was UV-crosslinked to the nylon membrane (UV-crosslinker, Stratagene) and subsequently air-dried for 2 hours.

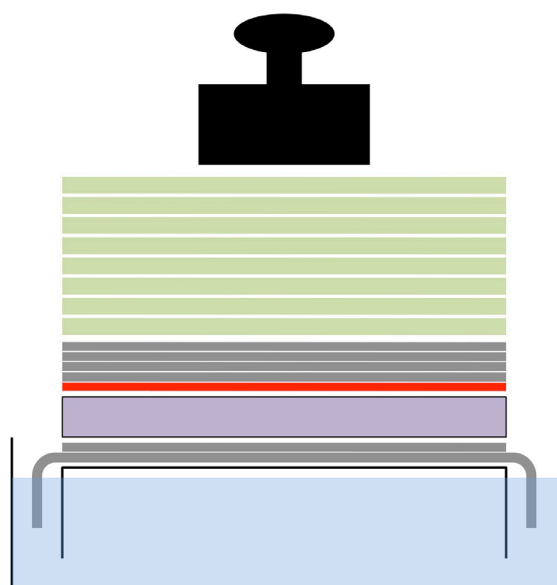


**Figure 37: Assembly of Southern blot**

The Blot is assembled in two nested pipet-tip boxes. grey: whatman-filter paper; purple: agarose gel; red: nylon membrane; green: paper towel

#### 4.5.1.2. Radiolabeling of egfp probe

5µg of plasmid pEGFP-N1 (Clontech) were double-digested in a volume of 20µl with BamHI and NotI (both Fermentas) to excise an *egfp* fragment. The digest was analyzed on a 1% agarose/1xTAE gel and the *egfp*-containing fragment was cut out from the gel with a scalpel. After purification and elution in 40µl of ddH<sub>2</sub>O, 12µl of the *egfp* fragment were radiolabeled with alpha-<sup>32</sup>P dCTP (3000Ci/mmol) using the Radprime DNA labeling System (Invitrogen) following the manufacturer's protocol. Unincorporated nucleotides were separated from the radiolabeled *egfp* probe using illustra microspin G25 column (GE Healthcare).

#### 4.5.1.3. Southern Hybridization

The blotted nylon membrane was rinsed with 2xSSC and transferred into a Hybridization tube containing 8ml of Rapid-hyb buffer (Amersham). After 30min of pre-hybridization at 65°C in a Hybridization oven, 25 µl of the radiolabeled probe was added into the tube and hybridized overnight at 65°C. The nylon membrane was washed twice with 50ml of 2xSSC/0.1%SDS and twice with 50ml of 0.2xSSC/0.1%SDS at 65°C for 20min each washing step. To detect genomic DNA fragments with bound egfp probe the blot was placed in an exposure cassette with an imaging plate and exposed for 3-7 days. The imaging plate was developed using a Phosphoimager and brightness and contrast of the image was adjusted using imageJ software.

### 4.5.2. Identification of specific RACE-PCR fragments and Colony lift

#### 4.5.2.1. Blotting of RACE-PCR fragments to nylon membrane

20µl of RACE-PCR and Nested RACE-PCR of *Platynereis ilp1*, *ilp2* and *IMaf* were analyzed on 1%agarose/1xTAE gel. An image of the gel was taken using a ruler as scale for later identification of specific PCR products. The gel was incubated in Denaturing solution (1.5M NaCl, 0.5M NaOH) for 30min and a Blot was assembled as shown in Figure 37. After blotting overnight, the nylon membrane was UV-crosslinked and air-dried for 2 hours.

#### 4.5.2.2. Radiolabeling of probes

*Platynereis ilp1*, *ilp2* and *lMaf* fragments were released from the pGEM T-easy vector backbone by EcoRI digest (New England Biolabs) at 37°C for 1hr. After gel cleanup as described above, 12µl of the probe templates were radiolabeled using Radprime DNA labeling system (Invitrogen) and unincorporated nucleotides were removed using illustra microspin G25 column (GE Healthcare) as described.

#### 4.5.2.3. Southern Hybridization

Nylon membranes were briefly soaked in 2xSSC and transferred into Hybridization tubes containing 8ml of Rapid-hyb buffer (Amersham). After 30 minutes of pre-hybridization at 65°C in a hybridization oven, 25µl of the radiolabeled probe were added and hybridized with the membrane for 2 hours. Nylon membranes were washed once with 50ml of 2xSSC/0.1%SDS and twice with 50ml of 0.2xSSC/0.1%SDS at 65°C for 20min each washing step. After washing, nylon membranes were placed in an exposure cassette (Kodak) with an imaging plate (GE Healthcare) and exposed for 24h. The imaging plate was developed using a Phosphorimager and specific RACE-PCR products were detected by autoradiographic hybridization signals.

#### 4.5.2.4. Cloning of specific RACE-PCR products and Colony lifts

25µl of RACE-PCR and nested RACE-PCR were run on 1%agarose/1xTAE gel and specific RACE-PCR products were excised, purified and cloned into pGEM-Teasy vector. TOP 10' chemically competent cells were transformed with 5µl of the cloning reaction, plated on ampicillin plates and incubated overnight at 37°C. Transfer of colonies to nylon membrane (colony lifts) were done as described in a protocol by J. Sambrook (Sambrook, 1989) and Southern Hybridization for *ilp1*, *ilp2* and *lMaf* RACE-PCR products was performed as described above.

## 4.6. Rapid Amplification of c-DNA Ends (RACE-PCR)

### 4.6.1. Protocol RACE-PCR

To obtain full-length sequences of *Platynereis* transcripts of *Platynereis ilp1*, *ilp2* and *IMaf*, RACE-PCR was performed. Gene-specific Primers (GSP) and nested gene-specific Primers (NGSP) ip1\_GSP3', ilp1\_NGSP3', ilp2\_GSP3', ilp2\_NGSP3', IMaf\_GSP3', IMaf\_NGSP3', ilp1\_GSP5', ilp1\_NGSP5', ilp2\_GSP5', ilp2\_NGSP5', IMaf\_GSP5' and IMaf\_NGSP5' were designed for 3' and 5' RACE-PCR. Total RNA was extracted from 48hpf, 72hpf, 5dpf larvae and adult heads using RNeasy kit (Qiagen). RNA quality was analyzed on a 1% agarose/1xTAE gel and RNA concentrations were measured. 1.2 µg of a pool of total RNA from the different developmental stages and tissues were used to generate cDNA templates for 5' and 3' RACE-PCR using the SMART RACE cDNA Amplification kit (Clontech) according to the manufacturer's instructions. First strand cDNA synthesis was performed with SuperScript II reverse transcriptase (Invitrogen) and all steps were carried out 200µl thin-walled PCR tubes on a thermal cycler (VWR). 100µl Tricine-EDTA buffer were added after cDNA synthesis and samples were stored at -20°C.

3µl of 5'- or 3'-RACE-Ready cDNA were used as template for RACE-PCR reaction.

RACE-PCR reaction mixture: 3µl 5'- or 3'-RACE Ready cDNA; 5µl 10x PCR buffer (Qiagen); 1µl dNTP's (10mM); 5µl 10x Universal Primer A Mix (UPM, Clontech); 1µl Gene-Specific-Primer (GSP, 10µM); 34.75µl ddH<sub>2</sub>O; 0.25µl HotStarTag Plus (Qiagen).

RACE-PCR program: 95°C-5'; 5x{94°C-30''; 67°C-30''; 72°C-4'}; 25x{94°C-30''; 66°C-30''; 72°C-4'}; 72°C-10'; 10°C-∞.

To increase the specificity of RACE-PCR products, nested RACE-PCR was performed.

Reaction mixture nested RACE-PCR: 1µl 5'- or 3' RACE-PCR reaction; 5µl 10x PCR buffer (Qiagen); 1µl dNTP's (10mM); 5µl Nested Universal Primer A (NUP, 10µM, Clontech); 1µl Nested Gene-Specific-Primer (NGSP, 10µM); 36.75µl ddH<sub>2</sub>O; 0.25µl HotStarTag Plus (Qiagen).

Nested RACE-PCR program: 95°C-5'; 25x{94°C-30''; 66°C-30''; 72°C-4'}; 72°C-10'; 10°C-∞.

## 4.7. Microscopy

### 4.7.1. Preparation of specimens for live imaging

Larvae were sacrificed directly before mounting in 4% PFA in seawater and subsequently transferred into fresh seawater on a microscope slide.

Juvenile worms were paralyzed by adding dropwise 1M  $\text{MgCl}_2$  into sea water until no movement of the animals occurred, then mounted in a small petri dish or on a microscope slide for microscopy.

### 4.7.2. Confocal laser microscopy

Confocal images of specimens were acquired as z-stacks on a Zeiss LSM 510 confocal microscope using a 40x oil immersion objective. Images were processed using the ImageJ software package (<http://imagej.nih.gov/ij/>), and confocal images were reconstructed as z-projections of scans and saved as tif-files.

### 4.7.3. DIC microscopy

DIC images were taken with a Zeiss Axioplan II microscope with Normarski optic settings using a 10x or a 40x oil immersion objective and a Zeiss AxioCam MR5 camera. Microscopic images were saved in tif-format.

### 4.7.4. Lumar stereomicroscopic images

Low magnification images of fluorescent specimens were acquired using a Zeiss Lumar V.12 Stereomicroscope with a FITC fluorescence filter and Kuebler HXP120 light source for fluorescence illumination and a Zeiss AxioCam MR4 camera. Images were saved in tif-format.

## 4.8. PhiC31 activity and plasmid recombination assay

### 4.8.1. Construction of attB-rps9::egfp

Primers attB-Rps9\_1.6kup\_f and EGFP-ISceI\_r were used to modify the rps9::egfp reporter by attaching the 39 nucleotide attB site 5' to the rps9 upstream region in a single PCR step. The resulting amplicon rps9::egfp\_5'attB was cloned into pJet2.1 vector.

### 4.8.2. Construction of attP-tuba::egfp

Primers ISceI/KpnI/attP/tuba\_f and EGFP-ISceI\_r were used in a PCR to modify tuba::egfp by attaching the 40-nucleotide attP site and a KpnI restriction site 5' to tuba:egfp. The resulting amplicon tuba::egfp\_5'attP was cloned into pJet2.1 vector and subcloned into pTol2 vector using the I-SceI meganuclease sites located on both 5' and 3' end of the construct.

### 4.8.3. Synthetic phiC31 integrase mRNA

The plasmid pCS2+-phiC31 containing the phiC31 integrase coding sequence was a generous gift from Johannes Bischof (Konrad Basler lab, University of Zurich, Switzerland). To generate synthetic phiC31 mRNA for microinjections, 5µg of the plasmid was linearized with NotI restriction enzyme (Fermentas), gel purified and eluted in 40µl of ddH<sub>2</sub>O. 6µl of the linearized template were used for Sp6 transcription. After DNaseI digest, the synthetic mRNA was purified and stored at -80°C.

### 4.8.4. Microinjection and analysis

Zygotes were injected with 0.15µg/µl of plasmid rps9::egfp\_5'attB, 0.15µg/µl of plasmid tuba::egfp\_5'attP, 0.2µg/µl of synthetic phiC31 integrase mRNA and 0.6% (w/v) TRITC-Dextrane (MW 70k, Invitrogen). After 5 hours of development, 4 injected embryos for each sample were collected in a volume of 1µl of sea water and transferred into 24µl PCR mastermix (2.5µl 10x CL buffer (Qiagen); 1µl primer phi\_test\_f; 1µl primer phi\_test\_r; 1µl

dNTP's (10mM); 0.25µl HotStar Taq Plus Polymerase (Qiagen); 18.25µl ddH<sub>2</sub>O) and PCR was performed (PCR program: 95°C-5'; 38x{94°C-30''; 60°C-30''; 72°C-1'45''}; 72°C-10'; 10°C-∞). PCR products were analyzed on 1% agarose/1xTAE gel, a 360bp PCR fragment was excised from the gel and cloned into pGEM-Teasy vector and sequenced.

## 4.9. Generation of reporter constructs

### 4.9.1. tuba::egfp reporter

To generate the tuba::egfp reporter construct pMos{tuba::egfp}, a 4.4kb fragment of the *Platynereis tuba* gene upstream of the putative start codon was PCR-amplified from purified BAC-DNA (CH305\_105D17) (Raible et. al., 2005) using primers „ISceI-tuba\_f“ and „tuba-GFP\_fusion\_r“. The *egfp* gene including a SV40 polyadenylation sequence was PCR-amplified from plasmid pEGFP-N1 (Clontech) using primers „EGFP-ISceI\_r“ and „EGFP-ATG\_f“. The PCR products were subsequently fused by fusion PCR with primers ISceI-tuba\_f and EGFP-ISceI\_r, and the final product was cloned into pCRII-TOPO (Invitrogen). In the final product, the *egfp* moiety is fused to the second exon of tuba, retaining the reading frame, as confirmed by sequencing. The I-SceI recognition sites flanking the reporter construct were used to release the product from pCRII-TOPO and to clone it into pMosSce and pTol2Sce destination vectors. F.Raible constructed the tuba::egfp reporter construct, I did the cloning into the destination vectors.

### 4.9.2. rps9::egfp reporter

3kb upstream region of rps9 were determined by sequencing fragments of a rps9-specific genomic TAIL-PCR. To generate the rps9 reporter construct, a 1.6kb fragment directly upstream of the start codon (ATG) was amplified by PCR using primers „ISceI-rps9\_1.6k\_f“ and „rps9-GFP\_fusion\_r“. The resulting amplicon was analyzed on 1% agarose gel, excised and purified. In a second PCR step the rps9 upstream amplicon was fused to *egfp* coding sequence derived from pEGFP-N1 (Clontech) amplified with primers „EGFP-ISceI\_r“ and „EGFP-ATG\_f“. The fusion product was cloned into pJet2.1 vector (Fermentas) and



subcloned into the transgenesis vectors pMos and pTol2 using the I-SceI sites that were attached to the 5' and 3' end of the reporter construct during PCR by the primers.

PCR mix rps9: 1µl (0.2µg) genomic DNA; 1µl dNTP's (10mM); 5µl 5x HF buffer (Finnzymes, Thermo Scientific, Thermo Scientific); 1µl primer ISceI-rps9\_1.6k\_f (5µM); 1µl primer rps9-GFP\_fusion\_r (5µM); 0.25µl (0.5U) Phusion DNA Polymerase (Finnzymes, Thermo Scientific); 15.75µl ddH<sub>2</sub>O.

PCR mix egfp: 1µl (1ng) pEGFP-N1 plasmid DNA (Clontech); 1µl dNTP's (10mM); 5µl 5x HF buffer (Finnzymes, Thermo Scientific); 1µl primer EGFP-ATG\_f (5µM); 1µl primer EGFP-ISceI\_r (5µM); 0.25µl (0.5U) Phusion DNA Polymerase (Finnzymes, Thermo Scientific); 15.75µl ddH<sub>2</sub>O.

Fusion PCR mix: 1µl egfp PCR fragment; 2µl rps9 PCR fragment; 1µl dNTP's (10mM); 5µl 5x HF buffer (Finnzymes, Thermo Scientific); 1µl primer ISceI-rps9\_1.6k\_f (5µM); 1µl primer EGFP-ISceI\_r (5µM); 0.25µl (0.5U) Phusion DNA Polymerase (Finnzymes, Thermo Scientific); 13.75µl ddH<sub>2</sub>O.

PCR program: 98°C-30''; 35x{98°C-15''; 60°C-30''; 72°C-90''}; 72°C-10'; 10°C-∞

Fusion PCR program: 98°C-30''; 35x{98°C-15''; 58°C-30''; 72°C-2''}; 72°C-10'; 10°C-∞

### 4.9.3. lMaf::egfp reporter

A 5kb genomic fragment containing the *Platynereis* lMaf locus and 3.8kb of its upstream region was identified by blast search in *Platynereis* genomic resources (<http://4dx.embl.de/platy/>). Primers ISceI-Maf\_3.6k\_f and Maf-GFP\_fusion\_r were designed to PCR amplify a 3.6kb fragment upstream of the start codon (ATG). The 3.6kb amplicon was linked by fusion PCR to the *egfp* coding sequence as outlined for the rps9::egfp reporter, cloned into pJet2.1 vector and subcloned into transgenesis vectors pMos and pTol2 using I-SceI sites.

PCR mix large Maf: 1µl (0.2µg) genomic DNA; 1µl dNTP's (10mM); 5µl 5x HF buffer (Finnzymes, Thermo Scientific); 1µl primer ISceI-Maf\_3.6k\_f (5µM); 1µl primer Maf-GFP\_fusion\_r (5µM); 0.25µl (0.5U) Phusion DNA Polymerase (Finnzymes, Thermo Scientific); 15.75µl ddH<sub>2</sub>O

Fusion PCR mix: 1µl egfp PCR fragment; 3µl large Maf PCR fragment; 1µl dNTP's (10mM); 5µl 5x HF buffer (Finnzymes, Thermo Scientific); 1µl primer ISceI-Maf\_3.6k\_f (5µM); 1µl primer EGFP-ISceI\_r (5µM); 0.25µl (0.5U) Phusion DNA Polymerase (Finnzymes, Thermo Scientific); 13.75µl ddH<sub>2</sub>O.

PCR program: 98°C-30''; 35x{98°C-15''; 60°C-30''; 72°C-3'}; 72°C-10'; 10°C-∞  
Fusion PCR program: 98°C-30''; 35x{98°C-15''; 60°C-30''; 72°C-4'}; 72°C-10'; 10°C-∞

#### 4.9.4. r-opsin::egfp reporter

A BAC containing the endogenous *Platynereis* r-opsin locus has been previously identified (Raible, 2005). An Egfp containing cassette (modified from Ejsmont et. al., 2009) was amplified using the primer and primer and inserted into the first exon of the *r-opsin* coding sequence using an established BAC recombineering protocol (Sarov et. al., 2006). Subsequently, an 8kbp region of the recombineered r-opsin locus was amplified using primers and placed into pMosSce by restriction cloning using SclI, resulting in the transgenesis vector pMos{r-opsin::egfp}. V.Babu Rajan generated the r-opsin reporter construct.

### 4.10. Morpholino antisense oligo design

To knockdown *Platynereis Maf* expression, I designed Morpholino antisense Oligos using oligo design support center by GeneTools (www.gene-tools.com, GENE TOOLS, LLC, USA).

#### 4.10.1. lMaf Morpholino antisense oligo

The *Platynereis lMaf* transcript including 5'UTR was determined by RACE-PCR. A 26 nucleotides translation blocking Morpholino antisense oligo binding 17 nucleotides in front of the start codon (ATG) was designed. The sequence of the antisense oligo is as follows: 5'-GGCTCCATAAGCCTGTTCTAAATAT-3'.

### 4.10.2. egfp Morpholino antisense oligo

As a control, an antisense oligo was designed for *egfp*.

A 25-nucleotide translation blocking Morpholino antisense oligo binding at the start codon (ATG) was designed for *egfp*. The sequence of the antisense oligo is as follows: 5'-ACAGCTCCTCGCCCTTGCTCACCAT-3'.

### 4.10.3. Morpholino antisense oligo injections

Zygotes were injected with 500µM Morpholino antisense oligo and 0.6% (w/v) TRITC-Dextrane (MW 70k, Invitrogen). After injection zygotes were transferred into fresh seawater and kept at 18°C.

## 4.11. Starvation assay

Immature animals were separated in 6-well dishes (1 animal/well) in sterile filtered seawater and kept without food during starvation period. The seawater was changed on a daily basis. After starvation of seven days, animals were divided into two groups. One group ( $I_f$ ) of the animals received a mixture of spinach, fish food (Tetramin) and algae, the other group ( $I_s$ ) was kept without food. 8 hours after donation of food to  $I_f$ ,  $I_f$  and  $I_s$  were decapitated and heads were immediately frozen in liquid nitrogen and subsequently stored at -80°C. One biological sample consisted of 5 heads.

## 4.12. Quantitative RT-PCR

### 4.12.1. Primer design

For optimal performance of quantitative RT-PCR, intron-spanning primer pairs with a melting temperature of 60°C and a PCR amplicon length ranging between 60 to 120 nucleotides were designed. Exon-Intron boundaries of *Platynereis* candidate genes were determined by spidey

mRNA-to-genomic alignment program (<http://www.ncbi.nlm.nih.gov/spidey/>) and gene structure of Medaka candidate genes was extracted from Ensembl homepage ([www.ensembl.org/](http://www.ensembl.org/)). Mainly, primer pairs for quantitative RT-PCR were designed using Roche Universal ProbeLibrary Assay Design Center (<https://www.roche-applied-science.com/sis/rtpcr/upl/index.jsp?id=UP030000>). In case no primer pairs were suggested by Universal ProbeLibrary Assay Design Center, primers were designed manually and primer properties were tested using Oligocalc webpage (<http://www.basic.northwestern.edu/biotools/oligocalc.html>). Specificity and efficiency of primer pairs were assayed in dilution series, with melting curve analysis and negative controls (-RT reaction, H<sub>2</sub>O control) according to general quantitative RT-PCR protocols.

In this study, I designed qRT-PCR primers for the following genes:

*Pdu ilp1*, *Pdu ilp2*, *Pdu ilp3*, *Pdu ilp4*, *Pdu ilp5*, *Pdu pax6*, *Ol ins*, *Ol igfI*, *Ol igfII*, *Ol rps9*, *Ol rpl7*, *Ol clk1*, *Ol clk2* (see Annex).

#### 4.12.2. Extraction of total RNA from tissues

Total RNA from tissues and whole animals was extracted using the RNeasy kit (Qiagen) RNA extraction protocol for animal tissues. Frozen specimens were disrupted in tubes using a sterile pestle. 350µl of RLT buffer containing 10µl/ml β-Mercaptoethanol were added and tissue was homogenized by pipetting. The lysate was centrifuged at 17.000g for 3 min and the supernatant was transferred into a fresh tube. After adding 350µl of 70% Ethanol the lysate was transferred to RNeasy spin columns and centrifuged at 8.000g for 15s. The spin column was washed once with 700µl of buffer RW1 and twice with 500µl of buffer RPE according to manufacturer's instructions and RNA was eluted in 30µl of RNase-free water. RNA concentration was determined using a nanodrop spectrophotometer and RNA was stored at -80°C.

#### 4.12.3. cDNA synthesis

Reverse transcription reaction was performed using the Quantitec reverse transcription kit (Qiagen) according to manufacturer's instructions. Typically, amounts of total RNA applied for generating cDNA ranged in different assays from 200ng for larval RNA to 400ng for adult

tissues. When 400ng (200ng) of total RNA were applied in the reverse transcription reaction, 80µl (40µl) of ddH<sub>2</sub>O were added after cDNA synthesis. cDNA was stored at -20°C.

#### 4.12.4. quantitative RT-PCR

Quantitative RT-PCR was performed on realtime PCR system using Microamp optical 96-well reaction plates sealed with MicroAmp optical Adhesive Film (all Applied Biosystems).

qRT-PCR program: 95°C-10'; 40x{95°C-15''; 60°C-1'}

qRT-PCR mix: 5µl cDNA; 1µl primer forward (10µM); 1µl primer reverse (10µM); 10µl SybrGreen mix (Applied Biosystems); 3µl ddH<sub>2</sub>O.

A dissociation curve analysis (melting curve) was performed as the last step of the PCR reaction by slowly raising the temperature of the sample from 60°C to 95°C.

#### 4.12.5. Analysis

qRT-PCR data were collected with the StepOne software v2.2 (ABI Biosystems). Thresholds of C<sub>T</sub> values of target genes were adjusted manually and C<sub>T</sub> values were exported to Excel software (Microsoft). All calculations, statistical analysis and diagrams of qRT-PCR data were done with Excel software.

### 4.13. Standard cloning procedures

#### 4.13.1. TA-cloning

Taq DNA Polymerase creates A-overhangs at the 3'-ends of each strand of a PCR product. To ligate PCR products generated with Taq DNA Polymerase into plasmid vector, TA cloning using the pGEM T-easy cloning kit (Promega) was performed. Half of the reaction volume recommended by the manufacturer was prepared for ligation in this study. 5µl of the ligation reaction were transformed into TOP 10' chemically competent cells (Invitrogen).

### 4.13.2. blunt-end cloning

Blunt-end PCR products generated with a proofreading DNA Polymerase were ligated into pJet2.1 vector (Fermentas) using blunt-end cloning protocol. Half of the recommended reaction volume was prepared for ligation and subsequently transformed into TOP 10' chemically competent cells (Invitrogen).

## 4.14. Plasmid preparation

### 4.14.1. Miniprep

3ml per culture LB media containing ampicillin (50µg/ml) or kanamycin (15µg/ml) were inoculated with a bacterial clone using a sterile pipet tip and incubated overnight at 37°C shaking with 160rpm. 1.5ml of overnight culture were transferred into a 1.5ml microcentrifuge tube, centrifuged at 5.000g for 9 min and the supernatant was removed. The bacterial pellet was resuspended in 200µl of Buffer P1 (50 mM TrisHCl pH 8.0; 10 mM EDTA; RNase A), 200µl of Buffer P2 (0.2M NaOH; 1%SDS) were added, mixed by inverting the tube and incubated for 5 min at room temperature. 200µl of Buffer P3 were added mixed by inverting the tube and centrifuged for 10 min at 17.000g. The clear lysate was transferred into a fresh tube, 450µl of Isopropanol were added and centrifuged for 20 min at 17.000g. The supernatant was removed, the DNA pellet was washed once with 1ml of 80% Ethanol and centrifuged for 5 min at 17.000g. The DNA pellet was air-dried for 15 min and resuspended in 50µl of ddH<sub>2</sub>O. Plasmid DNA was stored at -20°C.

### 4.14.2. Endotoxin-free Maxiprep

Bacterial endotoxin-free plasmid DNA was generated for microinjections in *Platynereis* zygotes. 100ml LB media containing ampicillin (50µg/ml) or kanamycin (15µg/ml) were inoculated with bacterial clones carrying the plasmid construct of interest and incubated overnight at 37°C shaking with 160rpm. To remove endotoxins during plasmid DNA preparation, Endofree Maxiprep kit (Qiagen) was used according to manufacturers instructions.

## 4.15. Thermal asymmetric interlaced PCR (TAIL-PCR)

TAIL-PCR uses three nested specific primers and one degenerated primer designed to bind arbitrary to sequences in consecutively PCR reactions. In process of the reactions, a specific PCR product is preferred, primed on one site by the specific primer and on the other site by the degenerated primer (Figure 38). In this study, a TAIL-PCR protocol provided by Y. Sasakura was used.

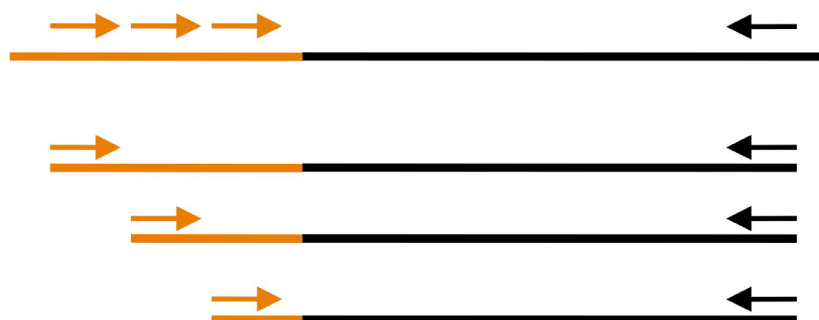


**Figure 38: Principle of TAIL-PCR**

Three consecutive nested primers are designed to bind a known region (orange). An arbitrary degenerated primer binds to random sequences (black). Successively, PCR reactions with the three nested primers (1st, 2nd, 3rd) and the arbitrary degenerated primer (ad) are performed.

The final product is primed on one site by the 3rd specific primer and on the other site by the degenerated primer.

### 4.15.1. Protocol

Nested specific primers were designed to have a melting temperature of 60°C. Sequences of degenerated primers I-VIII were designed according to Y. Sasakura.

For each of the degenerated primers consecutively PCR reaction with the three TAIL primers was performed. Starting amount in the first TAIL PCR was 200ng of genomic DNA. First TAIL-PCR reaction was diluted 1:25 with ddH<sub>2</sub>O and 1μl was used as template in the second TAIL-PCR reaction. Second TAIL-PCR reaction was diluted 1:25 and 1μl was used as template in the third TAIL-PCR reaction.

Reaction mixture 1<sup>st</sup> TAIL-PCR: 200ng DNA; 1μl dNTP's (10mM); 0.8μl specific primer TAIL1 (5μM); 1μl degenerated primer (100μM); 4μl 5xHF buffer (Finnzymes, Thermo Scientific); 0.2μl Phusion DNA Polymerase (Finnzymes, Thermo Scientific); ad 20μl ddH<sub>2</sub>O

Reaction mixture 2<sup>nd</sup> TAIL-PCR: 1µl 1<sup>st</sup> TAIL-PCR (1:25 dilution); 1µl dNTP's (10mM); 0.8µl specific primer TAIL1 (5µM); 1µl degenerated primer (100µM); 4µl 5xHF buffer (Finnzymes, Thermo Scientific); 0.2µl Phusion DNA Polymerase (Finnzymes, Thermo Scientific); 12µl ddH<sub>2</sub>O

Reaction mixture 3<sup>rd</sup> TAIL-PCR: 1µl 2<sup>nd</sup> TAIL-PCR (1:25 dilution); 1µl dNTP's (10mM); 0.8µl specific primer TAIL1 (5µM); 1µl degenerated primer (100µM); 4µl 5xHF buffer (Finnzymes, Thermo Scientific); 0.2µl Phusion DNA Polymerase (Finnzymes, Thermo Scientific); 12µl ddH<sub>2</sub>O

PCR program 1<sup>st</sup> TAIL-PCR: 98°C-30''; 94°C-1'; 95°C-1'; 6x{94°C-1'; 65°C-1'; 72°C-45''}; 94°C-1'; 25°C-3'; 72°C-3'; 15x{94°C-30''; 64°C-1'; 72°C-3'; 94°C-30''; 64°C-1'; 72°C-3'; 94°C-30''; 44°C-1'; 72°C-3'}; 72°C-5'; 10°C-∞

PCR program 2<sup>nd</sup> TAIL-PCR: 98°C-10''; 14x{94-30''; 64°C-1'; 72°C-3'; 94°C-30''; 64°C-1'; 72°C-3'; 94°C-30''; 44°C-1'; 72°C-3'}; 72°C-5'; 10°C-∞

PCR program 3<sup>rd</sup> TAIL-PCR: 98°C-10''; 12x{94-30''; 64°C-1'; 72°C-3'; 94°C-30''; 64°C-1'; 72°C-3'; 94°C-30''; 44°C-1'; 72°C-3'}; 72°C-5'; 10°C-∞

## 4.15.2. Detection of genomic integrations of reporter constructs

### 4.15.2.1. Mos integrations

TAIL-PCR was performed to PCR amplify genomic regions adjacent to the integration site of pMos tuba::egfp reporter construct in the transgenic line. Genomic DNA from a pMos tuba::egfp transgenic animal was extracted. Nested specific primers for consecutive PCR MosLIR-1, MosLIR-2, Mos-LIR3 and MosRIR-1, MosRIR-2, MosRIR-3 were designed to bind the left and right Mariner inverted repeats. After the 3<sup>rd</sup> TAIL-PCR, an 800bp fragment was obtained for the right inverted repeat primer set and a 1.2kb fragment was obtained for the left inverted repeat primer set. The fragments were cloned into pJet1.2 vector and sequenced.



#### 4.15.2.2. Tol2 integrations

TAIL-PCR was used to identify a genomic integration site of the pTol2 rps9::egfp reporter construct in a transgenic animal by PCR amplification of genomic regions adjacent to the Tol2 left and right terminal repeats. After breeding, genomic DNA was extracted from a mature animal that was injected with p{Tol2 rps9::egfp} as zygote.

Nested specific primers Tol2L-1, Tol2L-2, Tol2L-3 and Tol2R-1, Tol2R-2, Tol2R-3 were designed to bind sequences between the tol2 terminal repeats and the cloning sites (I-SceI) of the reporter construct. After the 3<sup>rd</sup> TAIL-PCR, a 1kb fragment was obtained for the left inverted repeat primers. The fragment was cloned into pJet1.2 vector and sequenced.

#### 4.15.3. Enhancer isolation

TAIL-PCR was used to isolate the enhancer of rps9 gene. Genomic DNA was extracted from a wild-type animal. In a first round of consecutive TAIL-PCR, a 700bp fragment upstream of the start codon was identified using nested specific primers rps9\_TAIL1, rps9\_TAIL2, rps9\_TAIL3 designed to bind in the first exon of rps9 near the start of the coding sequence. A second set of nested specific primers rps9\_TAILII-1, rps9\_TAILII-2, rps9\_TAILII-3 was designed to bind near the 5'-end of the 700bp upstream fragment identified in the first round of TAIL-PCR. An approximately 2.5kb fragment specific for the rps9 upstream region was identified. Combination of the 700bp and 2.5kb upstream fragments obtained in the two rounds of TAIL-PCR resulted in a total rps9 upstream region of about 3.000 nucleotides in length.

#### 4.16. Construction of Phylogenetic trees

To search for candidate genes of interest in *Platynereis*, the protein sequences of orthologous genes from different species were compiled from uniprot database (<http://www.uniprot.org/>) and from ncbi website (<http://www.ncbi.nlm.nih.gov/>) using non-redundant protein sequence database (nr). Blast searches for *Platynereis* candidates were performed against *Platynereis* larval transcriptome, head transcriptome and *Platynereis* 4dx library (<http://4dx.embl.de/platy/>). *Platynereis* nucleotide sequences of candidate genes were extracted and translated into protein sequence using EnzymeX software and confirmed by

BLAST search on ncbi website (<http://blast.ncbi.nlm.nih.gov/Blast.cgi>). *Platynereis* candidate protein sequences were included into the set of orthologues from different species and phylogenetic analysis were performed on phyML website ([http://www.phylogeny.fr/version2\\_cgi/one\\_task.cgi?task\\_type=phym1](http://www.phylogeny.fr/version2_cgi/one_task.cgi?task_type=phym1)). Sequence alignments were done using MUSCLE multiple alignment program. Poorly aligned positions and divergent regions were removed from the alignments using GBlocks software. Maximum-likelihood phylogeny was calculated with phyML program using bootstrapping procedure set to 300 bootstraps (maximum). Phylogenetic trees were visualized using TreeDyn tool, exported in nexus format and processed using FigTree software (v1.3.1).

#### 4.17. PCR Primer design

PCR primers used in this study were designed manually and primer properties were tested using Oligocalc webpage (<http://www.basic.northwestern.edu/biotools/oligocalc.html>). Optimal melting temperature for PCR primers calculated with Nearest Neighbor method was 60°C. Calculation parameters defined for potential hairpin formation was four nucleotides minimum, self-annealing of primers was defined as five nucleotides minimum.

#### 4.18. Identification of genomic loci of *Platynereis* insulin-like peptide1 and insulin-like peptide2

Genomic loci of *Platynereis insulin-like peptide1* and *insulin-like peptide2* were obtained by screening of a *Platynereis* BAC-library (CHORI-305, BACPAC Resources). To screen *Platynereis* BAC Filters, radiolabeled probes for *insulin-like peptide1* and *insulin-like peptide2* were generated as described in 4.5.2.2 and hybridized with the filters as described in 4.5.2.3.. Individual positive BAC clones were identified and ordered from BACPAC as stab cultures. Stab cultures were singled out on agar plates containing chloramphenicol in a concentration of 15µg/ml and incubated overnight at 37°C. Three colonies of each individual BAC clone were picked and BAC minipreps were done according to an established protocol. Diagnostic digests of BAC DNA using EcoRI and HindIII restriction enzymes (both Fermentas) were analyzed on 1% agarose/1xTAE gel, blotted on nylon membrane and hybridized with radiolabeled probes for *ilp1* and *ilp2* as described previously. One BAC clone

for *ilp1* and one BAC clone for *ilp2* were selected and were sent for sequencing to Genoscope, Institut de Génomique du CEA, Evry, France as glycerol stock.

## 4.19. Transposase activity test

To test the activity of transposase used for transgenesis in *Platynereis*, a PCR-based excision assay was performed. Primer pairs for the excision assay were designed to bind in the vector backbone in proximity to the terminal repeats. A PCR fragment specific for the empty vector indicates successful excision of the reporter from the vector backbone whereas non-cut plasmid yields no PCR fragment due to length restriction of PCR fragments set by a short extension interval during PCR.

### 4.19.1. Tol2 excision test

Primers T2f and T2r were designed to bind the pTol2 vector backbone at 138 / 96nt distance to the Tol2 inverted repeats. Zygotes were injected with 0.2µg/µl of pTol2Sce{rps9::egfp} DNA, 0.2µg/µl synthetic *tol2* mRNA and 0.6% (w/v) TRITC-Dextrane (MW:70.000, Invitrogen). Control zygotes were injected with 0.2µg/µl of reporter plasmid DNA and 0.6% (w/v) TRITC-Dextrane. Four hours after injection, three embryos per sample were collected in 1µl of seawater and transferred into PCR mix (2.5µl 10x Cl buffer (Qiagen); 1µl dNTP-mix (10mM); 0.25µl (1.25U) Hot Star Taq Plus DNA Polymerase (Qiagen); 1µl primer T2\_f (5µM), 1µl primer T2\_r (5µM); 18.25µl ddH<sub>2</sub>O). PCR for excision assay was performed under following conditions: 95°C - 5min, 35x (95°C - 30s, 60°C - 30s, 72°C - 1min), 72°C - 10min. Samples were analyzed on 1% agarose/1xTAE gel. A 200bp fragment was excised from the gel and sequenced

### 4.19.2. Mos1 excision test

Primers Mos\_test\_fw and Mos\_test\_rv were designed to bind the pMos1 vector backbone at 76/88 nt distance to the Mos1 terminal repeats.

Zygotes were injected with 0.2µg/µl of pMos{rps9::egfp} DNA, 0.2µg/µl synthetic *mos1* mRNA and 0.6% (w/v) TRITC-Dextrane (MW:70.000, Invitrogen). Control zygotes were

injected with 0.2µg/µl of reporter plasmid DNA and 0.6% (w/v) TRITC-Dextrane. Four hours after injection, three embryos per sample were collected in 1µl of seawater and transferred into PCR mix (2.5µl 10x Cl buffer (Qiagen); 1µl dNTP-mix (10mM); 0.25µl (1.25U) Hot Star Taq Plus DNA Polymerase (Qiagen); 1µl primer Mos\_test\_f (5µM), 1µl primer Mos\_test\_r (5µM); 18.25µl ddH<sub>2</sub>O). PCR for excision assay was performed under following conditions: 95°C - 5min, 35x (95°C - 30s, 60°C - 30s, 72°C - 1min), 72°C - 10min. Samples were analyzed on 1% agarose/1xTAE gel. A 150bp fragment was excised from the gel and sequenced.

## 4.20. Transposases

In order to establish Transgenesis in *Platynereis* different transposases were tested during this study. Transposases are co-injected as mRNA along with the reporter construct into zygotes. Translated into protein, the transposase is supposed to integrate the reporter construct into the genome.

### 4.20.1. Minos Transposase

For in-vitro synthesis of *Minos mRNA* for microinjections, the plasmid pBlueSKMimRNA (Pavlopoulos et al, 2004) was used. The plasmid was linearized with NotI restriction enzyme and transcribed using the T7 mMessage Machine kit (Ambion)

### 4.20.2. Mos1 Transposase

The Mos1 transposase was PCR-amplified from plasmid pKhsp82MOS (Coates et. al., 1997) using tagged primers, digested and directionally cloned into the BamHI/EcoRI sites of pCS2+ by F.Raible. To generate *mos1* synthetic mRNA, pCS2+ Mos1 was digested with NotI and transcribed using the Sp6 mMessage Machine kit (Ambion).

### 4.20.3. Tol2 Transposase

Synthetic *tol2* mRNA for microinjections was generated from plasmid pCS2FA Tol2-Transposase (Kwan et. al., 2007) by NotI linearization of the plasmid and subsequent Sp6 transcription using the Sp6 mMessage Machine kit (Ambion).

## 4.21. Vectors for Transgenesis

In order to establish Transgenesis in *Platynereis*, different transposon vectors were tested. The transposon vectors were designed to have two I-SceI meganuclease sites, which were used to insert the reporter constructs via I-SceI digest and T4 ligation.

### 4.21.1. pMiSce

pMiSce is a derivative of the vector pMi that possesses two additional SceI sites between the AscI cloning site. The plasmid was generated by inserting an AscI-flanked oligo containing two SceI sites into the AscI cloning site of pMi{3xP3-DsRedafm} (kindly provided by E. Wimmer). F. Raible constructed pMiSce with additional help from R. Tomer.

### 4.21.2. pMosSce

pMosSce is a derivative of the vector pMos that possesses two additional I-SceI sites between the AscI/FseI cloning sites. The plasmid was generated by inserting an AscI-flanked oligo containing two SceI sites into the AscI cloning site of pMos{3xP3-DsRedafm} (Horn and Wimmer, 2000). F. Raible constructed pMosSce.

### 4.21.3. pTol2Sce

pTol2Sce is a derivative of the tol2 kit vector pDestTol2pA2 (Kwan et. al., 2007) that possesses two additional I-SceI sites next to the XhoI and KpnI cloning sites of pDestTol2pA2. S. Kirchmaier constructed pTol2Sce.

### 4.22. *Platynereis dumerilii* primary cell culture

*Platynereis* larvae were transferred into a droplet (~20µl) of Schneider's insect medium containing penicillin and streptomycine on a microscope slide. The larvae were crushed between the microscope slide and a coverslip and sealed with mineral oil to prevent desiccation of specimens.

### 4.23. Standard sequencing of plasmid DNA

Standard sequencing of plasmids was done by LGC genomics (LGC, Berlin, Germany). Length of sequencing reads received from LGC genomics ranged between 800-1.000 nucleotides. Typically, sequencing of inserts cloned into pJet2.1 vector primers pJet\_fw and pJet\_rv were used and primers Sp6-20 and T7-prom were used to sequence inserts of pGEM T-easy vector.

### 4.24. Genotyping PCR for transgenic animals

To test for the presence of *egfp* in genomic DNA preparations of potentially transgenic individuals and their offspring, an *egfp* fragment of 700 nucleotides in length was PCR-amplified using primers EGFP\_f and EGFP\_r

As a control, a 700 nucleotide fragment of the *Platynereis large Maf* gene was PCR-amplified using primers Maf\_f and Maf\_r. Further controls for PCR included: no genomic template, wild-type genomic DNA, genomic DNA from transgenic animals, *egfp* plasmid DNA.

Reaction mixture: 1µl (100-150ng) genomic DNA; 2.5µl 10x CL buffer (Qiagen); 1µl dNTP's (10mM); 1µl primer forward (5µM); 1µl primer reverse (5µM); 0.25µl (1.25U) HotStar Taq Plus DNA Polymerase (Qiagen); 18.25µl ddH<sub>2</sub>O.

PCR program: 95°C-5'; 38x{94°C-30''; 60°C-30''; 72°C-1'}; 72°C-10'; 10°C-∞

## 4.25. *Platynereis dumerilii* rps9 gene-structure

Primers Rps9\_f and Rps9\_r were designed to bind the 5' and the 3' end of the *rps9* coding sequence. PCR on *Platynereis* genomic DNA as template revealed a PCR product of 750bp in length, which was cloned into pGEM T-easy vector and sequenced.

The sequencing product was aligned to *rps9* transcript to determine the *rps9* exon-intron structure.

Reaction mixture: 2µl genomic DNA; 2.5µl 10x buffer (Qiagen); 1µl dNTP's (10mM); 1µl primer Rps9\_f (5µM); 1µl primer Rps9\_r (5µM); 0.25µl (1.25U) HotStar Taq Plus DNA Polymerase (Qiagen); 17.25µl ddH<sub>2</sub>O.

PCR program: 95°C-5'; 35x{94°C-30''; 60°C-30''; 72°C-2'}; 72°C-10'; 10°C-∞

## 4.26. List of genes that were cloned in this study using specific primers

List of genes that were cloned using specific primers in this study. Genes were cloned into pGEM T-easy vector and sequences were validated.

*Platynereis dumerilii*:

*ptf1a*, *inR*, *glut2*, *foxo*, *cpa*, *insulin-like peptide1*, *insulin-like peptide2*, *insulin-like peptide3*, *insulin-like peptide4*, *insulin-like peptide5*, *dach*, *neuroD*, *pax2/5/8*, *g(q)*,

*Oryza latipes*:

*Ol clock1*, *Ol clock2*

## 4.27. Equipment

Microscopy:

- Stereomicroscope SteREO Lumar.V12 (Zeiss)
- light source for fluorescence illumination HXP120 (Kuebler)
- Axioplan2 Microscope (Zeiss)
- Confocal microscope LSM 510 (Zeiss)
- Stereomicroscope Stemi 2000 (Zeiss)

- Axiocam MRc5 camera (Zeiss)

Centrifuges:

- Microcentrifuge Heraeus Pico 17 (Thermo Scientific)
- Centrifuge 5810R (Eppendorf)

Thermal cycler:

- Thermal Cycler Quattro Chassi (VWR)
- StepOnePlus Realtime PCR system (ABI Biosystems)

Thermomixer:

- Thermomixer compact (Eppendorf)

Waterbath:

- Waterbath Julabo 13

Nylon nets:

- nylon nets for collecting *Platynereis* embryos for microinjection and WMISH fixation: Falcon cell strainer, mesh size 70µm (BD Bioscience) glued onto a bottomless 50ml Falcon tube (BD Bioscience)
- nylon nets for collecting *Platynereis* embryos in small volumes prior fixation for WMISH: nylon sieve tissue NITEX mesh width of 100µm (Gebr. Stallmann, Reilingen, Germany) glued onto bottomless 2 ml microcentrifuge tubes

Agarose gel electrophoresis:

- AGT2 electrophoresis chamber (VWR)
- MSMINI electrophoresis chamber (Biozym)
- Power source 250V (VWR)
- Alphaimager HP gel documentation system (Biozym)
- Safe imager blue light Transilluminator (Invitrogen)

Microinjections:

- LC2 microscope (Leica)
- Transferman NK2 micromanipulator (Eppendorf)
- Femtojet express microinjector (Eppendorf)
- Femtotips II microcapillaries (Eppendorf)
- injection mould

Molecular biology kits:

- RNeasy mini kit (Qiagen)
- Qiaquick gel extraction kit (Qiagen)
- Endofree plasmid maxi kit (Qiagen)



- Nucleospin tissue kit (Macherey-Nagel)
- T7/Sp6 mMessage mMachine kit (Ambion)
- Radprime DNA labeling kit (Invitrogen)
- Quantitec reverse transcription kit (Qiagen)

Southern blot equipment:

- Nylon membrane (39-2010, Peqlab, Germany)
- Hybridization oven
- exposure cassette (Kodak)
- phosphoimager
- imaging plate (GE Healthcare)
- UV crosslinker (Stratagene)

Nucleic acid concentration measurement:

- NanoDrop spectrophotometer (Peqlab)



## 5. References

- Ackermann AM, Gannon M (2007). Molecular regulation of pancreatic beta-cell mass development, maintenance, and expansion. *J Mol Endocrinol*, 38(1-2), 193-206.
- Aljanabi SM, Martinez I (1997). Universal and rapid salt-extraction of high quality genomic DNA for PCR-based techniques. *Nucleic Acids Res*, 25(22), 4692-3.
- Allaman-Pillet N, Roduit R, Oberson A, Abdelli S, Ruiz J, Beckmann JS, Schorderet DF, Bonny C (2004). Circadian regulation of islet genes involved in insulin production and secretion. *Mol Cell Endocrinol*, 226(1-2), 59-66.
- Allshire RC, Javerzat JP, Redhead NJ, Cranston G (1994). Position effect variegation at fission yeast centromeres. *Cell*, 76(1), 157-69.
- Arendt D, Wittbrodt J (2001). Reconstructing the eyes of Urbilateria. *Philos Trans R Soc Lond B Biol Sci*, 356(1414), 1545-63.
- Arendt D, Tessmar K, de Campos-Baptista MI, Dorresteijn A, Wittbrodt J (2002). Development of pigment-cup eyes in the polychaete *Platynereis dumerilii* and evolutionary conservation of larval eyes in Bilateria. *Development*, 129(5), 1143-54.
- Arendt D, Tessmar-Raible K, Snyman H, Dorresteijn AW, Wittbrodt J (2004). Ciliary photoreceptors with a vertebrate-type opsin in an invertebrate brain. *Science*, 306(5697), 869-71.
- Arnone MI, Bogarad LD, Collazo A, Kirchhamer CV, Cameron RA, Rast JP, Gregorians A, Davidson EH (1997). Green Fluorescent Protein in the sea urchin: new experimental approaches to transcriptional regulatory analysis in embryos and larvae. *Development*, 124(22), 4649-59.
- Artner I, Le Lay J, Hang Y, Elghazi L, Schisler JC, Henderson E, Sosa-Pineda B, Stein R (2006). MafB: an activator of the glucagon gene expressed in developing islet alpha- and beta-cells. *Diabetes*, 55(2), 297-304.
- Asakawa K, Kawakami K (2009). The Tol2-mediated Gal4-UAS method for gene and enhancer trapping in zebrafish. *Methods*, 49(3), 275-81.
- Azami S, Wagatsuma A, Sadamoto H, Hatakeyama D, Usami T, Fujie M, Koyanagi R, Azumi K, Fujito Y, Lukowiak K, Ito E (2006). Altered gene activity correlated with long-term memory formation of conditioned taste aversion in *Lymnaea*. *J Neurosci Res*, 84(7), 1610-20.
- Bach MA, Shen-Orr Z, Lowe WL Jr, Roberts CT Jr, LeRoith D (1991). Insulin-like growth factor I mRNA levels are developmentally regulated in specific regions of the rat brain. *Brain Res Mol Brain Res*, 10(1), 43-8.

- Backfisch B, Veedin Rajan VB, Fischer RM, Lohs C, Arboleda E, Tessmar-Raible K, Raible F (2013). Stable transgenesis in the marine annelid *Platynereis dumerilii* sheds new light on photoreceptor evolution. *Proc Natl Acad Sci U S A*, 110(1), 193-8.
- Banting FG, Best CH, Collip JB, Campbell WR, Fletcher AA (1922). Pancreatic Extracts in the Treatment of Diabetes Mellitus. *Can Med Assoc J*, 12(3), 141-6.
- Banting, F. G. and Best, C. H. (1922) The internal secretion of the pancreas. *J Lab Clin Med*, 7, 251±266
- Beiler JM, McBurney EA, Pachtmab EA, Pizzaia LM, Martin GJ (1960). Effects of relaxin on wound healing. *Arch Int Pharmacodyn Ther*, 123, 291-4.
- Bessa J, Tena JJ, de la Calle-Mustienes E, Fernández-Miñán A, Naranjo S, Fernández A, Montoliu L, Akalin A, Lenhard B, Casares F, Gómez-Skarmeta JL (2009). Zebrafish enhancer detection (ZED) vector: a new tool to facilitate transgenesis and the functional analysis of cis-regulatory regions in zebrafish. *Dev Dyn*, 238(9), 2409-17.
- Bischof J, Maeda RK, Hediger M, Karch F, Basler K (2007). An optimized transgenesis system for *Drosophila* using germ-line-specific  $\phi$ C31 integrases. *Proc Natl Acad Sci U S A*, 104(9), 3312-7.
- Boden G, Ruiz J, Urbain JL, Chen X (1996). Evidence for a circadian rhythm of insulin secretion. *Am J Physiol*, 1996 271, 246-52.
- Bonal C, Herrera PL. Genes controlling pancreas ontogeny (2008). *Int J Dev Biol*, 52(7), 823-35.
- Boquist L, Falkmer S, Mehrotra BK (1971). Ultrastructural search for homologues of pancreatic  $\beta$ -cells in the intestinal mucosa of the mollusc *Buccinum undatum*. *Gen Comp Endocrinol*, 17(1), 236-9.
- Breitman ML, Clapoff S, Rossant J, Tsui LC, Glode LM, Maxwell IH, Bernstein A (1987). Genetic ablation: targeted expression of a toxin gene causes microphthalmia in transgenic mice. *Science*, 238(4833), 1563-5.
- Brogiolo W, Stocker H, Ikeya T, Rintelen F, Fernandez R, et al. (2001) An evolutionarily conserved function of the *Drosophila* insulin receptor and insulin-like peptides in growth control. *Curr Biol*, 11, 213–221.
- Brooke NM, Garcia-Fernández J, Holland PW (1998). The ParaHox gene cluster is an evolutionary sister of the Hox gene cluster. *Nature*, 392(6679), 920-2.
- Brown MR, Crim JW, Arata RC, Cai HN, Chun C, Shen P (1999). Identification of a *Drosophila* brain-gut peptide related to the neuropeptide Y family. *Peptides*, 20(9), 1035-42.
- Bryan G, Garza D, Hartl D (1990). Insertion and excision of the transposable element mariner in *Drosophila*. *Genetics*, 125(1), 103-14

- Candiani S, Kreslova J, Benes V, Oliveri D, Castagnola P, Pestarino M, Kozmik Z (2003). Cloning and developmental expression of amphioxus Dachschund. *Gene Expr Patterns*, 3(1), 65-9.
- Cerf ME (2006). Transcription factors regulating beta-cell function. *Eur J Endocrinol*, 155(5), 671-9.
- Chan SJ, Cao QP, Steiner DF (1990). Evolution of the insulin superfamily: cloning of a hybrid insulin/insulin-like growth factor cDNA from amphioxus. *Proc Natl Acad Sci U S A*, 87(23), 9319-23.
- Chen DY, Stern SA, Garcia-Osta A, Saunier-Rebori B, Pollonini G, Bambah-Mukku D, Blitzner RD, Alberini CM (2011). A critical role for IGF-II in memory consolidation and enhancement. *Nature*, 469(7331), 491-7.
- Christodoulou F, Raible F, Tomer R, Simakov O, Trachana K, Klaus S, Snyman H, Hannon GJ, Bork P, Arendt D (2010). Ancient animal microRNAs and the evolution of tissue identity. *Nature*, 463(7284), 1084-8.
- Cissell MA, Zhao L, Sussel L, Henderson E, Stein R (2003). Transcription factor occupancy of the insulin gene in vivo. Evidence for direct regulation by Nkx2.2. *J Biol Chem*, 278(2), 751-6.
- Clements J, Hens K, Francis C, Schellens A, Callaerts P (2008). Conserved role for the *Drosophila* Pax6 homolog Eyeless in differentiation and function of insulin-producing neurons. *Proc Natl Acad Sci U S A*, 105(42), 16183-8.
- Coates, C. J., Turney, C. L., Frommer, M., O'Brochta, D. A. & Atkinson, P. W. (1997) *Mol. Gen. Genet*, 253, 728–733
- Cooley L, Berg C, Spradling A (1988). Controlling P element insertional mutagenesis. *Trends Genet*, 4(9), 254-8.
- Cooley L, Kelley R, Spradling A (1988). Insertional mutagenesis of the *Drosophila* genome with single P elements. *Science*, 239(4844), 1121-8.
- Davidson EH (2006). *The Regulatory Genome: Gene Networks in Development*. Academic Press.
- Davidson JK, Falkmer S, Mehrotra BK, Wilson S (1971). Insulin assays and light microscopical studies of digestive organs in protostomian and deuterostomian species and in coelenterates. *Gen Comp Endocrinol*, 17(2), 388-401.
- Denes AS, Jékely G, Steinmetz PR, Raible F, Snyman H, Prud'homme B, Ferrier DE, Balavoine G, Arendt D (2007). Molecular architecture of annelid nerve cord supports common origin of nervous system centralization in bilateria. *Cell*, 129(2), 277-88.
- de Velasco B, Erclik T, Shy D, Sclafani J, Lipshitz H, McInnes R, Hartenstein V (2007). Specification and development of the pars intercerebralis and pars lateralis, neuroendocrine command centers in the *Drosophila* brain. *Dev Biol*, 302(1), 309-23.

- Devaskar SU, Giddings SJ, Rajakumar PA, Carnaghi LR, Menon RK, Zahm DS (1994). Insulin gene expression and insulin synthesis in mammalian neuronal cells. *J Biol Chem*, 269(11), 8445-54.
- Devaskar SU, Singh BS, Carnaghi LR, Rajakumar PA, Giddings SJ (1993). Insulin II gene expression in rat central nervous system. *Regul Pept*, 48(1-2), 55-63.
- Dorer DR, Henikoff S (1994). Expansions of transgene repeats cause heterochromatin formation and gene silencing in *Drosophila*. *Cell*, 77(7), 993-1002.
- Dunlap JC (1999). Molecular bases for circadian clocks. *Cell*, 96(2), 271-90.
- Duret L, Guex N, Peitsch MC, Bairoch A (1998). New insulin-like proteins with atypical disulfide bond pattern characterized in *Caenorhabditis elegans* by comparative sequence analysis and homology modeling. *Genome Res*, 8(4), 348-53.
- Ebberink RH, Joosse J (1985). Molecular properties of various snail peptides from brain and gut. *Peptides*, 6 Suppl 3, 451-7.
- Essig M, Schoenfeld C, Amelar RD, Dubin L, Weiss G (1982). Stimulation of human sperm motility by relaxin. *Fertil Steril*, 38(3), 339-43.
- Fischer AH, Henrich T, Arendt D (2010). The normal development of *Platynereis dumerilii* (Nereididae, Annelida). *Front Zool*, 7, 31.
- Fischer A, Dorresteijn A (2004). The polychaete *Platynereis dumerilii* (Annelida): a laboratory animal with spiralian cleavage, lifelong segment proliferation and a mixed benthic/pelagic life cycle. *Bioessays*, 26(3), 314-25.
- Fischer A (1969). [A pigment deficient mutant in the polychaete *Platynereis dumerilii*]. *Mol Gen Genet*, 104(4), 360-70. German.
- Floyd PD, Li L, Rubakhin SS, Sweedler JV, Horn CC, Kupfermann I, Alexeeva VY, Ellis TA, Dembrow NC, Weiss KR, Vilim FS (1999). Insulin prohormone processing, distribution, and relation to metabolism in *Aplysia californica*. *J Neurosci*, 19(18), 7732-41.
- Franks RR, Anderson R, Moore JG, Hough-Evans BR, Britten RJ, Davidson EH (1990). Competitive titration in living sea urchin embryos of regulatory factors required for expression of the *CyIIIa* actin gene. *Development*, 110(1), 31-40.
- Franks RR, Hough-Evans BR, Britten RJ, Davidson EH (1988). Direct introduction of cloned DNA into the sea urchin zygote nucleus, and fate of injected DNA. *Development*, 102(2), 287-99.
- Franks RR, Hough-Evans BR, Britten RJ, Davidson EH (1988). Spatially deranged though temporally correct expression of *Strongylocentrotus purpuratus* actin gene fusion in transgenic embryos of a different sea urchin family. *Genes Dev*, 2(1), 1-12.
- Franz G, Loukeris TG, Dialektaki G, Thompson CR, Savakis C (1994). Mobile Minos elements from *Drosophila hydei* encode a two-exon transposase with similarity to the paired DNA-binding domain. *Proc Natl Acad Sci USA*, 91, 4746-4750.

- Franz G, Savakis CC (1991). *Minos*, a new transposable element from *Drosophila hydei*, is a member of the *Tc1*-like family of transposons Nucleic Acid Res, 19, 6646
- Fritsch HA, Van Noorden S, Pearse AG (1976). Cytochemical and immunofluorescence investigations of insulin-like producing cells in the intestine of *Mytilus edulis* L. (Bivalvia). Cell Tissue Res, 165(3), 365-9.
- Fröblius AC, Seaver EC (2006). ParaHox gene expression in the polychaete annelid *Capitella* sp. I. Dev Genes Evol, 216(2), 81-8.
- Galloway SM, Cutfield JF (1988). Insulin-like material from the digestive tract of the tunicate *Pyura pachydermatina* (sea tulip). Gen Comp Endocrinol, 69(1), 106-13.
- Garofalo RS, Rosen OM (1988). Tissue localization of *Drosophila melanogaster* insulin receptor transcripts during development. Mol Cell Biol, 8(4), 1638-47.
- Garrick D, Fiering S, Martin DI, Whitelaw E (1998). Repeat-induced gene silencing in mammals. Nat Genet, 18(1), 56-9.
- Geraerts WP, Smit AB, Li KW, Hordijk PL (1992). The Light Green Cells of *Lymnaea*: a neuroendocrine model system for stimulus-induced expression of multiple peptide genes in a single cell type. Experientia, 48(5), 464-73.
- Geraerts WP (1976). Control of growth by the neurosecretory hormone of the light green cells in the freshwater snail *Lymnaea stagnalis*. Gen Comp Endocrinol, 29(1), 61-71.
- Geraerts WP (1992). Neurohormonal control of growth and carbohydrate metabolism by the light green cells in *Lymnaea stagnalis*. Gen Comp Endocrinol, 86(3), 433-44.
- Gladon S, Holland LZ, Gehring WJ, Holland ND (1998). Isolation and developmental expression of the amphioxus Pax-6 gene (AmphiPax-6): insights into eye and photoreceptor evolution. Development, 125(14), 2701-10.
- Golding DW (1970). The infracerebral gland in *Nephtys*--a possible neuroendocrine complex. General and comparative endocrinology, 14(1)
- Groth AC, Fish M, Nusse R, Calos MP (2004). Construction of transgenic *Drosophila* by using the site-specific integrase from phage  $\phi$ C31. Genetics, 166(4), 1775-82.
- Hall K (1957). The effect of relaxin extracts, progesterone and oestradiol on maintenance of pregnancy, parturition and rearing of young after ovariectomy in mice. J Endocrinol, 15(1):108-17.
- Hang Y, Stein R (2011). MafA and MafB activity in pancreatic  $\beta$  cells. Trends Endocrinol Metab, 22(9), 364-73.
- Hauenschild C, Fischer A (1969) *Platynereis dumerilii*. Mikroskopische Anatomie, Fortpflanzung und Entwicklung [Platynereis dumerilii. Microscopical anatomy, reproduction and development]. Grosses Zoologisches Praktikum, (G. Fischer Verlag, Stuttgart). German.

- Henikoff S (1992). Position effect and related phenomena. *Curr Opin Genet Dev*, 2(6), 907-12.
- Hesse R (1898) Untersuchungen über die Organe der Lichtempfindung bei niederen Thieren. IV. Die Sehorgane des Amphioxus [Studies on the light sensation in lower animals. IV. The visual organs of amphioxus]. *Z Wiss Zool*, 65, 456–464. German.
- Hesse R (1899) Untersuchungen über die Organe der Lichtempfindung bei niederen Thieren. V. Die Augen der polychäten Anneliden [Studies on the light sensation in lower animals. V. The eyes of polychaete annelids]. *Z Wiss Zool*, 65, 446–516, German.
- Heremans Y, Van De Castele M, in't Veld P, Gradwohl G, Serup P, Madsen O, Pipeleers D, Heimberg H (2002). Recapitulation of embryonic neuroendocrine differentiation in adult human pancreatic duct cells expressing neurogenin 3. *J Cell Biol*, 159(2), 303-12.
- Hofmann DK (1976) Regeneration and endocrinology in the polychaete *Platynereis dumerilii*. An experimental and structural study. *Roux Arch Dev Biol*, 180(1):47–71
- Hogan A, Heyner S, Charron MJ, Copeland NG, Gilbert DJ, Jenkins NA, Thorens B, Schultz GA (1991). Glucose transporter gene expression in early mouse embryos. *Development*, 113(1), 363-72.
- Holland PW (2001). Beyond the Hox: how widespread is homeobox gene clustering? *J Anat*, 199(Pt 1-2), 13-23.
- Holthuizen PE, Cleutjens CB, Veenstra GJ, van der Lee FM, Koonen-Reemst AM, Sussenbach JS (1993). Differential expression of the human, mouse and rat IGF-II genes. *Regul Pept*, 48(1-2), 77-89.
- Hrytsenko O, Wright JR Jr, Morrison CM, Pohajdak B (2007). Insulin expression in the brain and pituitary cells of tilapia (*Oreochromis niloticus*). *Brain Res*, 1135(1), 31-40.
- Hrzenjak M, Kobrehel D, Levanat S, Jurin M, Hrzenjak T (1993). Mitogenicity of the earthworm's (*Eisenia foetida*) insulin-like proteins. *Comp Biochem Physiol B*, 104(4), 723-9.
- Hui JH, Raible F, Korchagina N, Dray N, Samain S, Magdelenat G, Jubin C, Segurens B, Balavoine G, Arendt D, Ferrier DE (2009). Features of the ancestral bilaterian inferred from *Platynereis dumerilii* ParaHox genes. *BMC Biol*, 7, 43.
- Ikeya T, Galic M, Belawat P, Nairz K, Hafen E (2002). Nutrient-dependent expression of insulin-like peptides from neuroendocrine cells in the CNS contributes to growth regulation in *Drosophila*. *Curr Biol*, 12(15), 1293-300.
- Iser WB, Gami MS, Wolkow CA (2006). Insulin signaling in *Caenorhabditis elegans* regulates both endocrine-like and cell-autonomous outputs. *Dev Biol*, 303(2), 434-47.
- Ito E, Okada R, Sakamoto Y, Otshuka E, Mita K, Okuta A, Sunada H, Sakakibara M (2012). Insulin and memory in *Lymnaea*. *Acta Biol Hung*, 63 Suppl 2, 194-201.
- Jonsson J, Carlsson L, Edlund T, Edlund H (1994). Insulin-promoter-factor 1 is required for pancreas development in mice. *Nature*, 371(6498), 606-9.



- Kelly JV, Posse N (1956). The hormone relaxin in labor; tocometric studies of its effect on uterine contractions at term. *Obstet Gynecol*, 8(5), 531-5.
- Ketting RF, Fischer SE, Plasterk RH (1997). Target choice determinants of the Tc1 transposon of *Caenorhabditis elegans*. *Nucleic Acids Res*, 25(20), 4041-7.
- Kim SK, Rulifson EJ (2004). Conserved mechanisms of glucose sensing and regulation by *Drosophila corpora cardiaca* cells. *Nature*, 431(7006), 316-20.
- Koga A, Suzuki M, Inagaki H, Bessho Y, Hori H (1996). Transposable element in fish. *Nature*, 383 (6595), 30.
- Korner J, Chun J, Harter D, Axel R (1991). Isolation and functional expression of a mammalian prohormone processing enzyme, murine prohormone convertase 1. *Proc Natl Acad Sci U S A*, 88(15), 6834-8.
- Kozmik Z, Holland ND, Kreslova J, Oliveri D, Schubert M, Jonasova K, Holland LZ, Pestarino M, Benes V, Candiani S (2007). Pax-Six-Eya-Dach network during amphioxus development: conservation in vitro but context specificity in vivo. *Dev Biol*, 306(1), 143-59.
- Kulakova MA, Cook CE, Andreeva TF (2008). ParaHox gene expression in larval and postlarval development of the polychaete *Nereis virens* (Annelida, Lophotrochozoa). *BMC Dev Biol*, 8, 61.
- Kwan KM, Fujimoto E, Grabher C, Mangum BD, Hardy ME, Campbell DS, Parant JM, Yost HJ, Kanki JP, Chien CB (2007). The Tol2kit: a multisite gateway-based construction kit for Tol2 transposon transgenesis constructs. *Developmental Dyn*, 236(11), 3088-99.
- La Fleur SE, Kalsbeek A, Wortel J, Buijs RM (1999). A suprachiasmatic nucleus generated rhythm in basal glucose concentrations. *J Neuroendocrinol* 11(8), 643-52.
- Larhammar D (1996). Evolution of neuropeptide Y, peptide YY and pancreatic polypeptide. *Regul Pept*, 62(1), 1-11.
- Lauterio TJ, Aravich PF, Rotwein P (1990). Divergent effects of insulin on insulin-like growth factor-II gene expression in the rat hypothalamus. *Endocrinology*, 126(1), 392-8.
- Le Roith D, Shiloach J, Roth J, Lesniak MA (1980). Evolutionary origins of vertebrate hormones: substances similar to mammalian insulins are native to unicellular eukaryotes. *Proc Natl Acad Sci U S A*, 77(10), 6184-8.
- LeRoith D, Lesniak MA, Roth J (1981). Insulin in insects and annelids. *Diabetes*, 30(1), 70-76.
- Li KW, Geraerts WP, van Loenhout H, Joosse J (1992). Biosynthesis and axonal transport of multiple molluscan insulin-related peptides by the neuroendocrine light green cells of *Lymnaea stagnalis*. *Gen Comp Endocrinol*, 87(1), 79-86.
- Li MA, Alls JD, Avancini RM, Koo K, Godt D (2003). The large Maf factor Traffic Jam controls gonad morphogenesis in *Drosophila*. *Nat Cell Biol*, 5(11), 994-1000.

- Liu YG, Mitsukawa N, Oosumi T, Whittier RF (1995). Efficient isolation and mapping of *Arabidopsis thaliana* T-DNA insert junctions by thermal asymmetric interlaced PCR. *Plant J*, 8(3), 457-63.
- Livingstone C, Lyall H, Gould GW (1995). Hypothalamic GLUT 4 expression: a glucose- and insulin-sensing mechanism? *Mol Cell Endocrinol*, 107(1), 67-70.
- Marcheva B, Ramsey KM, Buhr ED, Kobayashi Y, Su H, Ko CH, Ivanova G, Omura C, Mo S, Vitaterna MH, Lopez JP, Philipson LH, Bradfield CA, Crosby SD, JeBailey L, Wang X, Takahashi JS, Bass J (2010). Disruption of the clock components CLOCK and BMAL1 leads to hypoinsulinaemia and diabetes. *Nature*, 466(7306), 627-31.
- McClintock B (1950). The origin and behavior of mutable loci in maize. *Proc Natl Acad Sci U S A*, 36(6), 344-55.
- Meester I, Ramkema MD, van Minnen J, Boer HH (1992). Differential expression of four genes encoding molluscan insulin-related peptides in the central nervous system of the pond snail *Lymnaea stagnalis*. *Cell Tissue Res*, 269(1), 183-8.
- Metaxakis A, Oehler S, Klinakis A, Savakis C (2005). Minos as a genetic and genomic tool in *Drosophila melanogaster*. *Genetics*, 171, 571-581
- Miguel-Aliaga I, Thor S, Gould AP (2008) Postmitotic specification of *Drosophila* insulinergic neurons from pioneer neurons. *PLoS Biol*, 6: e58.
- Miller CP, McGehee RE Jr, Habener JF (1994). IDX-1: a new homeodomain transcription factor expressed in rat pancreatic islets and duodenum that transactivates the somatostatin gene. *EMBO J*, 13(5), 1145-56.
- Miskey C, Papp B, Mátés L, Sinzelle L, Keller H, Izsvák Z, Ivics Z (2007). The ancient mariner sails again: transposition of the human Hsmar1 element by a reconstructed transposase and activities of the SETMAR protein on transposon ends. *Mol Cell Biol*, 27(12), 4589-600.
- Morley JE, Hernandez EN, Flood JF (1987). Neuropeptide Y increases food intake in mice. *Am J Physiol*, 253(3 Pt 2), R516-22.
- Müller WA (1973). [Autoradiographic studies on the synthetic activity of neurosecretory cells in the brain of *Platynereis dumerilii* during sexual development and regeneration]. *Z Zellforsch Mikrosk Anat*, 139(4), 487-510.
- Mutoh H, Fung BP, Naya FJ, Tsai MJ, Nishitani J, Leiter AB (1997). The basic helix-loop-helix transcription factor BETA2/NeuroD is expressed in mammalian enteroendocrine cells and activates secretin gene expression. *Proc Natl Acad Sci U S A*, 94(8), 3560-4.
- Nagasawa H, Kataoka H, Isogai A, Tamura S, Suzuki A, Ishizaki H, Mizoguchi A, Fujiwara Y, Suzuki A (1984). Amino-terminal amino Acid sequence of the silkworm prothoracicotropic hormone: homology with insulin. *Science*, 226(4680), 1344-5.

- Nässel DR, Wegener C (2011). A comparative review of short and long neuropeptide F signaling in invertebrates: Any similarities to vertebrate neuropeptide Y signaling? *Peptides*, 32(6), 1335-55. Epub 2011 Mar 31.
- Nässel DR (2002). Neuropeptides in the nervous system of *Drosophila* and other insects: multiple roles as neuromodulators and neurohormones. *Prog Neurobiol*, 68(1), 1-84.
- Naya, F.J., Huang, H.P., Qiu, Y., Mutoh, H., Demayo, F.J., Leiter, A.B. and Tsai, M.J. (1997). Diabetes, defective pancreatic morphogenesis, and abnormal enteroendocrine differentiation in BETA2/NeuroD-deficient mice. *Genes Dev*, 11, 2323-34.
- Neerman-Arbez M, Cirulli V, Halban PA (1994). Levels of the conversion endoproteases PC1 (PC3) and PC2 distinguish between insulin-producing pancreatic islet beta cells and non-beta cells. *Biochem J*, 300 ( Pt 1), 57-61.
- Neerman-Arbez M, Sizonenko SV, Halban PA (1993). Slow cleavage at the proinsulin B-chain/connecting peptide junction associated with low levels of endoprotease PC1/3 in transformed beta cells. *J Biol Chem*, 268(22), 16098-100.
- Nishimura W, Kondo T, Salameh T, El Khattabi I, Dodge R, Bonner-Weir S, Sharma A (2006). A switch from MafB to MafA expression accompanies differentiation to pancreatic beta-cells. *Dev Biol*, 293(2), 526-39.
- Ogura K, Yamamoto MT (2003). A mariner-like element with a 5' lesion in *Drosophila simulans*. *Genetica*, 119(3), 229-35.
- Ohagi S, LaMendola J, LeBeau MM, Espinosa R 3rd, Takeda J, Smeekens SP, Chan SJ, Steiner DF (1992). Identification and analysis of the gene encoding human PC2, a prohormone convertase expressed in neuroendocrine tissues. *Proc Natl Acad Sci U S A* 89(11), 4977-81.
- Ohlsson H, Karlsson K, Edlund T (1993). IPF1, a homeodomain-containing transactivator of the insulin gene. *EMBO J*, 12(11), 4251-9.
- Okamoto N, Nishimori Y, Nishimura T (2012). Conserved role for the Dachshund protein with *Drosophila* Pax6 homolog Eyeless in insulin expression. *Proc Natl Acad Sci U S A*, 109(7), 2406-11
- Okamoto N, Yamanaka N, Yagi Y, Nishida Y, Kataoka H, O'Connor MB, Mizoguchi A (2009). A fat body-derived IGF-like peptide regulates postfeeding growth in *Drosophila*. *Dev Cell*, 17(6), 885-91.
- Olbrot M, Rud J, Moss LG, Sharma A (2002). Identification of beta-cell-specific insulin gene transcription factor RIPE3b1 as mammalian MafA. *Proc Natl Acad Sci U S A*, 99(10), 6737-42.
- Palmiter RD, Behringer RR, Quaife CJ, Maxwell F, Maxwell IH, Brinster RL (1987). Cell lineage ablation in transgenic mice by cell-specific expression of a toxin gene. *Cell*, 50(3), 435-43.

- Park CR (2001). Cognitive effects of insulin in the central nervous system. *Neurosci Biobehav Rev*, 25(4), 311-23.
- Pavlopoulos A, Averof M (2005). Establishing genetic transformation for comparative developmental studies in the crustacean *Parhyale hawaiiensis*. *Proc Natl Acad Sci U S A*, 102(22), 7888-93.
- Pera EM, Kessel M (1998). Demarcation of ventral territories by the homeobox gene NKX2.1 during early chick development. *Dev Genes Evol*, 208(3), 168-71.
- Plasterk RH, Groenen JT (1992). Targeted alterations of the *Caenorhabditis elegans* genome by transgene instructed DNA double strand break repair following Tc1 excision. *EMBO J*, 11(1), 287-90.
- Prud'homme B, de Rosa R, Arendt D, Julien JF, Pajaziti R, Dorresteyn AW, Adoutte A, Wittbrodt J, Balavoine G (2003). Arthropod-like expression patterns of engrailed and wingless in the annelid *Platynereis dumerilii* suggest a role in segment formation. *Curr Biol*, 13(21), 1876-81.
- Purschke G, Ding Z, Müller MC (1995). Ultrastructural differences as a taxonomic marker: The segmental ocelli of *Polyophthalmus pictus* and *Polyophthalmus qingdaoensis* sp.n. (Polychaeta, Opheliidae). *Zoomorphology*, 115(4), 229-241.
- Raff RA (2000). Evo-devo: the evolution of a new discipline. *Nat Rev Genet*, 1(1), 74-9.
- Raible F, Tessmar-Raible K, Osoegawa K, Wincker P, Jubin C, Balavoine G, Ferrier D, Benes V, de Jong P, Weissenbach J, Bork P, Arendt D (2005). Vertebrate-type intron-rich genes in the marine annelid *Platynereis dumerilii*. *Science*, 310(5752), 1325-6.
- Rast JP (2000). Transgenic manipulation of the sea urchin embryo. *Methods Mol Biol*, 136, 365-73.
- Rhode B (1992) Development and Differentiation of the Eye in *Platynereis dumerilii* (Annelida, Polychaeta). *J Morphol*, 212, 71-85.
- Richardson A, Liu F, Adamo ML, Van Remmen H, Nelson JF (2004). The role of insulin and insulin-like growth factor-I in mammalian ageing. *Best Pract Res Clin Endocrinol Metab*, 18(3), 393-406.
- Ripperger JA, Schibler U (2001). Circadian regulation of gene expression in animals. *Curr Opin Cell Biol*, 13(3), 357-62.
- Roovers E, Vincent ME, van Kesteren E, Geraerts WP, Planta RJ, Vreugdenhil E, van Heerikhuizen H (1995). Characterization of a putative molluscan insulin-related peptide receptor. *Gene*, 162(2), 181-8.
- Rulifson EJ, Kim SK, Nusse R (2002). Ablation of insulin-producing neurons in flies: growth and diabetic phenotypes. *Science*, 296(5570), 1118-20.
- Rutter J, Reick M, McKnight SL (2002). Metabolism and the control of circadian rhythms. *Annu Rev Biochem*, 71, 307-31.

- Saltiel AR, Kahn CR (2001). Insulin signalling and the regulation of glucose and lipid metabolism. *Nature*, 414(6865), 799-806.
- Samadi L, Steiner G (2010). Conservation of ParaHox genes' function in patterning of the digestive tract of the marine gastropod *Gibbula varia*. *BMC Dev Biol*, 10, 74.
- Sander M, Neubüser A, Kalamaras J, Ee HC, Martin GR, German MS (1997). Genetic analysis reveals that PAX6 is required for normal transcription of pancreatic hormone genes and islet development. *Genes Dev*, 11(13), 1662-73.
- Saudemont A, Dray N, Hudry B, Le Gouar M, Vervoort M, Balavoine G (2008). Complementary striped expression patterns of NK homeobox genes during segment formation in the annelid *Platynereis*. *Dev Biol*, 317(2), 430-43.
- Sijen T, Plasterk RH (2003). Transposon silencing in the *Caenorhabditis elegans* germ line by natural RNAi. *Nature*, 426(6964), 310-4.
- Smeekens SP, Avruch AS, LaMendola J, Chan SJ, Steiner DF (1991). Identification of a cDNA encoding a second putative prohormone convertase related to PC2 in AtT20 cells and islets of Langerhans. *Proc Natl Acad Sci U S A*, 88(2), 340-4.
- Smit AB, Spijker S, Van Minnen J, Burke JF, De Winter F, Van Elk R, Geraerts WP (1996). Expression and characterization of molluscan insulin-related peptide VII from the mollusc *Lymnaea stagnalis*. *Neuroscience*, 70(2), 589-96.
- Smit AB, Vreugdenhil E, Ebberink RH, Geraerts WP, Klootwijk J, Joosse J (1988). Growth-controlling molluscan neurons produce the precursor of an insulin-related peptide. *Nature*, 331(6156), 535-8.
- Sussel L, Kalamaras J, Hartigan-O'Connor DJ, Meneses JJ, Pedersen RA, Rubenstein JL, German MS (1998). Mice lacking the homeodomain transcription factor Nkx2.2 have diabetes due to arrested differentiation of pancreatic beta cells. *Development*, 125(12), 2213-21.
- Sussel L, Marin O, Kimura S, Rubenstein JL (1999). Loss of Nkx2.1 homeobox gene function results in a ventral to dorsal molecular respecification within the basal telencephalon: evidence for a transformation of the pallidum into the striatum. *Development*, 126(15), 3359-70.
- Tahara Y, Otsuka M, Fuse Y, Hirao A, Shibata S (2011). Refeeding after fasting elicits insulin-dependent regulation of Per2 and Rev-erb $\alpha$  with shifts in the liver clock. *J Biol Rhythms*, 26(3), 230-40.
- Tessmar-Raible K, Steinmetz PR, Snyman H, Hassel M, Arendt D (2005). Fluorescent two-color whole mount in situ hybridization in *Platynereis dumerilii* (Polychaeta, Annelida), an emerging marine molecular model for evolution and development. *Biotechniques*, 39(4), 460, 462, 464.

Tessmar-Raible K, Raible F, Christodoulou F, Guy K, Rembold M, Hausen H, Arendt D (2007). Conserved sensory-neurosecretory cell types in annelid and fish forebrain: insights into hypothalamus evolution. *Cell*, 129(7), 1389-400.

Tessmar-Raible K, Raible F, Arboleda E (2011) Another place, another timer: Marine species and the rhythms of life. *Bioessays*, 33(3), 165–172.

Thor S, Thomas JB (1997). The *Drosophila* islet gene governs axon pathfinding and neurotransmitter identity. *Neuron*, 18(3), 397-409.

Tomer R, Denes AS, Tessmar-Raible K, Arendt D (2010). Profiling by image registration reveals common origin of annelid mushroom bodies and vertebrate pallium. *Cell*, 142(5), 800-9.

van der Krol AR, Mur LA, Beld M, Mol JN, Stuitje AR (1990). Flavonoid genes in petunia: addition of a limited number of gene copies may lead to a suppression of gene expression. *Plant Cell*, 2(4), 291-9.

van Heemst D, Beekman M, Mooijaart SP, Heijmans BT, Brandt BW, Zwaan BJ, Slagboom PE, Westendorp RG (2005). Reduced insulin/IGF-1 signalling and human longevity. *Aging Cell*, 4(2), 79-85.

van Heumen WR, Roubos EW (1991). Immuno-electron microscopy of sorting and release of neuropeptides in *Lymnaea stagnalis*. *Cell Tissue Res*, 264(1), 185-95.

van Heumen WR, Roubos EW (1990). Ultrastructural evidence for synthesis, storage and release of insulin-related peptides in the central nervous system of *Lymnaea stagnalis*. *Neuroscience*, 39(2), 493-500.

van Luenen HG, Plasterk RH (1994). Target site choice of the related transposable elements Tc1 and Tc3 of *Caenorhabditis elegans*. *Nucleic Acids Res*, 22(3), 262-9.

van Minnen J, Smit AB, Joosse J (1989). Central and peripheral expression of genes coding for egg-laying inducing and insulin-related peptides in a snail. *Arch Histol Cytol*, 52 Suppl, 241-52.

van Minnen J (1994). Axonal localization of neuropeptide-encoding mRNA in identified neurons of the snail *Lymnaea stagnalis*. *Cell Tissue Res*, 276(1), 155-61.

Weiler KS, Wakimoto BT (1995). Heterochromatin and gene expression in *Drosophila*. *Annu Rev Genet*, 29, 577-605.

Wendelaar Bonga SE (1970). Ultrastructure and histochemistry of neurosecretory cells and neurohaemal areas in the pond snail *Lymnaea stagnalis* (L.). *Z Zellforsch Mikrosk Anat*, 108(2), 190-224.

Wilkinson TN, Bathgate RA (2007). The evolution of the relaxin peptide family and their receptors. *Adv Exp Med Biol*, 612, 1-13.

Winchell CJ, Valencia JE, Jacobs DK (2010). Expression of Distal-less, dachshund, and optomotor blind in *Neanthes arenaceodentata* (Annelida, Nereididae) does not support

homology of appendage-forming mechanisms across the Bilateria. *Dev Genes Evol*, 220(9-10), 275–295.

Xiang M, Zhou L, Macke JP, Yoshioka T, Hendry SH, Eddy RL, Shows TB, Nathans J (1995). The Brn-3 family of POU-domain factors: primary structure, binding specificity, and expression in subsets of retinal ganglion cells and somatosensory neurons. *J Neurosci*, 15(7 Pt 1), 4762-85.

Yamaguchi T, Fernandez R, Roth RA (1995). Comparison of the signaling abilities of the *Drosophila* and human insulin receptors in mammalian cells. *Biochemistry*, 34(15), 4962-8.

Yang CH, Belawat P, Hafen E, Jan LY, Jan YN (2008). *Drosophila* egg-laying site selection as a system to study simple decision-making processes. *Science*, 319(5870), 1679-83.

Yang G, Weil CF, Wessler SR (2006). A rice Tc1/mariner-like element transposes in yeast. *Plant Cell*, 18(10), 2469-78.

Yang XJ, Kow LM, Funabashi T, Mobbs CV (1999). Hypothalamic glucose sensor: similarities to and differences from pancreatic beta-cell mechanisms. *Diabetes*, (9), 1763-72.

Yu JK, Holland ND, Holland LZ (2004). Tissue-specific expression of FoxD reporter constructs in amphioxus embryos. *Dev Biol*, 274(2), 452-61.

Zecchin E, Mavropoulos A, Devos N, Filippi A, Tiso N, Meyer D, Peers B, Bortolussi M, Argenton F (2004). Evolutionary conserved role of *ptfla* in the specification of exocrine pancreatic fates. *Dev Biol*, 268(1), 174-84.





## 6. Appendix

### Primer list:

ilp2_GSP2_3'RACE	CGTCATGGCGAAACCTCGGCAGTCTC
ilp2_GSP1_5'RACE	GCAGCCATGTGAGGTTGTTTGCACCTCGG
ilp2_GSP2_5'RACE	GGAGATCAGAGTTTCTTTTGGCTTGAGGG
ilp1_GSP2_5'RACE	GATGCCTTGACTGCCACGTTTGCCTCGG
ilp1_GSP1_3'RACE	GCATTACAGCTGCTGGGGCCCAGGATGG
ilp1_GSP2_3'RACE	GTTCAGCATATCATTGCTTCAGCAGGGGTC
ilp2_GSP1_3'RACE	GTTGTGGAAGCCTGCTGTTATCGCACATG
ilp1_GSP1_5'RACE	CGGAACAAGGGTGTCTGCAACATTACAGG
Maf_5'RACE_GSP	GCTTCAGCTTGAGTACGGCCTCCTTGGGG
Maf_5'RACE_NGSP	CCCTGCAGCCTGCGGTTGAGTTCTCTC
Maf_3'RACE_GSP	GAACTACTAGATACGGCGAGGCGAGATGATC
Maf_3'RACE_NGSP	GCCCATCGTACCTGGCATAATTATAGCGCG
attB-Rps9_1.6kup_f	GGTGCCAGGGCGTGCCCTTGGGCTCCCCGGGCGCGTTCCCAGAAAAACGCTGATGTATGG
ISceI/KpnI/attP/tuba_f	TAGGGATAACAGGGTAATgggtaccCCCCAACTGGGGTAACCTTTGAGTTCTCTCAGTTGGGGGcaattcgctctgccactctgcaac
EGFP-ISceI_r	tagggataacagggtaatGCTTAAGATACATTGATGAGTTTGGAC
EGFP-ATG_f	ATGGTGAGCAAGGGCGAGGAGC
tuba-GFP_fusion_r	gtggcgaccggtggatCCTGTCCGACGTGGATGCTG
ISceI-tuba_f	TAGGGATAACAGGGTAATcaattcgctctgccactctgcaac
ISceI-rps9_1.6k_f	TAGGGATAACAGGGTAATTTCCCAGAAAAACGCTGATGTATGG
rps9-GFP_fusion_r	ctctcgcccttctcaccatCTGAAATGTTAATAATAGATAAAATAAAAAACATTG
ISceI-Maf_3.6k_f	TAGGGATAACAGGGTAATGGGTGGCTTTAGAAGTATGTCTG
Maf-GFP_fusion_r	GCTCCTCGCCCTTGCTCACCATAAGCCTGTTCTAAATATAGCTCCG
rps9_TAIL1	GCTTCAACTCCTGATCCAAACGCTC
rps9_TAIL2	GCGCCGGGGAGTTGTGTAGG
rps9_TAIL3	TGGAGTACACCAATGGTATGCGCG
rps9_TAILII-1	CCAGATACATGGATTTTCGCCATCGAC
rps9_TAILII-2	CCTGGCCACAGGTCCCACC
rps9_TAILII-3	GCCAATATTGGCATTGATTTTGAAGGAGC
MosLIR-1	GGCACGAAACTCGACATGTTGACTGC
MosLIR-2	AACAATTATGACGCTCAATTTCGCGCC
MosLIR-3	GGTGGTTCGACAGTCAAGGTTGACACTTC
MosRIR-1	AGCGCTTCGATTCTTACGAAAGTGTG
MosRIR-2	GGTTCGCGCAAAAGACGATGAGTTC
MosRIR-3	GGAATCCACAAATTGCCCGAGAGATGG
Tol2L-1	CTAAAGCAGGATAAAACCTTGTATGCATTTT
Tol2L-2	CCTTAATACTCAAGTACAATTTTAATGGAGTAC
Tol2L-3	CTTTTACTCAAGTAAGATTCTAGCCAGATAC
Tol2R-1	CGTCACTTCCAAAGGACCAATGAACATGTC
Tol2R-2	CTGGGCATCAGCGCAATTCAATTGG
Tol2R-3	GCAAGGGAAAAATAGAATGAAGTGATCTCC
degenerated primer I	NGTCGASWGANAWGTT
degenerated primer II	GTNCGASWCANAWGTT
degenerated primer III	WGTGNAGWANCANAGA
degenerated primer IV	NGTCGASWGANAWCTT
degenerated primer V	GTNCGASWCANAWCAA
degenerated primer VI	GTNCGASWCANAWCAA
degenerated primer VII	NGTCGASWGANAWAGA
degenerated primer VIII	WGTGNAGWANCANGTT
T2_f	GCCAAGCGCGCAATTAACCCCTC
T2_r	GTACGCCTACCTGTTGGACCCAGG
Mos_test_f	CCCTCACTAAAGGGAACAAAAGCTTTATGG
Mos_test_r	ATATATGCGTAAGAACGGGGACCTAG
EGFP_f	GGTGAGCAAGGGCGAGGAGC
EGFP_r	CTCGTCCATGCCGAGAGTGATCC
ilp1_RT_f	GATATCACCATGGAAAACGATC
ilp1_RT_f	GTGTCTGCAACATTACAGG
ilp2_RT_f	GGCTCAGACAAAAAGATCACAAA
ilp2_RT_r	CGCAGTATGATTCCATTTCCTC
ilp3_RT_f	GAAAACGATCCGACAGGCAC
ilp3_RT_r	CATTACAGATGATGCCACG
ilp4_RT_f	GGAAAACGCTCTGCAGGAAC
ilp4_RT_r	CAACATTACAGATGATGCCAC
ilp5_RT_f	GATCTCAACTTTATAATACCCCTTCGAC
ilp5_RT_r	AGAAGGGGACTGTCTTCGAGAAAT
pax6_RT_f	CTCCAGTTTCCCCAACTCAA
pax6_RT_r	GCTGAATGACCCAAAACAG
Ol_ins_RT_f	GACGTGGACCCTCTTCTCG
Ol_ins_RT_r	GCGAACTCAGCCACTTCATT

Ol_igf1_RT_f	TGTCTGTGGAGATAGAGGCTTTT
Ol_igf1_RT_r	CGCGCAGTACATCTCCAG
Ol_igf2_RT_f	GTCTCCGCAGGTCATTCC
Ol_igf2_RT_r	CCTCACAGTCATAGGCTGCTT
Ol_clk1_RT_f	CCTTTTCTCAGCAACGAGGA
Ol_clk1_RT_r	TGCTATGAAGAAACCGTCCA
Ol_clk2_RT_f	CCATCTGTCCCGTAACCAGT
Ol_clk2_RT_r	CAGGACTGTGCAGCTCAGATA
Ol_rps9_RT_f	GAAGGCTGCAGACTCAGGTC
Ol_rps9_RT_r	GGATATTCACCACTTGCTTGC
Ol_rpl7_RT_f	GCTGAACAAGGCTTCAATCA
Ol_rpl7_RT_r	TGAGCTCTCGCACAGACTTC
Ol_rpl7_publ_f	GTCGCCTCCCTCCACAAAG
Ol_rpl7_publ_r	AACTTCAAGCCTGCCAACAAC
Maf_r	GAGAGCACACTGTCCGGGGATCC
Maf_f	CAGTGAGTCCCTTCCAGCCCC
Rps9_f	ATGCCGCGCATACCATTTGGTGAC
Rps9_r	GATATGTCTCTGACGAATGAGCACACG
ptf1a_f	GAATAGTTCACAGATCTGCCGAGAGG
ptf1a_r	GGATTCTAGCTCAATCAGTTAACAGCAC
cpa_f	CATACTGACTTGGCACTGTTGGCAG
cpa_r	CGATGGACGGCCTCACGTTGG
glut2_f	GAGACGTAGGCCAACCACTGGACTG
glut2_r	GTGGGATCCTCGTCTCCAGGCC
neuroD_f	CCTGCCCCGTTTCCTGGATTTACTCTC
neuroD_r	GCGGCTGGTAGAAAGCCAAGGG
foxo_f	GGACGCAGCAGACATCGACCCC
foxo_r	GGGCAAGGACTGCTGCTGGGTC
dach_f	CTCCGGTGTGAGTCCTCAGCC
dach_r	GAGGAGGCGGCCATCTTGTCAG
inR_f	CCGGACCATTTGACATCAGGAACAACG
inR_r	GTCGACCTCCGGCCTGCACTC
pax258_f	ATGGACGTCCTCACCCACCTGCC
pax258_r	CTAGGGTACTGAGCGGTGTAAGCAG
g(q)_f	GTGGCATTCTGCTGGAGGAGCTC
g(q)_r	CCACTGACTGGTCTGGCATCATTAACC
phi_test_f	GCCAAGCGCGCAATTAACCCCTC
phi_test_r	CAATTCTGCTGCCACTCTGCAAC



## Summary

A main focus of this study was the comparative analyses of insulinergetic cells in the marine annelid *Platynereis dumerilii* to study their regulation in larvae and adult animals. I have identified 5 different *Platynereis* insulin-like peptides that are specifically expressed by neurosecretory cells in the larval and postlarval brain. Based on optimized in-situ staining protocols that I developed to study gene expression patterns in adult worms, I analyze the expression of known vertebrate insulin regulators and found that *Platynereis* IMaf, pax6 and islet genes are associated with insulinergetic cells in larval and postlarval brains, respectively. Further molecular analyses of *Platynereis* insulinergetic cells revealed, that insulin-like peptides are associated with centers of clock gene-expression and exhibit a 24-hour rhythm of expression, which is maintained even under constant darkness. These findings suggest that the expression of *Platynereis* insulin like peptides may be under the control of the circadian clock, possibly reflecting an ancient mechanism to integrate metabolic processes and the circadian clock. Evidences for a function of *Platynereis* insulin-like peptides in nutrient metabolism were shown in this study, which implies that *Platynereis* insulin-like peptides have a conserved role in carbohydrate metabolism. Moreover, a role for the *Platynereis* infracerebral gland as blood glucose-sensing organ was proposed and a mechanism of insulin secretion was suggested in this study.

The findings of this study provide new insights into the regulation of insulin-like peptides in *Platynereis* and indicate possibly ancient features of insulin transcription, their function and interconnection to the circadian clock in bilaterian animals. Moreover, the findings support the hypothesis that insulinergetic cells are of neuronal origin.

Another goal of this work was to develop methods to label cells in *Platynereis dumerilii* larval and postlarval stages in vivo. Based on an optimized zygotic microinjection protocol and specific transposon-derived vectors, I generated the first stable transgenic strains and established a robust protocol for transient transgenic applications in *Platynereis*. A *Mos1*-derived transgenic fluorescent reporter line that recapitulates the endogenous expression of *r-opsin*, a characteristic marker for rhabdomeric photoreceptors, led to the discovery of non-cephalic photoreceptors. Molecular analysis of these non-cephalic photoreceptors revealed that they differentiate independent of pax6, a gene that is involved in eye development in many metazoans, and that they could share a common origin with the amphioxus Hesse organ. Moreover, a second transgenic strain was established that drives expression of EGFP

under the control of cis-regulatory elements of an alpha-tubulin gene that enables to trace ciliated cells during development of the early trochophore larva. Analyses of the transgenic reporter lines revealed that Mos1-derived transgenes are integrated into the genome and are transmitted and expressed in subsequent generations. These findings establish that the Mos1 transposon is a suitable tool to generate transgenic strains in *Platynereis dumerilii*.

I explored transient transgenic approaches in *Platynereis* using a tol2-derived fluorescent reporter construct for rps9, a component of the ribosomal 40S subunit that drives ubiquitous EGFP expression. Zygotes that were co-injected with the rps9 reporter along with synthetic tol2 transposase mRNA gave rise to fully fluorescent adult animals. No EGFP expression was observed in the offspring of injected animals which might reflect a permanent silencing of the reporter, since *egfp* coding sequence can still be amplified from non-fluorescent batches derived from transgenic parents. Notwithstanding, Tol2-based vectors yield high numbers of complete expression patterns of transgenes in the injected animals and hence, Tol2-derived constructs are suitable tools for transient transgenic applications in *Platynereis*.

The establishments of transient transgenic technology and stable transgenic strains reported in this study, provide unprecedented tools to characterize and functionally study cell types throughout the lifetime of the animal. Moreover, the methodology described in this study, fills a critical gap in the toolkit currently available for *Platynereis dumerilii* and will help to address open biological questions in both developmental and evolutionary biology, as well as chronobiology.

## Zusammenfassung

Das Hauptziel dieser Arbeit war die vergleichende Analyse von insulinergen Zellen und deren Regulation in Larven sowie in adulten Stadien des Meeresringelwurms *Platynereis dumerilii*. In dieser Studie wurden fünf verschiedene insulin-ähnliche Peptidhormone (Insuline) in *Platynereis* beschrieben, welche in neurosekretorischen Zellen der Gehirne von Larven und adulten Würmern exprimiert sind. Basierend auf verbesserten in-situ Färbemethoden, welche im Zuge dieser Arbeit entwickelt wurden um Genexpressionsmuster in adulten Würmern zu erforschen, analysierte ich die Expressionsmuster bekannter Insulin-Regulatoren aus Wirbeltieren und entdeckte, dass deren *Platynereis*-Orthologe *lMaf*, *pax6* und *islet* mit insulinergen Zellen der Gehirne von Larven beziehungsweise adulte Stadien assoziiert sind. Weitere molekulare Analysen der insulinergen Zellen in *Platynereis* ergaben, dass die Zentren der Insulin-Expression und der circadianen Uhr miteinander assoziiert sind und Insuline in einem 24-Stunden Rhythmus exprimiert werden, welcher auch unter konstant dunklen Bedingungen beibehalten wird. Diese Ergebnisse deuten darauf hin, dass in *Platynereis* die Expression von Insulinen von der circadianen Uhr kontrolliert wird und dass es sich dabei möglicherweise um einen alten Mechanismus handelt, der Stoffwechselprozesse und die circadiane Uhr aufeinander abstimmt. Hinweise auf eine Funktion der *Platynereis* Insuline im Nahrungsstoffwechsel wurden in dieser Studie aufgezeigt, die auf eine konservierte Funktion der *Platynereis* Insuline im Kohlenhydrat-Stoffwechsel hindeuten. Darüber hinaus wurde in dieser Studie eine Funktion der Infracerebral-Drüse als ein den Blutzuckerspiegel messendes Organ vorgeschlagen und ein möglicher Mechanismus der Insulin-Sekretion in *Platynereis* diskutiert.

Die Ergebnisse dieser Studie liefern neue Einblicke in die Regulation Insulin-ähnlicher Peptide im Modellorganismus *Platynereis dumerilii*, die möglicherweise altertümliche Eigenschaften in der Transkription und Funktion von Insulinen und ihrer Verbindung zu der circadianen Uhr widerspiegeln. Darüber hinaus stützen die Ergebnisse die Hypothese, nach der insulinerge Zellen neuronalen Ursprungs sind.

Ein weiteres Ziel dieser Arbeit war die Entwicklung von Methoden, die die Markierung von Zellen in lebenden Larven und adulten Tieren ermöglichen. Mithilfe eines Mikoinjektionsprotokolls für Zygoten und Transposon-basierter Plasmid-Vektoren gelang mir die Etablierung der ersten stabilen transgenen Reporterlinien im Modellorganismus *Platynereis dumerilii*. Darüber hinaus entwickelte ich Methoden, die transiente Transgenese

in *Platynereis dumerilii* ermöglichen. Eine auf dem Transposon Mos1 basierende fluoreszente Reporterlinie, die die endogene Expression von r-opsin, einem charakteristischen Marker-Gen stäbchenförmiger Fotorezeptorzellen widerspiegelt, führte zu der Entdeckung von Fotorezeptorzellen außerhalb des Kopfes, die sich im Bereich des Bauchmarks und der Beinchen befinden. Diese Fotorezeptorzellen entwickeln sich unabhängig von *pax6*, einem Gen, das für die Augenentwicklung in vielen mehrzelligen Tieren zuständig ist und ähneln damit dem sogenannten Hesse-Organ, das im Lanzettfischchen beschrieben wurde. Darüber hinaus wurde in dieser Studie eine weitere transgene Reporterlinie etabliert, die die Expression des Fluoreszenzfarbstoffs EGFP unter der Kontrolle des Enhancers von alpha-tubulin treibt und die es erlaubt, ziliäre Zellen während früher Entwicklungsstadien zu verfolgen. Untersuchungen der transgenen Reporterlinien ergab, dass Mos1 basierte Reporterkonstrukte ins Genom von *Platynereis dumerilii* integriert und vererbt werden und in den Folgegenerationen exprimiert sind. Die Untersuchungen zeigen, dass auf dem Transposon Mos1 basierende Plasmid-Vektoren geeignet sind, um in *Platynereis* stabile transgene Reporterlinien zu erzeugen.

Um transiente Transgenese in *Platynereis* zu erforschen, verwendete ich ein auf dem Transposon Tol2 basierendes fluoreszentes Reporterkonstrukt, welches die Expression von EGFP unter der Kontrolle des Enhancers von *rps9* treibt, eines Komponenten der S40 ribosomalen Untereinheit. Dieses Reporterkonstrukt resultiert in einer starken Expression von EGFP in allen Zellen des Tieres. Zygoten, die mit diesem Reporterkonstrukt und synthetisch hergestellter Tol2 Transposase mRNA co-injiziert wurden, entwickelten sich zu komplett grün leuchtenden adulten Tieren. In Kontrast dazu, brachten die injizierten Tiere keinen fluoreszenten Nachwuchs hervor, was möglicherweise daran liegt, dass das Reporterkonstrukt gesilenced wurde. Hierfür spricht, dass aus dem Nachwuchs fluoreszenter Elterntiere egfp-kodierende Sequenzen mittels PCR amplifiziert werden konnten. Injektionen Tol2-basierter Reporterkonstrukte führen zu einer hohen Anzahl an Tieren, die ein komplettes Expressionsmuster des Reporters zeigen und daher ist das Tol2 Transposon für transiente Transgenese in *Platynereis* geeignet.

Die Etablierung transienter Transgenese und transgener Reporterlinien sind außerordentlich wertvolle Methoden bei der Charakterisierung und funktionalen Analyse von Zelltypen in Larven, sowie in adulten Tieren und schließen eine Lücke im Spektrum molekularbiologischer Methoden, die derzeit im Modellorganismus *Platynereis dumerilii* zur Verfügung stehen. Die hier vorgestellten Methoden werden dabei nützlich sein, offene Fragen

in der Entwicklungs- und Evolutionsbiologie, sowie der Chronobiologie mithilfe des Modells *Platynereis dumerilii* adressieren.





## Erklärung

Ich versichere hiermit, dass ich meine Dissertation „Regulatory tools and the characterization of insulinergic cells in the annelid *Platynereis dumerilii*“ selbst und ohne unerlaubte Hilfe verfasst und mich dabei keiner anderen Hilfsmittel als der von mir ausdrücklich bezeichneten Quellen und Hilfen bedient habe und dass ich die Dissertation in der vorliegenden oder einer ähnlichen Form bei keiner anderen Hochschule zu Prüfungszwecken eingereicht habe.

Wien, den 20. Januar 2013

Dipl.-Biol. Benjamin Backfisch





## Curriculum vitae

Name: Benjamin

Family Name: Backfisch

### Education:

June 2008  
- Dec 2012 Phd Student of the „VBC PhD programme“, MFPL, Vienna, Austria  
(Florian Raible lab)

Jan 2008: Diploma degree in Biology (Molecular Biology, Biochemistry,  
Ecology), Ruprecht-Karls University, Heidelberg, Germany

Mar 2007  
- Jan 2008: Diploma thesis at EMBL Heidelberg, Germany (Detlev Arendt lab)

June 2004: Intermediate Diploma (German Vordiplom)

2002-2008: Studies in Biology, Ruprecht-Karls University, Heidelberg, Germany

Sep 2001  
- Aug 2002: Civilian Service, MSBB, Heidelberg, Germany

June 2001: High school exam (German Abitur), Hölderlin-Gymnasium

1992-2001: Hölderlin-Gymnasium (High school), Heidelberg, Germany

### Publications:

**Backfisch B**, Veedin Rajan VB, Fischer RM, Lohs C, Arboleda E, Tessmar-Raible K, Raible F (2013). Stable transgenesis in the marine annelid *Platynereis dumerilii* sheds new light on photoreceptor evolution. Proc Natl Acad Sci U S A 110(1), 193-8.